

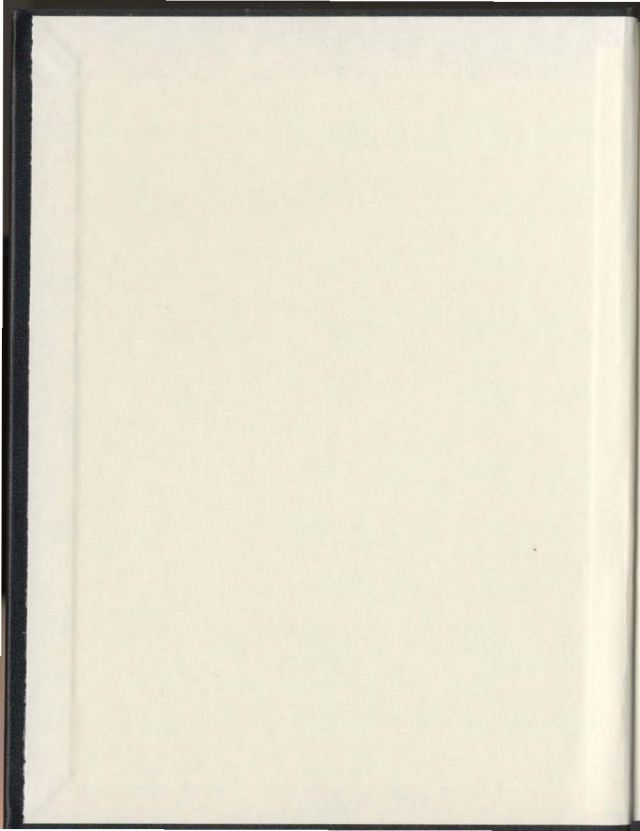
ROBUST LIMIT LOADS USING ELASTIC
MODULUS ADJUSTMENT TECHNIQUES

CENTRE FOR NEWFOUNDLAND STUDIES

**TOTAL OF 10 PAGES ONLY
MAY BE XEROXED**

(Without Author's Permission)

SATHYA PRASAD MANGALARAMANAN





INFORMATION TO USERS

This manuscript has been reproduced from the microfilm master. UMI films the text directly from the original or copy submitted. Thus, some thesis and dissertation copies are in typewriter face, while others may be from any type of computer printer.

The quality of this reproduction is dependent upon the quality of the copy submitted. Broken or indistinct print, colored or poor quality illustrations and photographs, print bleedthrough, substandard margins, and improper alignment can adversely affect reproduction.

In the unlikely event that the author did not send UMI a complete manuscript and there are missing pages, these will be noted. Also, if unauthorized copyright material had to be removed, a note will indicate the deletion.

Oversize materials (e.g., maps, drawings, charts) are reproduced by sectioning the original, beginning at the upper left-hand corner and continuing from left to right in equal sections with small overlaps. Each original is also photographed in one exposure and is included in reduced form at the back of the book.

Photographs included in the original manuscript have been reproduced xerographically in this copy. Higher quality 6" x 9" black and white photographic prints are available for any photographs or illustrations appearing in this copy for an additional charge. Contact UMI directly to order.

UMI

A Bell & Howell Information Company
300 North Zeeb Road, Ann Arbor MI 48106-1346 USA
313/761-4700 800/521-0600

**ROBUST LIMIT LOADS USING ELASTIC
MODULUS ADJUSTMENT TECHNIQUES**

By

Sathya Prasad Mangalaramanan

A DISSERTATION
SUBMITTED TO THE SCHOOL OF GRADUATE STUDIES
IN PARTIAL FULFILLMENT OF THE REQUIREMENTS
FOR THE DEGREE OF
DOCTOR OF PHILOSOPHY

FACULTY OF ENGINEERING AND APPLIED SCIENCE
MEMORIAL UNIVERSITY OF NEWFOUNDLAND

St. John's, Newfoundland, Canada

August 1997

©Copyright: Sathya Prasad Mangalaramanan 1997



National Library
of Canada

Acquisitions and
Bibliographic Services

395 Wellington Street
Ottawa ON K1A 0N4
Canada

Bibliothèque nationale
du Canada

Acquisitions et
services bibliographiques

395, rue Wellington
Ottawa ON K1A 0N4
Canada

Your file / Votre référence

Our file / Notre référence

The author has granted a non-exclusive licence allowing the National Library of Canada to reproduce, loan, distribute or sell copies of this thesis in microform, paper or electronic formats.

The author retains ownership of the copyright in this thesis. Neither the thesis nor substantial extracts from it may be printed or otherwise reproduced without the author's permission.

L'auteur a accordé une licence non exclusive permettant à la Bibliothèque nationale du Canada de reproduire, prêter, distribuer ou vendre des copies de cette thèse sous la forme de microfiche/film, de reproduction sur papier ou sur format électronique.

L'auteur conserve la propriété du droit d'auteur qui protège cette thèse. Ni la thèse ni des extraits substantiels de celle-ci ne doivent être imprimés ou autrement reproduits sans son autorisation.

0-612-25774-6

Canada

Reverentially dedicated at the lotus feet of my

Mother: Shrimathi. Lakshmi Mangalaramanan
Father: Shri. Tiruchuzhi Mangala Ramanan Narayanaiyer
Teacher: Dr. R. M. Umesh, and
God: The "Self"

Abstract

Simple and systematic methods for determining lower and upper bound limit loads, based on two linear elastic finite element analyses, are presented in this thesis. The methods that are developed for estimating lower bound limit loads are designated as the m_α -method and the r-node (redistribution node) method. It is also shown that robust upper bound limit loads can be obtained from statically admissible stress distributions that satisfy the integral mean of the yield.

The m_α -method is based on the extended variational theorem of Mura et al., and utilizes the concept of leap-frogging to a near limit state and the notion of reference volume. The lower bound multiplier, m_α , is found to give limit load estimates that are better than the classical.

The r-node method invokes the concept of redistribution nodes, reference stress and the primary stress as defined in the ASME Pressure Vessels and Piping code. R-Nodes are load-controlled locations in a mechanical component or a structure. As such r-nodes lie on a distribution of stresses corresponding to primary stress as defined in the ASME code. On account of its load-controlled nature, the "combined r-node equivalent stress" can

be identified with the reference stress, which is widely used in the integrity assessment of components and structures.

The r-node method is also extended for analyzing two-layered beams and two-layered cylindrical shell structures. The proposed methods are applied to a number of pressure component configurations of practical interest. The results in all the cases are compared with those obtained using inelastic finite element analysis and the comparison is found to be good.

The concept of iso r-node stress is introduced in order to minimize the weight of mechanical components and structures. A relationship is established among the proposed minimum-weight method, the theorem of nesting surfaces and the extended variational theorem. The proposed method is applied for minimizing the weight of an indeterminate beam and for designing reinforcement in a spherical pressure vessel with a cylindrical nozzle.

Acknowledgments

The author wishes to thank his supervisor, Dr. R. Seshadri, for his support and guidance, and for the challenging technical discussions during the course of his doctoral program. Despite his heavy responsibilities as the Dean of the Faculty of Engineering and Applied Science, Dr. Seshadri had always been available for discussions, both as a supervisor and also as a well-wisher. Thanks are directed to Dr. A. S. J. Swamidas, Dr. M. R. Haddara, Dr. W. J. D. Shaw, Dr. C. C. Monahan and Dr. C. Daley for their helpful comments. The financial support provided by the Faculty of Engineering and Applied Science, and the School of Graduate Studies, Memorial University of Newfoundland, is gratefully acknowledged. The partial funding provided by the Natural Sciences and Engineering Research Council of Canada is also thankfully acknowledged. Finally, the author would like to acknowledge the inspiration provided by his grand parents Shri. R. Krishnamurthi Aiyer and Shrimathi. K. Gomathi.

Contents

Dedication	i
Abstract	ii
Acknowledgments	iv
Table of Contents	v
List of Figures	xiii
List of Tables	xviii
List of Symbols	xxi
1 Introduction	1
1.1 General Background	1
1.2 Limit Analysis of Mechanical Components and Structures . . .	3
1.3 Need for Robust Techniques in Pressure Component Design . .	4
1.4 Objectives of the thesis	7
1.5 Organization of the Thesis	8

1.6	Original Contributions	11
2	Theoretical Background	14
2.1	Introduction	14
2.2	Elastic Analysis and Plastic Design	16
2.3	Classical Lower and Upper Bound Theorems	20
2.3.1	Statically Admissible Stress Fields	20
2.3.2	Kinematically Admissible Velocity Fields	21
2.3.3	Application of Lower and Upper Bound Theorems - Determination of the Limit Pressure for a Thick-Walled Cylinder	22
2.4	Extended Variational Theorems of Limit Analysis	27
2.5	Evolution of Robust Methods in Pressure Component Design .	34
2.6	Robust Methods of Limit Load Determination	37
2.6.1	Limit Analysis based on Partial Elastic Modulus Mod- ification	37
2.6.2	The R-Node Method	38
2.6.3	The Elastic Compensation Method	43
2.6.4	Strain-Hardening and Strain-Softening: Limit Load Ap- proximations	44
2.7	Reference Stress Method in Pressure Component Design . . .	45
2.8	Theorem of Nesting Surfaces	49
2.9	Closure	52

3	Finite Element Implementation of Modified Elastic Modulus	
	Methods of Limit Analysis	53
3.1	Introduction	53
3.2	Limit Analysis based on Partial Elastic Modulus Modification	55
3.3	The R-Node Method	56
3.4	The Elastic Compensation Method	64
3.5	The Theorem of Nesting Surfaces	65
3.6	The Extended Lower Bound Theorem	66
3.7	Closure	69
4	Improved Lower Bound Limit Load Estimates: The m_α-method	70
4.1	Introduction	70
4.2	Advantages and Limitations of the Existing Robust Limit Analysis Techniques	71
	4.2.1 Classical Limit Theorems	71
	4.2.2 Extended Lower Bound Theorem	76
	4.2.3 Theorem of Nesting Surfaces	78
4.3	Robustness of Structural Behavior during Repeated Elastic Iterations	79
	4.3.1 Class I, II and III Components and Structures	82
4.4	Local Plastic Collapse - Notion of Reference Volume (V_R)	84
4.5	The m_α -method	87
4.6	Illustrative Example - Torispherical Head	92

4.7	Numerical Examples	97
4.7.1	Thick-Walled Cylinder	98
4.7.2	Indeterminate Beam	98
4.7.3	Torispherical Heads	99
4.7.4	Spherical Pressure Vessel with a Cylindrical Nozzle . .	101
4.7.5	Pressure Vessel Support Skirt	104
4.7.6	Non-symmetric Rectangular Plate Structures	106
4.7.7	Cracked Components	109
4.8	Closure	111
5	In Search of the Redistribution Nodes	114
5.1	Introduction	114
5.2	R-Node Peaks and Collapse Mechanism	115
5.3	Virtual R-Node Peaks and Convergence of R-Node Stresses . .	116
5.4	Identification of Real R-Node Peaks	124
5.5	Criteria for Lower-Bound Limit Loads	128
5.6	Illustrative Example - Pressure Vessel Support Skirt	137
5.7	Numerical Examples	140
5.8	Closure	140
6	Limit Loads of Layered Beams and Layered Cylindrical Shells using the R-Node Method	150
6.1	Introduction	150

6.2	Limit Load Estimates of Two-Layered Beams subjected to Uniform Load	151
6.2.1	Elastic Modulus Modification Index based on Deformation Control ($q = 1$)	151
6.2.2	General Elastic Modulus Modification Scheme ($0 \leq q \leq 1$)	157
6.2.3	Numerical Examples	160
6.3	Limit Load Estimates of Two-Layered Axisymmetric Cylindrical Shells under Uniform Internal Pressure	162
6.3.1	Formulations for Layered-Cylinder Problem	162
6.3.2	Numerical Examples	173
6.4	Closure	173
7	Minimum Weight Design of Pressure Components using the Iso R-Node Stress Concept	180
7.1	Introduction	180
7.2	Minimum Weight Design based on the Iso R-Node Stress Concept	181
7.3	Minimum Weight Design - Another Perspective	186
7.4	Step-by-step Procedure for Minimizing the Weight of Structures using the R-Node Method	187
7.5	Numerical Examples	189
7.5.1	Indeterminate Beam subjected to Uniform Load	189

7.5.2	Design of Reinforcement and Nozzle of an Axisymmetric Spherical Pressure Vessel with a Cylindrical Nozzle subjected to Internal Pressure	190
7.6	Closure	202
8	Conceptual Models for Understanding the Role of R-Nodes in Plastic Collapse	203
8.1	Introduction	203
8.2	Idealization of an R-Node	204
8.3	Analogous Systems that Depict Plastic Collapse	204
8.3.1	Thick Cylinder subjected to Uniform Internal Pressure	205
8.3.2	Indeterminate Beam subjected to Uniformly distributed Load	206
8.4	Closure	206
9	Conclusions and Future Research	212
9.1	Conclusions	212
9.2	Future Research	214
	References	215
	Publications during the Course of the Ph.D Program	226
	Appendices	228
A	Fortran Program for determining the R-Node Locations and	

Stresses	228
B Fortran Program for determining the Minimum Weight Ge- ometry of Mechanical Components and Structures	240
C ANSYS Commands Listing of Mechanical Components and Structures	275
C.1 Isotropic Components	275
C.1.1 Linear Elastic Analysis	275
C.1.2 Non-linear Analysis	302
C.2 Two-Layered Beams	305
C.2.1 Linear Elastic Analysis	305
C.2.2 Non-linear Analysis	318
C.3 Two-Layered Cylinder under Uniform Internal Pressure	323
C.3.1 Linear Elastic Analysis	323
C.3.2 Non-linear Analysis	326
D Elastic Moduli Softening Macro for R-Node Analysis	330
D.1 Isotropic Structures and Two-Layered Beams	330
D.2 Two-Layered Cylindrical Shells	335
E Essential Macros for performing a Number of Elastic Itera- tions	340
E.1 First Elastic Iteration - 'iter1'	340
E.2 Second Elastic Iteration - 'iter2'	347

E.3 Macro that Links all the Individual Elastic Iteration Macros - 'repeat'	350
F Input File for determining the Elastic Moduli Ratio for a Two-Layered Cylinder	352
F.1 Axisymmetric Two-Layered Cylinder under Plane-Strain Con- ditions	352

List of Figures

2.1	Uniaxial Stress-Strain Curve	18
2.2	Thick-Walled Cylinder subjected to Uniform Internal Pressure	23
2.3	Comparison of Exact and Lower Bound Limit Loads of a Thick-Walled Cylinder	28
2.4	Follow-up Angle (θ) on the GLOSS Diagram	36
2.5	R-Nodes in a Beam subjected to Bending	40
2.6	Indeterminate Beam subjected to Uniform Load - Collapse Mechanism	42
2.7	Strain-Hardening and Strain-Softening in Mechanical Compo- nents	46
2.8	Nesting Surfaces for a Pin-Jointed Two-Bar Structure	51
3.1	A Square Plate Simply Supported on All Sides under Uniform Pressure	59
3.2	R-Node Stress Surface of the Square Plate Simply Supported on All Sides	60

3.3	Spline Interpolated R-Node Stress Surface of the Square Plate Simply Supported on All Sides	62
3.4	Iso R-Node Stress Contour of the Square Plate Simply Sup- ported on All Sides	63
4.1	Dimensions of a Torispherical Head	73
4.2	Typical Response of Structures to Repeated Elastic Iterations	74
4.3	Total and Reference Volumes	86
4.4	Variation of m^o and m' with Elastic Iterations	88
4.5	Determination of Reference Volume	89
4.6	Leap-frogging of Elastic Iterations to a Limit State	93
4.7	Variation of m^o , m' and m_α with Volume in an Indeterminate Beam	100
4.8	Variation of m^o , m' and m_α with Volume in a Torispherical Head	103
4.9	Dimensions of the Spherical Pressure Vessel with a Cylindrical Nozzle	105
4.10	Pressure Vessel Support Skirt	107
4.11	Non-symmetric Rectangular Plate Structures	108
4.12	Compact Tension Specimen	110
5.1	Indeterminate Beam subjected to Uniform Load - Dimensions and Convergence of Peak R-Node Stresses	117

5.2	Spherical Pressure Vessel with a Cylindrical Nozzle subjected to Uniform Internal Pressure - Dimensions and Plasticity Spread at Collapse	118
5.3	R-Node Diagrams of the Spherical Pressure Vessel with a Cylindrical Nozzle ($q = 1$)	119
5.4	Interpolation Errors while determining R-Nodes - Effect of Stress Distributions	121
5.5	R-Node Diagram of a Torispherical Head subjected to Uniform Internal Pressure ($q = 1$)	122
5.6	R-Node Diagram of a Torispherical Head ($q = 0.25$)	126
5.7	Stress Distribution across the Thickness of an Indeterminate Beam	132
5.8	Influence of q for a Thick-Walled Cylinder analyzed in Section 4.7.1	133
5.9	R-Node Diagram for a Pressure Vessel Support Skirt ($q = 1$) .	138
5.10	R-Node Stress Surface for the Non-Symmetric Plate Structure shown in Figure 4.11a	143
5.11	Spline Interpolated R-Node Stress Surface for the Non-Symmetric Plate Structure shown in Figure 4.11a	144
5.12	Iso R-Node Stress Contour for the Non-Symmetric Plate Structure shown in Figure 4.11a	145
5.13	R-Node Stress Surface for the Non-Symmetric Plate Structure shown in Figure 4.11b	146

5.14	Spline Interpolated R-Node Stress Surface for the Non-Symmetric Plate Structure shown in Figure 4.11b	147
5.15	Iso R-Node Stress Contour for the Non-Symmetric Plate Structure shown in Figure 4.11b	148
5.16	Stress Distributions for a Compact Tension Specimen	149
6.1	Two-Layered Beam under Pure Bending	152
6.2	Relationship between R-Node Stresses and Yield Stresses in a Two-Layered Beam	156
6.3	Dimensions of the Two-Layered Beams Analyzed	161
6.4	Stress Distribution in a Typical Section - Two-Layered Beam subjected to Pure Bending ($t_1 = t_2 = 1.27$ cm., $\psi = 1/3$ and $q = 1$)	163
6.5	Stress Distribution in a Typical Section - Two-Layered Beam subjected to Pure Bending ($t_1 = t_2 = 1.27$ cm., $\psi = 1/3$ and $q = 1$)	164
6.6	R-Node Diagram of a Two-Layered Indeterminate Beam subjected to Uniform Loading ($t_1 = t_2 = 1.27$ cm., $\psi = 1/3$ and $q = 1$)	165
6.7	Two-Layered Cylinder under Internal Pressure	177
6.8	Typical Stress Distributions across a Layered Cylinder - Case No. 1, Configuration 1 ($q = 1$)	178
6.9	Typical Stress Distributions across a Layered Cylinder - Case No. 1, Configuration 2 ($q = 1$)	179

7.1	An Arbitrary Beam of Varying Cross-section - Application of the Iso R-Node Stress Concept	183
7.2	Discretized Indeterminate Beams	191
7.3	Plasticity Spread at Collapse for the Indeterminate Beams	192
7.4	R-Node Diagrams for the Indeterminate Beams	193
7.5	Spherical Pressure Vessel with Equal Nozzle and Shell Thickness	196
7.6	Reinforced Spherical Pressure Vessel	197
7.7	Unreinforced Spherical Pressure Vessel	198
7.8	R-Node Diagrams for the Spherical Pressure Vessels	199
8.1	Idealization of an R-Node	208
8.2	Determination of R-Node in a Thick Cylinder Subjected to Uniform Internal Pressure	209
8.3	Analogous Model for a Thick Cylinder Subjected to Uniform Internal Pressure	210
8.4	Analogous Model for an Indeterminate Beam Subjected to Uniform Loading	211

List of Tables

4.1	Values of Elastic Moduli of Two Elements in a Compact Tension Specimen - Elastic Iteration Number 6 ($q = 1$)	75
4.2	Dimensions of Torispherical Heads	101
4.3	Limit Load Estimates of Torispherical Heads	102
4.4	Configurations of Mechanical Components Analyzed	111
4.5	Limit Load Estimates of Mechanical Components	112
5.1	Maximum Values of Equivalent and R-Node Stresses in a Torispherical Head ($q = 1$)	129
5.2	Maximum Values of Equivalent and R-Node Stresses in a Pressure Vessel Support Skirt ($q = 1$)	130
5.3	Values of $(\sigma_e)_{max}$, m^o and Maximum Stress Location for the Cylinder considered in Figure 5.8	134
5.4	Variation of R-Node Peak Stresses with Elastic Iterations in an Indeterminate Beam	136
5.5	Limit Loads of Torispherical Heads using the R-Node Method	141

5.6	Limit Loads of Mechanical Components using the R-Node Method	142
6.1	Limit Loads for a Two-Layered Beam subjected to Pure Bending ($t_1 = t_2 = 1.27$ cm.)	166
6.2	Limit Loads for a Two-Layered Beam subjected to Pure Bending ($t_1 = 0.846$ cm.; $t_2 = 1.694$ cm.)	167
6.3	Limit Loads for a Two-Layered Simply Supported Beam subjected to Uniform Pressure ($t_1 = t_2 = 1.27$ cm.)	168
6.4	Limit Loads for a Two-Layered Indeterminate Beam subjected to Uniform Pressure ($t_1 = t_2 = 1.27$ cm.)	169
6.5	Limit Load Estimates for a Two-Layered Cylinder - Configuration 1	175
6.6	Limit Load Estimates for a Two-Layered Cylinder - Configuration 2	176
7.1	Comparison of a Uniform Indeterminate Beam with an Optimized Beam	194
7.2	Comparison of Optimized Pressure Vessel Design with Conventional Pressure Vessel Design	195
7.3	Limit Load Estimates based on the R-Node Method - Indeterminate Beam	200
7.4	Limit Load Estimates based on the R-Node Method - Spherical Pressure Vessel with a Cylindrical Nozzle	201

8.1 Correspondence between the Actual Structure and the Analogous System for a Thick Cylinder subjected to Uniform Internal Pressure	207
--	-----

Nomenclature

B, n	creep parameters for second stage power law creep
D	diameter of a torispherical head
E_1, E_2	elastic moduli of a two-layered beam
E_o	original elastic modulus of a mechanical component or structure
E_R, E_s	modified value of elastic modulus of a mechanical component or structure
f_N	normal force
$f(s_{ij}), f(s_{ij}^o)$	von Mises yield function
$F(s_{ij}^o, \sigma^o, m^o, \mu^o, \phi^o)$	functional associated with Mura's formulation
H	height of a torispherical head
i	iteration number corresponding to a set of linear elastic finite element analyses
I_1, I_2	moments of inertia of a two-layered beam
k	yield stress of a material in pure shear; curvature of a beam in bending

L	length of an indeterminate beam
L_s	radius of curvature of the spherical portion in a torispherical head
m	safety factor corresponding to an applied load P
m_{LC}	classical lower bound multiplier corresponding to an applied load, P
m^o	a multiplier based on the average surface of dissipation corresponding to an applied load P
m_R^o	m^o based on the reference volume
m'	lower bound multiplier corresponding to an applied load P
m'_R	m' based on the reference volume
m_α	proposed lower bound multiplier corresponding to an applied load P
M	applied external bending moment in a beam
M_p	plastic moment of the indeterminate beam
N	number of plastic hinges or plastic hinge contours in a mechanical component or a structure at collapse; total number of finite elements
P	applied external load
P_{exact}	limit load determined using closed form solutions (or inelastic finite element analysis)

P_{int}	interface pressure in a two-layered cylinder
P_L	proposed limit load ($= m_\alpha P$)
P_{LC}	classical lower bound limit load
P_{LM}	lower bound limit load based on extended variational method
$(P_L)_{r-node}$	limit load determined using the r-node method
P_{UC}	classical upper bound limit load
q	elastic modulus adjustment index
Q_1, Q_2, \dots	generalized loads applied to a mechanical component or structure
Q_e	effective generalized stress
r	inner radius of the nozzle in a spherical pressure vessel
r_1	inner radius of a two-layered cylinder
r_2	interface radius of a two-layered cylinder
r_3	outer radius of a two-layered cylinder
r_c	radius of the torus in a torispherical head
R	inner radius of the shell in a spherical pressure vessel
\bar{s}_{ij}^σ	statically admissible deviatoric stress field corresponding to the traction P
s_{ij}^σ	statically admissible deviatoric stress field corresponding to the traction $m^\sigma P$
S_m	code allowable stress

S_T	surface area of a structure over which traction is prescribed
SI	von Mises equivalent stress in an element of a discretized structure
t	nozzle thickness of a spherical pressure vessel
t_c	thickness of the cylindrical region of a torispherical head
t_k	thickness of the knuckle region of a torispherical head
t_s	thickness of the spherical region of a torispherical head
t_o	time
T	shell thickness of a spherical pressure vessel
V	volume of a component or a structure
V_R	reference volume of a component or a structure
V_T	total volume of a component or a structure
V_g	partial volume of a component or a structure
Y	ratio of the outer radius to the inner radius for a thick cylinder; yield stress based on Tresca's yield criterion
β	geometric scaling factor that depends on the structure and boundary conditions
γ_1, γ_2	scaling parameters
δ	deflection
δ_{ij}	Kronecker delta
ΔV_i	volume of i th element
$\dot{\epsilon}$	strain rate at reference stress

ϵ^C	creep strain
ζ	linear elastic iteration variable; ratio of the yield stresses in a two-layered beam
ζ_1, ζ_2	interpolation errors pertaining to r-node locations
θ	follow-up angle on the GLOSS diagram
μ	coefficient of friction
μ^o	plastic flow parameter
ν	Poisson's ratio
ϕ^o	a point function defined in conjunction with yield criterion
ξ_1, ξ_2	interpolation errors pertaining to r-node stresses
σ	hydrostatic stress for an actual stress distribution
σ_{arb}	arbitrary stress in the modulus of elasticity softening process
$(\sigma_e)_{r-node}$	r-node equivalent stress
σ_e^o	von Mises equivalent stress evaluated at an element's centroid
σ_M	maximum stress intensity in a component
$(\sigma_e^o)_M, (\sigma_e)_M$	maximum von Mises equivalent stress in a structure for any arbitrary load P for an elastic stress distribution
$\bar{\sigma}_n$	combined r-node stress
σ_{n_j}	r-node peak stress
σ^o	hydrostatic stress for an assumed stress distribution

σ_r	radial stress in a thick cylinder
σ_{ref}	reference stress based on the theorem of nesting surfaces
σ_R	reference stress
σ_y	yield stress
σ'_y	assumed nominal yield stress for analyzing components fabricated out of strain-hardening or strain-softening materials
σ_z	longitudinal stress in a thick cylinder
σ_θ	hoop stress in a thick cylinder
ν	ratio of elastic moduli of a two-layered beam
ω	ratio of the upper and lower bound limit loads

Subscripts

arb	arbitrary
e	von Mises equivalent
i, j	tensorial indices
L	limit
R	reference
y	yield
I, II, \dots	linear elastic analyses I, II etc.

Superscript

o	assumed quantities
-----	--------------------

Acronyms and Abbreviations

ADPL	ANSYS Design Parametric Language ¹
FEA	Finite Element Analysis
GLOSS	Generalized Local Stress Strain
r-node	Redistribution Node

Chapter 1

Introduction

1.1 General Background

The primary objective in designing a mechanical component or a structure is to ensure its ability to perform the intended function at minimum capital and operational cost. Innovation by way of employing advanced analysis techniques, newer materials, sophisticated manufacturing methods and stringent quality control measures are some of the important requirements that are necessary for improving product design and performance. During the conceptual design stage, the designer should take into consideration all the failure modes that the component may possibly encounter during operation. An interesting discussion on the various failure modes and their significance, and the different types of loading conditions is presented by Burgreen.²

While it is important to design components by taking into account all the possible failure modes, it is also necessary, at the same time, to periodically assess the “integrity” of mechanical components and structures. By this

process, an estimate of the remaining life of critical components, especially in power, petroleum and chemical plants can be obtained.

Among the various modes that may govern the failure of a component, plastic collapse is important since it would lead to gross plastic deformation which can be potentially dangerous. Determination of loads which result in cross-sectional plasticity in structures leading to uncontained plastic flow is termed as limit analysis. Limit analysis is important since it provides a measure of the reserve strength that exists in structural members. Also, knowledge of limit load is necessary for estimating the reference stress which is widely used in the integrity assessment of mechanical components.³

Conventionally, limit loads are determined either analytically using the bounding theorems, or numerically by using methods such as inelastic finite element analysis, although efforts are currently being directed towards developing simplified methods.⁴⁻⁶ Analytical methods of limit analysis have evolved over a long period of time as compared to computer-aided numerical techniques, such as inelastic finite element analysis, which are fairly recent. An examination of the literature pertaining to limit analysis reveals that analytical solutions are available for only simple cases of loadings and geometric configurations. Inelastic finite element analysis, on the otherhand, has its own limitations because it requires enormous computational time, is an expensive process and produces a large amount of output data that has to be interpreted properly in order to make practical sense. The above factors thus create a need for the development of robust methods of limit analysis which

are simple, efficient and yet sufficiently accurate. Systematic development of such methods for performing limit analysis is the main aim of this thesis.

1.2 Limit Analysis of Mechanical Components and Structures

The importance of limit analysis in structural design is well documented.⁷⁻¹⁰ It is recognized that structures can withstand loads beyond the elastic limit of structural materials and with plastic design, advantage can be taken of the reserve strength that exists beyond the initial yielding. For statically indeterminate structures, especially those with large redundancies, this reserve strength is significant. Therefore, a knowledge of limit loads of components and structures becomes useful to a designer, since it enables the determination of the reserve strength and also addresses the mode of failure associated with load-controlled effects.

Plastic design not only produces economy in materials but also simplifies the design procedure through the use of the so-called "bounding theorems." Lack of fit in structural connections, residual stresses and other fabrication defects which are difficult to quantify do not affect plastic analysis, whereas it is necessary to take these factors into account when elastic analysis is carried out, thus making the latter more cumbersome. It is therefore more useful to analyze structures that are on the "verge of collapse" and then establish appropriate working levels of applied loads.

Conventionally, the bounding theorems and inelastic finite element analysis are the methods that are adopted for determining limit loads. However, both these methods have their own limitations - the former being intractable and the latter being laborious and expensive.

The above mentioned factors have provided sufficient motivation to direct efforts towards developing simpler and more general techniques that are capable of providing acceptable results based on minimum input and cost, using linear elastic analyses. In this thesis, robust methods for estimating lower and upper bound limit loads are developed. The methods proposed are based on linear elastic analyses and are intended to be generic in nature. The material properties are assumed to be elastic perfectly-plastic and components are considered to be subjected to “sustained loads”, i.e., non-cyclic loads that do not diminish because of structural deformation.

1.3 Need for Robust Techniques in Pressure Component Design

In the design of pressure vessels by analysis, finite element analysis is usually coupled with the use of appropriate rules contained in pressure vessel codes such as the ASME Pressure Vessel and Boiler Code Sections III and VIII (Division 2).¹¹ The stresses obtained from linear elastic finite element runs are partitioned into primary, secondary and peak stress categories in order to apply appropriate stress limits. Each of these stress categories is associated with distinct type of failure mechanisms such as gross distortion,

ratchetting and fatigue, respectively. The stress categorization procedure, however, becomes tedious when continuum results given by 2-D and 3-D finite element analysis are considered.

In order to avoid the complexity of the stress categorization procedures, the ASME code does, however, allow the designer to perform an elastic-plastic or limit analysis of the component in order to arrive at allowable loads. Plastic analysis, unlike elastic analysis, takes into account the stress redistribution upon yield. For a component that fails by gross distortion due to a single application of the load, a plastic analysis is the one that would give the design pressure sought by the analyst. Design pressures that are calculated by any other method are acceptable only as long as it is possible to prove that the estimates obtained do not exceed those obtained on the basis of plastic analysis.¹² This additional requirement is hard to be satisfied by design based on elastic analysis procedures for complex structures with limited amount of inelastic or limit design data.

An investigation into the literature pertaining to limit analysis reveals that a considerable amount of effort has been expended towards the analytical determination of limit loads of pressure components. The bounding methods for determining limit loads may turn out to be mathematically intractable with increasing complexity for problems such as oblique nozzle-shell intersections, and component configurations with non-symmetric loading and boundary conditions. Moreover, the accuracy of the method is affected by the underlying simplifying assumptions.

With the advent of high speed computers and the development of the finite element technique, inelastic finite element analysis (FEA) has emerged as a versatile tool for carrying out elastic-plastic analysis. Several commercial packages^{1,13} are available for performing inelastic FEA. The method is general and could be applied to a variety of engineering problems. A variety of element types and solid modeling techniques enable the simulation of field problems to a reasonable degree of accuracy.

Nevertheless, inelastic finite element analysis also has some inherent drawbacks as mentioned in the previous section. Apart from the method being elaborate and time consuming, the merit of applying a detailed nonlinear analysis for a given component is often questionable due to convergence problems and the requirement of enormous computer memory. The limit load values obtained by nonlinear finite element analysis, although accepted to be by far the most accurate, involves a higher cost per run. Therefore, a detailed nonlinear analysis may not be a viable alternative in situations where results acceptable for practical purposes are all that is needed in a stipulated time frame. This clearly shows the necessity for developing robust approximate techniques, which are simple, reliable methods based on linear elastic analysis and are capable of predicting inelastic response with acceptable accuracy. The reduced modulus methods are the robust techniques that are of interest in this thesis.

Robustness, in the present context, implies the ability to provide acceptable results on the basis of less than reliable input, together with conceptual

insight and economy of computational effort.¹⁴

The major application areas of robust methods are:

1. Initial scoping and feasibility study,
2. Screening of critical areas in large complex systems for further detailed analyses,
3. "Sanity" checks on the results obtained by non-linear analysis and
4. Approximate estimates of inelastic effects.

Robust methods are ideally suited for performing a preliminary analysis or design of components so that the feasibility of a specified system can be assessed. These methods can also be used for identifying critical locations in complex systems which can be the source of potential problems. Robust methods are sometimes the only recourse for an independent verification of the results of a detailed nonlinear analysis of a complex problem. While it is recognized that the conventional methods for the structures analyzed in this thesis provide reasonable results, it is imperative to note that robust methods are simple, inexpensive and pragmatic alternatives.

1.4 Objectives of the thesis

The objectives of this thesis are to:

1. Propose simple and systematic procedures for determining the limit loads of mechanical components and structures using linear elastic anal-

yses.

2. Investigate the conceptual basis and the functioning of the r-nodes in depth, and propose the necessary guidelines for determining lower bound limit loads.
3. Develop a procedure for reducing the stress concentration in pressure components on the basis of the iso r-node stress concept.
4. Apply the proposed methods to a variety of pressure component configurations and validate the methods by comparing with results obtained using conventional techniques.

1.5 Organization of the Thesis

Chapter 1 addresses the importance of limit analysis. The limitations of the existing methods are analyzed and the need for robust methods of limit analysis is brought out. The objectives and the organization of the thesis are also presented in this chapter. The chapter ends by providing a list of original contributions.

The theoretical aspects pertaining to the research reported in this thesis are explained in Chapter 2. The advantages of plastic design as compared to elastic design are discussed and the usefulness of the upper and lower bound limit loads are explained in this chapter. The extended variational theorem proposed by Mura and co-workers¹⁵ is introduced and the underlying formulations are reconstructed. Evolution of robust methods in pressure

component design is examined and the metamorphosis of these methods into limit analysis techniques is explored. The r-node and the elastic compensation methods of limit load determination are reviewed. The reference stress method in pressure component design is introduced and the relationship between reference stress and limit load is highlighted.

Chapter 3 deals with the finite element implementation of the existing robust limit analysis techniques based on linear elastic finite element analyses. The variational formulation proposed by Mura et al.^{15,16} is implemented and the method is rendered suitable for directly obtaining lower bound limit loads for generic structures using linear elastic finite element analyses stress distributions. The “theorem of nesting surfaces” proposed by Calladine and Drucker^{17,18} is also introduced as a direct way of determining the reference stress using elastic stress distributions. A relationship between the integral mean of the yield¹⁶ and the reference stress obtained by invoking the theorem of nesting surfaces is also identified.

In Chapter 4, the underlying problems in carrying out a number of elastic iterations are investigated and components are classified into three types based on their response to elastic iterations. The advantages and disadvantages of conventional limit analysis techniques are discussed from an engineering standpoint. An improved method, named the m_α -method, for determining lower bound limit loads is proposed in this chapter on the basis of the extended lower bound theorem, and uses the concept of “leap-frogging” to a near limit state and the notion of reference volume. The proposed method is

based on two linear elastic finite element analyses. The chapter is concluded by determining the limit loads of a number of pressure component configurations of practical significance and comparing the results with the existing ones.

One of the essential requirements while determining limit loads using the r-node method lies in the identification of valid r-node peaks. The procedure for identifying and eliminating virtual r-node peaks is explained and guidelines are provided for identifying valid r-node peaks in Chapter 5. The r-nodes are investigated in depth in this chapter and aspects pertaining to convergence of r-nodes are addressed. Requirements for obtaining lower bound limit loads are provided and limit loads are determined for the components considered in Chapter 4.

In Chapter 6, limit analysis of layered beams and layered cylindrical shells are discussed. While the formulations for the beam problems are based on the theory of bending, the theorem of nesting surfaces is invoked in order to determine the r-nodes in cylindrical shells.

Minimum weight design is important in engineering since a substantial amount of savings is possible by way of better utilization of material. Furthermore, such a design would help in minimizing stress concentrations and improving fatigue life. Chapter 7 utilizes the iso r-node concept for minimizing the weight of pressure components. Numerical examples are also illustrated in this chapter in order to demonstrate the applicability of the method.

Chapter 9 summarizes the advantages of the proposed methods. Suggestions are also provided for carrying out future work along the lines of this thesis.

The appendices contain the programs and ANSYS¹ macros that are necessary for solving the numerical examples. The Fortran programs in Appendices A and B are used for determining the r-nodes and for minimizing the weight of components, respectively. Appendix C contains the ANSYS listings for the numerical examples. The ANSYS macros, written using ADPL¹ (ANSYS DESIGN PARAMETRIC LANGUAGE) for carrying out the elastic moduli modification, are given in Appendix D. Appendix E provides the necessary macros for performing a number of elastic iterations. The Maple¹⁹ listing that is necessary for implementing the formulations for the two-layered cylinder is given in Appendix F.

1.6 Original Contributions

The following are the original contributions of this thesis:

- The extended variational theorem proposed by Mura et al.¹⁶ has been implemented so that stress distributions obtained from linear elastic finite element analyses could be directly used for estimating lower and upper bound limit loads.
- A relationship is identified between the integral mean criterion proposed by Mura et al. and the theorem of nesting surfaces.

- The underlying problems behind carrying out a number of elastic iterations are explored in this thesis and on this basis, mechanical components and structures are classified into three distinct categories depending on their response to elastic moduli changes. Methods are also proposed to overcome the stability related problems in carrying out repeated elastic iterations.
- The concept of reference volume is introduced in an attempt to isolate regions in structures that most likely do not participate in plastic collapse. Using this, a procedure for determining upper bound limit loads on the basis of the integral mean of the yield and the theorem of nesting surfaces is proposed.
- A method, designated as the m_α -method, is proposed for determining the lower bound limit loads of mechanical components. The method utilizes the concept of leap-frogging to a near limit state and the notion of reference volume, in order to obtain improved lower bound limit loads on the basis of two linear elastic analyses.
- The properties of r-nodes are investigated in detail and aspects pertaining to lower bound limit loads are discussed. Guidelines are also provided for determining the valid r-node peaks that are responsible for collapse.
- An r-node is idealized as a mechanical model. Based on this idealization, simple conceptual models that depict the stress redistribution

during collapse are proposed.

- Procedures for determining the limit loads of two-layered beams and two-layered axisymmetric cylindrical shell structures using r-nodes are proposed.
- The concept of iso r-nodes is proposed for determining the minimum weight of mechanical components and structures and for designing nozzle reinforcements.
- A number of numerical examples of varying complexity are worked out and the results are compared with conventional analyses techniques. It is demonstrated that the proposed methods are robust in nature and can be used for analyzing complex problems with minimum effort and resources.

Chapter 2

Theoretical Background

2.1 Introduction

Theoretical aspects germane to the forthcoming chapters of this thesis are presented here. In the era prior to the introduction of finite element analysis, robust approximations were commonplace in analysis and design methodologies. It was considered sufficient for all practical purposes to estimate load bearing capacity of engineered structures that were below the actual value. Obtaining a lower bound estimate of limit loads was seen by designers as a pragmatic way of ensuring safe designs. However, when estimating power requirements for metal cutting, for instance, the upper bound values of loads were considered to be appropriate. Conservative estimates of load were determined by invoking the upper bound theorem. The classical lower and upper bound theorems of plasticity still play an important role in engineering design although today's powerful computational tools can be used to great effect.

Alternate formulations to the lower and upper bound theorems that were based on variational concepts were proposed by Mura et al.^{15,16} By making use of “statically admissible” stress distributions and “kinematically admissible” strain distributions and invoking the notion of integral mean of yield, pseudoelastic distributions of stresses that exceed yield were utilized for determining upper and lower bound limit loads.

Mura et al.¹⁶ applied their variational method for determining the upper and lower bound limit loads of a uniaxial specimen. Their results compared well with the results obtained using the classical theorems of limit analysis. In this thesis the Mura’s lower bound theorem is implemented for directly using the stress distributions obtained from finite element analysis, for a generic structure. It is also shown that an upper bound multiplier can be obtained from stress distributions that satisfy the integral mean of the yield condition.

Calladine and Drucker¹⁷ proposed the “theorem of nesting surfaces” and obtained an expression for the reference stress by making use of a stress-strain relationship of the type $\epsilon = B\sigma^n$ and the concept of average dissipation. They demonstrated that the reference stress so obtained is strictly monotonic, and increases with the exponent n . It is bounded by the result for $n = 1$ (elastic material) and above by the limiting functional as $n \rightarrow \infty$ (perfectly-plastic).¹⁸ The reference stress obtained using the theorem of nesting surfaces could also be used for approximate estimation of limit loads, though it would be shown in this chapter that such estimates are unconservative in nature.

Despite the availability of various theories and advances in high speed computing for limit load determination, the application of conventional analysis methods such as bounding theorems and inelastic finite element analyses have proved to be elaborate, expensive and time-consuming. For instance, a recent paper by Berak and Gerdeen²⁰ proposed an effective technique using finite element analysis for simple two-dimensional problems and summarized that "...this procedure is particularly applicable to the solution of complex problems using parallel processing on a supercomputer." This clearly demonstrates the need for developing simplified methods if one is to take full advantage of the benefits of inelastic effects without a great deal of effort. Therefore, development of robust simplified methods of limit analyses that give acceptable results at minimum time and cost become useful during the initial stages of the design process. The modulus adjustment method, originally developed in order to assess inelastic effects such as follow-up in mechanical components and structures, was the pioneering work in this direction.^{21,22} Subsequent efforts by Marriott,⁴ Seshadri⁵ and Mackenzie et al.⁶ have led to the development of robust methods for estimating limit loads on the basis of linear elastic finite element analyses.

2.2 Elastic Analysis and Plastic Design

To carry out a complete stress analysis of mechanical components or structures, it is necessary to satisfy the equilibrium equations and the traction boundary conditions. Next, the strain displacement or geometric compati-

bility conditions and the kinematic boundary conditions should be satisfied. Finally, the stresses must be related to the strains by appropriate constitutive relations.

Both the equilibrium equations and strain-displacement relations are independent of the material under consideration. While the equilibrium equation is an expression of a physical law, the compatibility relations are geometric descriptions that express the aspect of continuity of the structure. Irrespective of whether the behavior of the structure is linear or non-linear, these conditions are valid. The difference between an elastic and an inelastic problem is therefore the constitutive equations. While this relationship is linear in the elastic range, it will generally be non-linear in the plastic range. This aspect can be understood by examining the uniaxial stress-strain curve illustrated in Figure 2.1.

In the elastic range the strains are uniquely determined by the state of stress regardless of how this stress state was reached. In the plastic range, however, the strains are in general not uniquely determined by the stresses but rather by the history of loading or in other words how the stress state was reached.

The elastic stress-strain relationship is given by

$$\epsilon_{ij} = \frac{1+\nu}{E}\tau_{ij} - \frac{\nu}{E}\tau_{kk}\delta_{ij} \quad (2.1)$$

where ϵ_{ij} is the strain, τ_{ij} is the stress, E is the Young's modulus, ν is the Poisson's ratio and δ_{ij} is the Kronecker's delta.

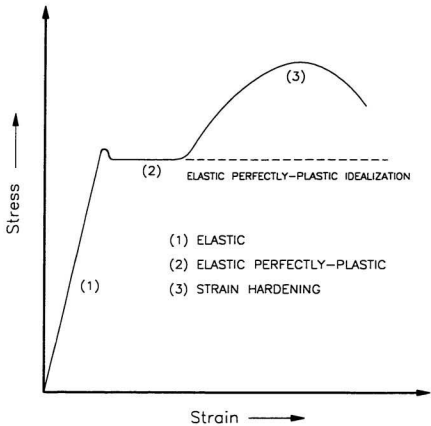


Figure 2.1: Uniaxial Stress-Strain Curve

The plastic stress-strain relationship considers the plastic strain increment which, at any instant of loading, is proportional to the instantaneous stress deviation, i.e.,

$$d\epsilon_{ij}^p = s_{ij} d\lambda. \quad (2.2)$$

In this equation, s_{ij} is the stress deviator tensor and $d\lambda$ is a non-negative constant which might vary throughout the loading history and is determined from the yield criterion. The above equation is called the "Prandtl-Reuss" equation.

Structures designed using the theory of elasticity are usually based on the allowable stress concept. The structure is designed so that the maximum stress as calculated for certain specified conditions of service is less than a stipulated value of stress defined as the "allowable stress." The margin between the allowable stress and the ultimate stress may be reduced in proportion to the certainty of the service conditions, intrinsic reliability of the material and the accuracy of the stress analysis etc..²³

The allowable stress is usually based on the yield stress. The design stress is a fraction of the allowable stress. Design of the structure is carried out so that the maximum stress can be no more than the stipulated allowable stress.

It is apparent, however, that the important consideration in an engineering structure is not whether the yield stress has been exceeded at some point, but whether the structure as a whole can carry out the intended function. There is no reason not to allow some parts of the structure to exceed yield

as long as there is adequate reserve strength in the entire structure. In many practical component configurations, local plastic flow will occur at stress raisers and at locations of discontinuity in the geometry. Residual stresses, while affecting partially plastic behavior of a structure, do not affect the plastic collapse load. Consequently, it makes sense to design a structure based on the limiting load at which it will collapse (uncontained plastic flow occurs).

The limit load can be used as a realistic basis for assessing the permissible working load on a structure through the use of a factor of safety. Different types of failures such as fatigue, fracture, or buckling may govern the design. In some cases the magnitude of deflection (elastic or plastic) is itself a criterion, rather than the imminence of plastic collapse. Avoidance of failure by plastic collapse is the governing criterion in the design of many structures, and the development of efficient methods for computing the collapse load has in recent years been of immense interest to engineers.²⁴

2.3 Classical Lower and Upper Bound Theorems

2.3.1 Statically Admissible Stress Fields

A stress field Q_1, Q_2, \dots, Q_n defined throughout a continuum is called statically admissible for the given loads if, in addition to satisfying the yield conditions, it represents a state of equilibrium under the given loads. Such a field is safe if at each point of the field, the state of stress is represented by

a point inside the yield surface.

The lower bound theorem states that, if any stress distribution throughout the structure can be found which is everywhere in equilibrium internally and balances certain external loads and at the same time does not violate the yield condition, those loads will be carried safely by the structure.²⁵ The limit load evaluated using this theorem is lower than the exact value of the limit load and therefore can be used for designing mechanical components that are safe against collapse.

2.3.2 Kinematically Admissible Velocity Fields

A strain rate field $\dot{q}_1, \dot{q}_2, \dots, \dot{q}_n$ defined throughout a continuum is called kinematically admissible for the given conditions of support, if it is derived from a velocity field which is compatible with the conditions of support and certain continuity conditions. Such a strain field is unsafe for the given loads, if the total rate of energy dissipated is less than the rate at which the given loads do work on the generating velocities.⁹

The upper bound theorem states that, if an estimate of the plastic collapse load of a structure is made by equating the internal rate of dissipation of energy to the rate at which the external forces do work in any postulated mechanism of deformation of the body, the estimate will be either correct, or high.²⁵ In processes such as metal forming and metal cutting, it is necessary to determine the load that is capable of performing the given operation. Determination of limit loads using the upper bound theorem ensures that

the limit load estimates obtained can cause “plastic flow” in the component.

2.3.3 Application of Lower and Upper Bound Theorems - Determination of the Limit Pressure for a Thick-Walled Cylinder

2.3.3.1 Lower Bound Limit Pressure

The lower bound theorem can be illustrated by considering the problem of limit load determination of a thick-walled cylinder (Figure 2.2) subjected to uniform internal pressure.

The equilibrium equation for the thick-walled cylinder can be expressed as:

$$\frac{d\sigma_r}{dr} = \frac{\sigma_\theta - \sigma_r}{r} \quad (2.3)$$

where σ_r and σ_θ are respectively the radial and hoop stresses and r is the radius.

The yield condition is assumed to be governed by the Tresca's yield criterion, which is given by

$$|\sigma_r - \sigma_\theta| = Y. \quad (2.4)$$

Since the equilibrium conditions hold good even at impending plastic collapse, equation (2.4) can be substituted into equation (2.3) resulting in

$$\frac{d\sigma_r}{dr} - \frac{Y}{r} = 0, \quad (2.5)$$

which on integrating leads to

$$\sigma_r = Y \ln r + C. \quad (2.6)$$

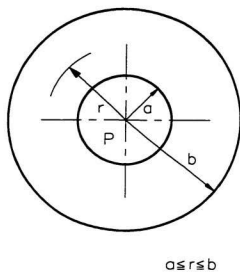


Figure 2.2: Thick-Walled Cylinder subjected to Uniform Internal Pressure

where C is an arbitrary constant of integration.

The boundary conditions can be expressed as:

$$\left. \begin{aligned} \sigma_r &= -P & \text{at } r &= a \\ \sigma_r &= 0 & \text{at } r &= b \end{aligned} \right\} \quad (2.7)$$

where a and b are the inside and outside radii of the cylinder respectively and P is the internal pressure.

Assuming the cylinder to be completely plastic at collapse and applying equations (2.7) on equation (2.6),

$$\left. \begin{aligned} Y \ln a + C &= -P_{LC} \\ Y \ln b + C &= 0 \end{aligned} \right\} \quad (2.8)$$

from which the limit pressure can be obtained as

$$P_{LC} = Y \ln \frac{b}{a}. \quad (2.9)$$

Alternately, in situations where such direct integration of the equilibrium equation as in equation (2.5) is not possible, it becomes necessary to assume some statically admissible stress distribution and proceed with the lower bound limit load calculations. The closer the assumed stress distribution is to the limit type, the more accurate would be the solution.

For the problem under consideration, a linear radial stress field can be assumed as

$$\sigma_r = Ar + B \quad (2.10)$$

Substituting the boundary conditions given by equation (2.7) in equation (2.10) the radial stress can be expressed as:

$$\sigma_r = -P(b-r)/(b-a) \quad a \leq r \leq b. \quad (2.11)$$

The limit pressure can be derived from equations (2.3) and (2.11) as

$$\sigma_\theta - \sigma_r = Pr/(b - a). \quad (2.12)$$

Clearly $|\sigma_\theta - \sigma_r|$ has its greatest value at $r = b$, so for the yield condition not to be violated anywhere, but just to be reached at $r = b$, the lower bound limit pressure can be determined as:

$$P_{LC} = Y(1 - a/b). \quad (2.13)$$

2.3.3.2 Upper Bound Limit Pressure

An upper bound limit load can be determined by considering any kinematically admissible velocity field, say, in this case based on the incompressibility condition, i.e.,

$$\epsilon_r + \epsilon_\theta + \epsilon_z = 0 \quad (2.14)$$

where ϵ_r , ϵ_θ and ϵ_z are the radial, hoop and the axial strains, respectively.

For a plane strain condition, equation (2.14) reduces to

$$\epsilon_r + \epsilon_\theta = 0. \quad (2.15)$$

The strains can be expressed in terms of the radial displacement field $u(r)$ as:

$$\epsilon_r = \frac{du}{dr} \quad ; \quad \epsilon_\theta = \frac{u}{r}. \quad (2.16)$$

Equations (2.15) and (2.16) lead to the expression:

$$\frac{du}{dr} + \frac{u}{r} = 0 \quad (2.17)$$

which on integrating becomes

$$\ln r = -\ln u + \ln C \quad (2.18)$$

or

$$u = \frac{C}{r}. \quad (2.19)$$

The arbitrary constant C can be determined by substituting the condition, at $r = a$, $u = u_a$, which leads to

$$u = \frac{u_a a}{r}. \quad (2.20)$$

Therefore, the strain field is given by

$$\epsilon_r = -\frac{u_a a}{r^2} \quad \text{and} \quad \epsilon_\theta = \frac{u_a a}{r^2}. \quad (2.21)$$

The internal energy dissipation per unit volume can be expressed as

$$\begin{aligned} D &= \epsilon_\theta \sigma_\theta + \epsilon_r \sigma_r \\ &= \frac{u_a a}{r^2} (\sigma_\theta - \sigma_r) \\ &= \frac{u_a a}{r^2} Y \quad \text{at yield.} \end{aligned} \quad (2.22)$$

The internal dissipation per unit length of the cylinder is given by

$$W_{\text{int}} = \int_a^b D 2\pi r \, dr = 2\pi a Y u_a \ln \frac{b}{a}. \quad (2.23)$$

The external work done per unit length of the cylinder is

$$W_{\text{ext}} = 2\pi a P_i u_a. \quad (2.24)$$

Equating the internal dissipation of energy to the external work, the upper bound limit pressure can be obtained as

$$P_{UC} = Y \ln \frac{b}{a} \quad (2.25)$$

which in this case is the same as the equilibrium solution given by equation (2.9). Therefore it is evident that the limit load obtained is exact. That the value of limit pressure given by equation (2.13) is less than that given by the exact solution [equation (2.9)] for $b > a$ is shown in Figure 2.3.

2.4 Extended Variational Theorems of Limit Analysis

Mura and Lee¹⁵ have demonstrated by means of the variational principle that the safety factor, the kinematically admissible multiplier and the statically admissible multiplier for a component or structure made out of a perfectly plastic material, and subjected to prescribed surface tractions are actually extremum values of the same functional under different constraint conditions.

In lower bound limit analysis, the statically admissible stress field cannot lie outside of the hypersurface of the yield criterion. Mura et al.¹⁶ showed that such a requirement can be eliminated if the integral mean of the yield criterion is used. They showed that the safety factor, m , can be obtained by rendering the following functional, F , stationary, i.e.,¹⁵

$$F[v_i, s_{ij}, \sigma, R_i, m, \mu, \phi] = \int_V s_{ij} \frac{1}{2} (v_{i,j} + v_{j,i}) dV + \int_V \sigma \delta_{ij} v_{i,j} dV$$

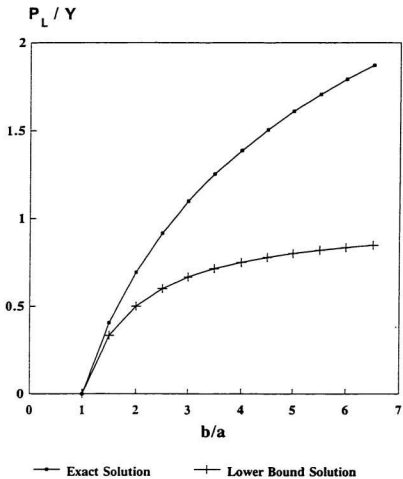


Figure 2.3: Comparison of Exact and Lower Bound Limit Loads of a Thick-Walled Cylinder

$$\begin{aligned}
& - \int_V R_i v_i dS - m \left(\int_{S_T} T_i v_i dS - 1 \right) \\
& - \int_V \mu [f(s_{ij}) + \phi^2] dV \quad (2.26)
\end{aligned}$$

with $\mu \geq 0$.

In the above equation, v_i is the velocity, s_{ij} is the deviatoric stress, and σ , R_i , m , μ and ϕ are the Lagrangian multipliers. The yield criterion is given by

$$f(s_{ij}) = \frac{1}{2} s_{ij} s_{ij} - k^2. \quad (2.27)$$

The total surface, S , of the structure is divided into S_T , where the traction is prescribed and S_V , where the velocity is prescribed.

Taking the variation of F leads to

$$\begin{aligned}
\delta F = & \int_V \delta s_{ij} \frac{1}{2} (v_{i,j} + v_{j,i}) dV + \int_V s_{ij} \frac{1}{2} (\delta v_{i,j} + \delta v_{j,i}) dV \\
& + \int_V \delta \sigma \delta_{ij} v_{i,j} dV + \int_V \sigma \delta_{ij} \delta v_{i,j} dV - \int_{S_V} \delta R_i v_i dS - \int_{S_V} R_i \delta v_i dS \\
& - \delta m \left(\int_{S_T} T_i v_i dS - 1 \right) - m \int_{S_T} T_i \delta v_i dS - \int_V \delta \mu [f(s_{ij}) + \phi^2] dV \\
& - \int_V \mu \frac{\partial f}{\partial s_{ij}} \delta s_{ij} dV - \int_V \mu 2\phi \delta \phi dV. \quad (2.28)
\end{aligned}$$

Integrating the above equation by parts gives the natural conditions

$$\frac{1}{2} (v_{i,j} + v_{j,i}) = \mu \frac{\partial f}{\partial s_{ij}} \quad \text{in } V, \quad (2.29)$$

$$\mu \geq 0, \quad \text{in } V, \quad (2.30)$$

$$(s_{ij} + \delta_{ij} \sigma)_{,j} = 0 \quad \text{in } V, \quad (2.31)$$

$$(s_{ij} + \delta_{ij} \sigma) n_j = m T_i \quad \text{on } S_T \quad (2.32)$$

$$(s_{ij} + \delta_{ij} \sigma) n_j = R_i \quad \text{on } S_V, \quad (2.33)$$

$$f(s_{ij}) + \phi^2 = 0 \text{ in } V, \quad (2.34)$$

$$\mu\phi = 0 \text{ in } V, \quad (2.35)$$

$$\delta_{ij}v_{i,j} = 0 \text{ in } V, \quad (2.36)$$

$$v_i = 0 \text{ on } S_V, \quad (2.37)$$

$$\int_{S_T} T_i v_i dS = 1. \quad (2.38)$$

Equation (2.29) is the plastic potential flow, equations (2.31) to (2.33) are the equilibrium conditions, and equations (2.36) to (2.38) define a kinematically admissible velocity field. Equations (2.34) and (2.35) define the admissible domain of the stress space, i.e.,

$$f(s_{ij}) = 0 \text{ if } \mu > 0 \quad (2.39)$$

$$f(s_{ij}) \leq 0 \text{ if } \mu = 0 \quad (2.40)$$

Obviously, equations (2.29) to (2.38) are the conditions for incipient plastic flow. Condition (2.33) can be used to determine R_i , the reaction at the boundary, which is arbitrary. Condition (2.38) is no more restrictive than the requirement

$$\int_{S_T} T_i v_i dS > 0. \quad (2.41)$$

Setting the integral equal to unity only determines the otherwise arbitrary size of the velocity vector.

Considering the arbitrary arguments

$$v_i^o = v_i + \delta v_i, \quad s_{ij}^o = s_{ij} + \delta s_{ij}, \dots \quad (2.42)$$

in which v_i, s_{ij}, \dots denote the stationary set of arguments of equation (2.26) and $\delta v_i, \delta s_{ij}, \dots$ etc. are the corresponding variations. If the arguments of equation (2.26) are substituted by equation (2.42), taking into account the conditions specified by equations (2.29) to (2.38) for v_{ij}, s_{ij} , etc., F can be written as

$$\begin{aligned} F[v_i^o, s_{ij}^o, \sigma^o, R_i^o, m^o, \mu^o, \phi^o] &= m + \int_V \delta s_{ij} \frac{1}{2} (\delta v_{i,j} + \delta v_{j,i}) dV \\ &\quad + \int_V \delta \sigma \delta_{ij} \delta v_{i,j} dV - \int_{S_V} \delta R_i \delta v_i dS - \delta m \int_{S_T} T_i \delta v_i dS \\ &\quad - \int_V \mu \left\{ \frac{1}{2} \delta s_{ij} \delta s_{ij} + (\delta \phi)^2 \right\} dV - \int_V \delta \mu \left\{ f(s_{ij}^o) + (\phi^o)^2 \right\} dV. \end{aligned} \quad (2.43)$$

Making use of the boundary conditions given by equations (2.31), (2.32), (2.33), the requirements for a statically admissible stress field, viz.,

$$(s_{ij}^o + \delta_{ij} \sigma^o)_j = 0 \quad \text{in } V, \quad (2.44)$$

$$(s_{ij}^o + \delta_{ij} \sigma^o) n_j = m^o T_i \quad \text{on } S_T, \quad (2.45)$$

and stipulating

$$(s_{ij}^o + \delta_{ij} \sigma^o) n_j = R_i^o \quad \text{on } S_V, \quad (2.46)$$

equation (2.26) can be rewritten as

$$F = m - \int_V \mu \left\{ \frac{1}{2} \delta s_{ij} \delta s_{ij} + (\delta \phi)^2 \right\} dV - \int_V \delta \mu \left\{ f(s_{ij}^o) + (\phi^o)^2 \right\} dV. \quad (2.47)$$

In equation (2.46), R_i^o denotes the reaction of the stress field on S_V . Also, integrating equation (2.26) with arbitrary arguments $v_i^o, s_{ij}^o, \sigma^o, R_i^o, m^o, \mu^o$ and ϕ^o and constraint conditions given by equations (2.44), (2.45) and (2.46),

the following expression can be obtained:

$$F = m^o - \int_V \mu^o \{f(s_{ij}^o) + (\phi^o)^2\} dV. \quad (2.48)$$

The integral mean of yield can be expressed as

$$\int_V \mu^o \{f(s_{ij}^o) + (\phi^o)^2\} dV = 0 \quad (2.49)$$

where

$$\mu^o \geq 0. \quad (2.50)$$

Substituting equation (2.49) in equation (2.48) results in

$$F = m^o. \quad (2.51)$$

Since $\mu^o = \mu + \delta\mu$, equation (2.49) can be written as

$$- \int_V \delta\mu \{f(s_{ij}^o) + (\phi^o)^2\} dV = \int_V \mu \{f(s_{ij}^o) + (\phi^o)^2\} dV. \quad (2.52)$$

Equation (2.52) can be substituted in equation (2.47) which can be rewritten as

$$F = m - \int_V \mu \left\{ \frac{1}{2} \delta s_{ij} \delta s_{ij} + (\delta\phi)^2 \right\} dV + \int_V \mu \{f(s_{ij}^o) + (\phi^o)^2\} dV. \quad (2.53)$$

Since the second term on the right hand side of equation (2.53) is always a positive quantity, equations (2.51) and (2.53) can be related by an inequality as

$$\begin{aligned} m^o &\leq m + \int_V \mu \{f(s_{ij}^o) + (\phi^o)^2\} dV \\ &\leq m + \max \{f(s_{ij}^o) + (\phi^o)^2\} \int_V \mu dV. \end{aligned} \quad (2.54)$$

where $\max\{f(s_{ij}^\circ) + (\phi^\circ)^2\} \geq 0$ because of conditions (2.49) and (2.50).

The safety factor which can be expressed as

$$\begin{aligned} m &= m \int_{S_T} T_i v_i dS = \int_S (s_{ij} + \delta_{ij} \sigma) n_j v_i dS \\ &= \int_V (s_{ij} + \delta_{ij} \sigma) v_{i,j} dV + \int_V (s_{ij} + \delta_{ij} \sigma) v_{i,j} dV \\ &= \int_V s_{ij} \frac{1}{2} (v_{i,j} + v_{j,i}) dV = \int_V s_{ij} \mu s_{ij} dV = 2k^2 \int_V \mu dV, \end{aligned}$$

can be rearranged as

$$\int_V \mu dV = m/2k^2. \quad (2.55)$$

From equations (2.54) and (2.55) the expression for the lower bound multiplier (m') for the safety factor (m) can be obtained as

$$m' = \frac{m^\circ}{1 + \max\{f(s_{ij}^\circ) + (\phi^\circ)^2\}/2k^2} \leq m \quad (2.56)$$

which holds for any set of s_{ij}° , σ° , m° , μ° and ϕ° satisfying

$$(s_{ij}^\circ + \delta_{ij} \sigma^\circ)_{,j} = 0 \quad \text{in } V, \quad (2.57)$$

$$(s_{ij}^\circ + \delta_{ij} \sigma^\circ) n_j = m^\circ T_i \quad \text{on } S_T, \quad (2.58)$$

$$\int_V \mu^\circ \{f(s_{ij}^\circ) + (\phi^\circ)^2\} dV = 0, \quad (2.59)$$

$$\mu^\circ \geq 0. \quad (2.60)$$

Equation (2.56) includes the classical definition of the lower bound, as is seen by taking equation (2.49) in the special form

$$f(s_{ij}^\circ) + (\phi^\circ)^2 = 0. \quad (2.61)$$

In this case, $\max\{f(s_{ij}^\circ)\}$ vanishes and equation (2.56) reduces to

$$m^\circ \leq m. \quad (2.62)$$

2.5 Evolution of Robust Methods in Pressure Component Design

The use of simplified methods for pressure component design started with the development of reduced modulus procedures for assessing inelastic effects in pressure components. The reduced modulus method was first introduced by Jones and Dhalla in 1981 as a robust procedure for classifying local clamp induced stresses in Liquid Metal Fast Breeder Reactors.^{21,22} They argued that clamp induced stresses could be categorized as secondary by showing that they redistribute on account of material or geometric non-linearity. By systematically reducing the elastic modulus, the inelastic response of this problem was investigated. It was found that the reduced modulus approach satisfactorily simulated the inelastic response.

By performing repeated elastic analyses and by judiciously modifying the elastic modulus at every stage, Dhalla²⁶ and Severud²⁷ analyzed the inelastic response and follow-up characteristics of piping systems.

Thus having understood that it is possible to use linear elastic analyses for simulating inelastic effects, efforts were directed towards developing procedures for categorizing stresses.²⁸ Subsequently, Marriott⁴ proposed a reduced elastic modulus procedure in 1988 for determining the primary stress of pressure components, which also opened up the possibility of determining limit loads.

Formal development of the reduced modulus procedure was systematically carried out for the first time by Seshadri.⁵ The method, called the GLOSS (Generalized Local Stress Strain) analysis, was applied by Seshadri and his co-workers to a number of areas. An elastic analysis was performed and all the elements having equivalent stress* greater than the material yield stress were identified. Assuming pure deformation control and an elastic perfectly plastic material, inelasticity would cause the stress to relax to σ_y while maintaining the strain at the original level. The modulus modification scheme used by Seshadri is given by:

$$E_s = E_o \frac{\sigma_y}{\sigma_e} \quad (2.63)$$

A simplified method was suggested by Seshadri^{29,30} for estimating creep damage in pressurized components in the presence of elastic follow-up. The procedure was also extended to elevated temperature component design. The procedure proposed by Seshadri demonstrated that inelastic effects could be simulated with sufficient accuracy^{31,32} and subsequently stress categorization methods were proposed.³³ The terms GLOSS plot (Figure 2.4) and GLOSS analysis were introduced into the modulus reduction vocabulary by Seshadri.

*Throughout this thesis, the term equivalent stress refers to the von Mises equivalent stress, unless otherwise stated.

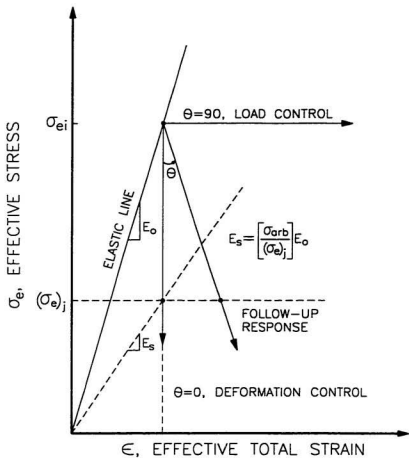


Figure 2.4: Follow-up Angle (θ) on the GLOSS Diagram

2.6 Robust Methods of Limit Load Determination

2.6.1 Limit Analysis based on Partial Elastic Modulus Modification

One of the main challenges in determining lower bound limit loads is in identifying a stress field that satisfies all the requirements that are necessary for “static admissibility” (Section 2.3.1). However, this problem can be circumvented by using stress distributions obtained from linear elastic finite element analyses. If the applied loads are greater than the loads corresponding to the first yield, the stress redistribution that takes place on account of inelastic effects should also be accounted for. In the procedure adopted by Marriott,⁴ this is made possible by identifying the elements that have exceeded the allowable stress limit in a discretized structure. The elastic moduli of these elements are suitably modified on an element-by-element basis and a second elastic analysis is carried out. In this manner, the elastic moduli are changed after every elastic analysis and a number of elastic iterations are performed. The stress field obtained as a result of this satisfies all the conditions that are necessary for being statically admissible. Since this procedure requires that the stresses are below yield, all the requirements necessary for lower bound limit analysis are satisfied. If the value of the maximum von Mises equivalent stress converges to a value less than the yield stress after some iterations, then the applied load can be assumed to be a lower bound

on the exact limit load.

It should, however, be noted that the procedure adopted by Marriott was primarily intended for finding the stress distribution with the least maximum stress for a given value of applied load, rather than determining the limit load itself. Selective softening of the elements does not assure that the converged value of stress would always be less than the code allowable. Since only specified portions of the structure are subjected to moduli modification, this procedure does not entirely characterize the actual stress redistribution that would occur in a component during plastic collapse.

2.6.2 The R-Node Method

The iterative procedure proposed by Marriott⁴ for determining lower bound limit loads has a number of limitations as explained in the previous section. Nevertheless, the procedure was a pioneering effort that opened up the possibility of determining limit loads on the basis of linear elastic analyses.

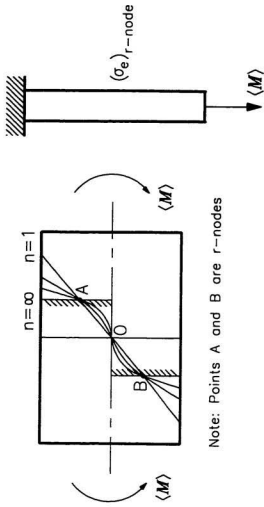
Cognizant of the practical difficulties that the analyst might encounter in carrying out a number of elastic iterations, Seshadri,³⁴ in 1991, proposed an approximate procedure for determining limit loads on the basis of two linear elastic analyses. This method, referred to as the GLOSS R-Node method, incorporated the concept of redistribution nodes and the reference stress method for determining limit loads.

R-Nodes are load-controlled locations within a structure. Therefore, the stresses at the r-nodes are directly proportional to the external tractions irrespective of the material constitutive relations. Hence any two stress distributions satisfying equilibrium with externally applied tractions will intersect at the r-nodes. This feature is useful in the practical determination of the r-nodes and the corresponding r-node equivalent stresses.

When widespread inelastic action (plasticity or creep) occurs, involving entire cross-sections, the statically indeterminate stresses undergo a redistribution except at the r-nodes which are almost statically determinate locations.

Plastic Collapse of Components and Structures: Consider a beam of rectangular cross-section that is subjected to a bending moment M . If the material constitutive relationship is given by $\epsilon = B\sigma^n$, where B and n are material parameters, then $n = 1$ corresponds to elastic behavior and $n \rightarrow \infty$ corresponds to perfect plasticity. The stationary stress distributions across the beam for various values of n are shown in Figure 2.5. The intersection of stress distributions for $n = 1$ and $n \rightarrow \infty$ is designated as the redistribution nodes or simply r-nodes. The stress distributions for all other n 's are assumed to pass through the r-nodes, i.e., points A and B in Figure 2.5.

Since the stresses at points A and B are almost invariant, they can be considered to be load-controlled, i.e., they are set up in order to equilibrate externally applied loads and moments. Therefore, the r-nodes are located on



Note: Points A and B are r-nodes

Figure 2.5: R-Nodes in a Beam subjected to Bending

a "limit type" of stress distribution. Since r-node stresses are load-controlled

$$(\sigma_e)_{r\text{-node}} = \gamma M, \quad (2.64)$$

where γ is a constant of proportionality that depends on the geometry and loading. For an elastic perfectly plastic material, when $(\sigma_e)_{r\text{-node}}$ approaches the yield stress (σ_y) corresponding to the von Mises criterion, the applied moment will correspond to the collapse moment, i.e.,

$$\sigma_y = \gamma M_L. \quad (2.65)$$

Eliminating γ between equations (2.64) and (2.65),

$$M_L = \frac{M \sigma_y}{(\sigma_e)_{r\text{-node}}}. \quad (2.66)$$

The collapse process can be represented by a single bar r-node model (locations A and B). For an indeterminate beam (Figure 2.6), for instance, where multiple plastic hinges form leading to plastic collapse, a multibar model can be used to represent the collapse process. This model enables "transfer of loads" to appropriate bars until collapse occurs. For such structures with generalized loads,

$$\left. \begin{aligned} P_L &= \left[\frac{\sigma_y}{\bar{\sigma}_n} \right] P \\ \langle P, M \rangle_L &= \left[\frac{\sigma_y}{\bar{\sigma}_n} \right] \langle P, M \rangle \end{aligned} \right\} \quad (2.67)$$

where

$$\bar{\sigma}_n = \frac{\sum_{j=1}^N \sigma_{nj}}{N} \quad (2.68)$$

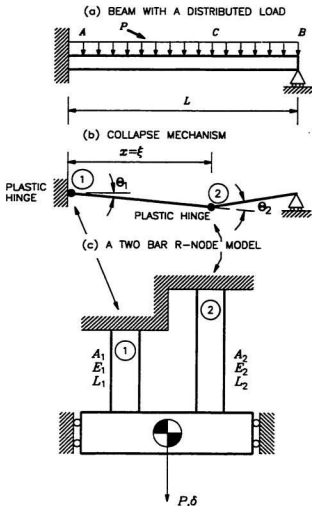


Figure 2.6: Indeterminate Beam subjected to Uniform Load - Collapse Mechanism

and σ_{n_j} 's are the r-node peaks.

The r-node method has been applied to a number of two-dimensional mechanical components and structures such as frames, arches^{34,35} and shells.³⁴ Limit loads of three-dimensional non-symmetric plate structures subjected to a variety of loading is made possible by plotting r-node stress surfaces.³⁶ The limit load estimates obtained using this method are found to compare well with analytical and inelastic finite element analysis results. Although the r-node method has consistently been giving conservative estimates of limit loads, rigorous guidelines for ensuring that the limit loads obtained are lower bounds would be of immense use for practicing engineers. In this thesis such guidelines are proposed and the properties and the usefulness of the r-nodes are investigated in detail.

2.6.3 The Elastic Compensation Method

Mackenzie and Boyle⁶ proposed a method in 1992 for determining limit loads based on iterative elastic analysis and called it the elastic compensation method. In this method the Seshadri's⁵ (r-node) method of limit load determination is adopted for modifying the elastic modulus of elements and at the same time repeated elastic iterations similar to that of Marriott's⁴ method are carried out.

The elastic compensation method typically aims at achieving a statically admissible stress field having a maximum equivalent stress value which is minimum for a given set of elastic iterations (typically six to ten). This value of

maximum stress is used for determining the limit load using the conventional lower bound theorem.^{6,37,38} This method however has disadvantages since it has to make use of a number of elastic iterations. Moreover, even after a number of elastic iterations there is no guarantee that the resulting stress distribution would correspond to limit type* of a stress distribution. While the stresses relax to almost limit type in case of problems such as a beam subjected to bending⁶ and a thick-walled cylinder subjected to uniform internal pressure, in case of problems such as a torispherical head under internal pressure, this method requires modifications in order to achieve a satisfactory trend in stress redistribution.³⁸

2.6.4 Strain-Hardening and Strain-Softening: Limit Load Approximations

The elastic modulus modification procedures for determining limit loads idealize the material behaviour to be elastic perfectly-plastic. However, this assumption may lead to overly conservative limit load estimates for components that are made out of strain-hardening materials (Figure 2.7). The reverse would be the case if strain-softening materials are used for component fabrication. A practical way for applying the limit analysis procedures in such situations would be to assume a nominal yield strength (σ'_y) for performing the computations. The value of this nominal yield strength may

*Limit type stress distribution can be defined as the distribution of stress corresponding to an arbitrary traction, P , such that this stress distribution, when scaled by a factor, m , becomes equal to the stress distribution at impending collapse. The scaling factor, m , otherwise known as the safety factor, is the ratio of a generic surface traction, P_{exact} at the instant of impending plastic flow to the applied surface traction (P).

typically be the value of the flow stress, i.e., the arithmetic mean of the yield and the ultimate stresses. Alternately, this value can be assumed to correspond to some limiting value of strain (say, 2-3% or S_m/E) in the uniaxial stress-strain curve.

2.7 Reference Stress Method in Pressure Component Design

The reference stress method is a simple technique wherein the effect of uncertainties in the material data on the behavior of structures in creep are reduced by relating the structural behavior to a simple tension test conducted at the "reference stress". By this method, the deflection δ at a point in a structure at some time t_o can be expressed as

$$\delta(t_o) = \beta \epsilon^C(t_o), \quad (2.69)$$

where β is a geometric scaling factor that depends on the structure and the boundary conditions, $\epsilon^C(t_o)$ is the creep strain at time t_o as obtained in a creep test performed on a sample of the material at the reference stress σ_R . Conventionally, experimental data are used to construct constitutive equations which are then used for performing the necessary structural calculations. However, the inherent inconsistency of the available test data together with an idealized form of the constitutive law are likely to produce errors in the final prediction of the structural behavior.³⁹ While it is possible to statistically control the uncertainties arising in the case of linear constitutive

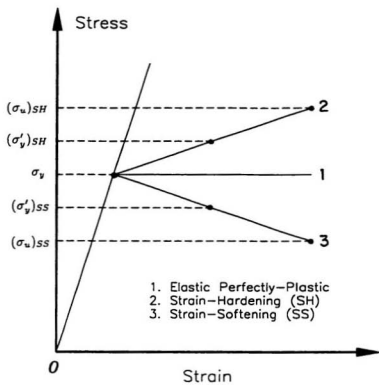


Figure 2.7: Strain-Hardening and Strain-Softening in Mechanical Components

theories, the same may not be the case for non-linear constitutive theories, which tend to amplify the errors.

The reference stress method fundamentally aims at controlling the effect of these errors by identifying a particular uniaxial test, performed at the “reference stress”, which could satisfactorily characterize the structural behavior under consideration. Thus the uncertainties in the available experimental data pertaining to creep are eliminated. The reference stress method is, of course, only an approximate method with possibilities of errors arising out of anisotropy and multiaxiality of the structure. Nevertheless, considering the advantages of the method, a practicing engineer would be willing to accept this compromise at least during the early stages of design.

Among the early investigators of the reference stress method are Soderberg,⁴⁰ who calculated the reference stress for pressurized tubes and Schulte,⁴¹ who observed skeletal points in creeping beams and estimated their deflections from uniaxial tests. Marriott and Leckie⁴² observed that there are points in components undergoing transient creep where the stress does not change with time. Such points are called as skeletal points. Anderson⁴³ analyzed creeping beams with various end conditions. Analytical methods for identifying the reference stress were proposed by Mackenzie,⁴⁴ Sim^{45,46} and Johnson.⁴⁷ The aforementioned methods involve procedures that rely on the existence of an analytical solution for the creep problem which is available only for simple geometries and loading.

Noting that the reference stress is independent of the creep exponent, Sim^{45,46} reasoned that as the creep exponent approaches infinity, the stress distribution will continue to pass through the point that defines it. Since the solution for an infinite creep exponent is analogous to the limit solution corresponding to perfect plasticity, Sim proposed that the reference stress can be obtained from

$$\sigma_R = \left(\frac{P}{P_L} \right) \sigma_y, \quad (2.70)$$

where P is the load on the structure, P_L is the limit load, and σ_y is the yield stress. To apply the above formula, the limit load is assumed to be available.

In 1991, Seshadri⁵ introduced the concept of r-nodes (Section 2.6.2) in an attempt to directly determine the reference stress and the limit loads of mechanical components and structures on the basis of two linear elastic analyses. In this method, stress redistribution similar to creep stress redistribution is simulated by suitably modifying the elastic moduli of the elements in the structure. The equivalent stresses at r-nodes does not change in the process. The invariant behavior of the r-node stress and the reference stress relates the two methods. As such, r-nodes lie on a distribution of stresses that corresponds to primary stresses as defined in the ASME codes.¹¹ The apparently disconnected concepts of r-nodes, limit loads, reference stress and the ASME stress classification concepts are unified in a paper by Seshadri and Marriott.³

In the last several decades, there has been a significant development of the reference stress method, mainly in the United Kingdom.⁴⁸ The “combined r-

node effective stress”, which can be obtained by the r-node method,³⁴ can be identified with the reference stress. The determination of the reference stress using the r-node method is useful since it has application in the integrity assessment of mechanical components and structures as described in Nuclear Electric’s R5 and R6 documents.^{49,50} The assessments include creep damage, low cycle fatigue, elastic-plastic fracture and stress-classification.

2.8 Theorem of Nesting Surfaces

The reference stress can be interpreted in another manner on the basis of energy dissipation considerations. The dissipation rate in a component or a structure under a system of loads is equated to the average dissipation rate at the “reference stress state,”

$$\sigma_R \epsilon_R V = \int_V \sigma_{ij} \epsilon_{ij} dV. \quad (2.71)$$

Using equivalent stresses and strains to represent three-dimensional stress-states, and stipulating that steady state creep is of the form $\epsilon = B\sigma^n$,

$$\sigma_R^{n+1} V = \int_V \sigma_e^{n+1} dV, \quad (2.72)$$

from which the reference stress can be obtained as:^{17,18}

$$\sigma_R = \left[\frac{1}{V} \int_V \sigma_e^{n+1} dV \right]^{\frac{1}{n+1}}. \quad (2.73)$$

The theorem of “nesting surfaces” due to Calladine and Drucker¹⁷ states that the functional

$$\sigma_R = F_n(\sigma_{ij}) = \left[\frac{1}{V} \int_V \sigma_e^{n+1} dV \right]^{\frac{1}{n+1}} \quad (2.74)$$

is strictly monotonically increasing with the exponent n . It is bounded below by the result of $n = 1$ (elastic) and above by the limiting functional as $n \rightarrow \infty$ (perfect plasticity). Thus, if one considers the hypersurfaces $F_n(\sigma_{ij}) = \text{constant}$, in the stress space, then they must “nest” inside each other for increasing n .

For a pin-jointed two-bar structure shown in Figure 2.8, the following development will clarify the aforementioned concepts:

The stresses in bars 1 and 2 can be expressed as

$$\begin{aligned}\sigma_1 &= \frac{Q_1 + Q_2}{A\sqrt{2}}, \\ \sigma_2 &= \frac{Q_1 - Q_2}{A\sqrt{2}}.\end{aligned}\tag{2.75}$$

For the simple statically determinate structure,

$$\begin{aligned}F_n(\sigma_1, \sigma_2) &= \left[\frac{1}{V} \int_V \sigma_e^{n+1} dV \right]^{\frac{1}{n+1}} \\ &= \left[\frac{1}{2} \left(\frac{Q_1 + Q_2}{A\sqrt{2}} \right)^{n+1} + \frac{1}{2} \left(\frac{Q_1 - Q_2}{A\sqrt{2}} \right)^{n+1} \right]^{\frac{1}{n+1}}\end{aligned}\tag{2.76}$$

where the total volume of the bars $V = 2LA$.

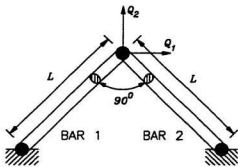
If $F_n(\sigma_1, \sigma_2)$ is further examined, it can be seen that, for $Q_1, Q_2 \geq 0$:

For $n = 1$ (elastic):

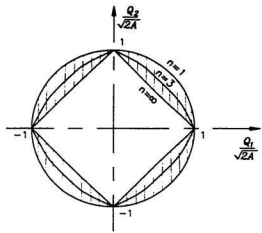
$$Q_e = F_n(\sigma_1, \sigma_2) = \sqrt{\left(\frac{Q_1}{A\sqrt{2}} \right)^2 + \left(\frac{Q_2}{A\sqrt{2}} \right)^2}.\tag{2.77}$$

For $n \rightarrow \infty$ (perfectly-plastic):

$$Q_e = F_n(\sigma_1, \sigma_2) \rightarrow \frac{Q_1}{A\sqrt{2}} + \frac{Q_2}{A\sqrt{2}}.\tag{2.78}$$



(a) A Pin-jointed Two-bar Structure



(b) Nesting Surfaces in Generalized Load Space for the Two-bar Structure

Figure 2.7: Nesting Surfaces for a Pin-Jointed Two-Bar Structure

It can be shown that

$$Q_e|_{n=1} \leq Q_e \leq \lim_{n \rightarrow \infty} (Q_e). \quad (2.79)$$

The nesting surfaces for the two-bar pin-jointed structure can be obtained as shown in Figure 2.8.

Thus, the functional $F_n(\sigma_1, \sigma_2) \equiv Q_e(Q_1, Q_2)$ is a strictly monotonic function that increases with exponent n . Geometrically, the hypersurfaces $Q_e = \text{constant}$, must "nest" inside each other for increasing n . They are enveloped above by the surface for $n = 1$ and below by the limit surface $n \rightarrow \infty$, which is the yield surface in generalized forces constructed on the assumption that the condition of plasticity is $Q_e = \text{constant}$.

2.9 Closure

It can be seen that robust concepts such as reference stress, load control and lower bound limit theorem can be conveniently coupled with linear elastic finite element analyses for obtaining limit load estimates. The extended lower bound theorem of Mura et al. introduces new ideas such as integral mean of yield and exceedance of the yield criterion. This has provided the impetus for investigating this method further, with the aim of obtaining improved lower bound limit load estimates. The finite element implementation of the extended lower bound theorem in order to obtain lower bound limit loads of generic components is discussed in the next chapter.

Chapter 3

Finite Element Implementation of Modified Elastic Modulus Methods of Limit Analysis

3.1 Introduction

In Chapter 2, the upper and lower bound theorems of limit analysis were discussed. The extended lower bound limit theorem proposed by Mura et al.¹⁶ was also introduced. With the emergence of high speed computing facilities and advances in finite element techniques in the last two decades, analytical methods were rapidly being replaced by the relatively easier numerical techniques. However, the time consuming aspect of conventional analyses, particularly non-linear finite element analysis, necessitated development of simpler techniques in order to study the inelastic effects in pressure components. The ease in carrying out linear elastic finite element analyses with modest resources motivated designers to develop techniques based on elastic

analyses. It was found that by systematically modifying the elastic moduli of structures, it is possible to obtain stress fields that would correspond to the stress redistribution associated with inelastic effects. The reduced modulus method was found to satisfactorily assess inelastic effects such as follow-up. This further encouraged researchers to develop methods based on linear elastic finite element analyses in order to determine limit loads.

The robust methods that are currently available for determining limit loads are:

1. the reduced modulus method by partially modifying the elastic moduli,⁴ which is based on the classical lower bound theorem,
2. the r-node method,⁵ which is based on the concepts of reference stress method in creep, load control and the notion of primary stress as defined in the ASME B&PV codes,¹¹ and
3. the elastic compensation method,⁶ which is an iterative method similar to the Marriott's method but based on the elastic modulus modification scheme as suggested by Seshadri. This method invokes the classical lower bound theorem for estimating limit loads*.

In this chapter, the finite element implementation of these three methods is explained. The extended lower bound method of Mura et al. is implemented for obtaining lower bound limit loads by directly using the stress distributions obtained from finite element analyses. By using the theorem of

*A similar method, referred to as the Modified Elastic Modulus (MEM) Method, has been proposed by Carter and Ponter⁵¹ which also involves a number of elastic iterations.

nesting surfaces it is also shown that the factor m^o defined in the previous chapter is actually an upper bound multiplier.

3.2 Limit Analysis based on Partial Elastic Modulus Modification

The iterative procedure adopted by Marriott,⁴ introduced in Section 2.6.1, was primarily intended to characterize the stress redistribution that would occur as a result of post yield loading and thereby estimate the primary stress in the component. In this method, an arbitrary load above the first yield load of the structure is applied and an initial elastic analysis is performed. All the elements that are above the code allowable stress are selected and the elastic moduli of these elements are modified on an element by element basis according to the equation:

$$E_R = E_o \frac{S_m}{SI} \quad (3.1)$$

where, for any given elastic iteration, E_o is the previous value of modulus. S_m is the code allowable stress and SI is the element equivalent stress. The analysis is then rerun to obtain a first reduced modulus solution. The elastic modulus procedure is then repeated in an iterative manner until any further iteration does not reduce the maximum stress, or until the element stress becomes less than S_m . Since the stress distribution corresponding to any iteration is a statically admissible stress field satisfying all the requirements of the classical lower bound theorem, a lower bound limit load can also be

obtained for every iteration as:

$$P_L = P \frac{\sigma_y}{\sigma_M} \quad (3.2)$$

where σ_y is the yield stress and σ_M is the maximum equivalent stress in the component.

3.3 The R-Node Method

The r-node method⁵ (Section 2.6.2) is a robust method for determining limit loads of mechanical components and structures based on two linear elastic finite element analyses. Identifying load controlled locations in a structure called as the r-nodes form the basis for using this method. The r-node method can be used to determine the limit loads of mechanical components and structures in the following manner:

- A linear elastic finite element analysis of a given mechanical component or structure is carried out for prescribed isothermal loadings. The resulting stresses would be pseudo-elastic quantities.
- The elastic modulus of each and every element, j , is modified according to the equation

$$(E_s)_j = \left[\frac{\sigma_{arb}}{\sigma_{\epsilon_j}^0} \right] E_0, \quad (3.3)$$

where σ_{arb} is an arbitrary non-zero stress value. A second linear elastic finite element analysis is carried out.

- On the basis of the two linear elastic analysis, the follow-up angle θ on the GLOSS diagram (Figure 2.4) can be determined for each element. The locations for which $\theta = 90$ deg. can then be identified as the r-node locations, through interpolation. In practice, the foregoing computations can be incorporated into the finite element code.
- A given structure can be visualized to be made of a finite number of sections across the thickness, through out its length. Every section is a potential plastic hinge location and may contain an r-node. A plot of these r-node stresses shows peaks at some locations along the structure which indicates that as the external load is increased these locations will become fully plastic at a lower load than the adjacent sections and form a plastic hinge. These peak r-node stresses for a structure having M peaks can be arranged in a numerically decreasing order, denoted by $\sigma_{n1}, \sigma_{n2}, \dots, \sigma_{nM}$.
- **Location of R-Node Peaks:**

Two-Dimensional Structures:

As the external load is increased, plastic hinges first form at the location with an r-node stress of σ_{n1} and then at the location with an r-node stress σ_{n2} and so on in that sequence. Thus the sequential formation of hinges in the structure is tracked until a local or global collapse mechanism can be identified. If the mechanism for the local or global

collapse requires the formation of N hinges, the effective r-node stress $\bar{\sigma}_n$ can be obtained by relating to an N bar mechanism (Figure 2.6). as:

$$\bar{\sigma}_n = \frac{\sum_{j=1}^N \sigma_{nj}}{N}. \quad (3.4)$$

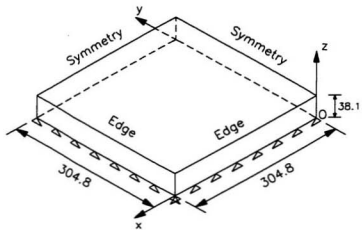
The limit load of the structure P_L is given by:

$$P_L = \left[\frac{\sigma_y}{\bar{\sigma}_n} \right] P. \quad (3.5)$$

Three-dimensional Structures:

In case of three-dimensional structures such as non-symmetric plates, r-node stress surfaces are required for the determination of r-node peaks. The three-dimensional plot of the r-node stress (on the z coordinate) versus the r-node location (on the x and y coordinates) produces the three-dimensional r-node stress surface.

A three-dimensional structure such as, say, a plate structure can be visualized to be made of a finite number of sections normal to the neutral plane. The number of r-nodes present in a section depends on whether bending or direct stresses are dominant in that section.³⁴ For the plate structure shown in Figure 3.1, the r-node stress surface (Figure 3.2) has peaks at certain regions. The relative numerical value of the peaks indicates the sequence of formation of plastic zones or



1. All dimensions in mm
2. O - Origin

Figure 3.1: A Square Plate Simply Supported on All Sides under Uniform Pressure

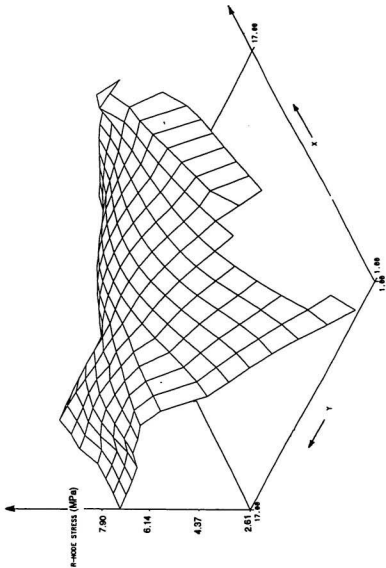


Figure 3.2: R-Node Stress Surface of the Square Plate Simply Supported on All Sides

hinges in the structure and respective locations. Thus the r-node peaks are potential nucleation points for plastic regions.

Since every section of the plate analyzed may not necessarily contain an r-node, the r-node stress surface may, at the first sight, be difficult to interpret. Therefore, a spline interpolated r-node stress surface is introduced (Figure 3.3). This plot gives a better picture of the likely locations of the r-node peaks. However, it should be noted that the purpose of the spline interpolated r-node stress surface is only to enable a better visual interpretation of the r-node stress surface. An iso r-node stress contour plot (Figure 3.4) may also be used to enable the determination of the r-node peaks.

The combined r-node effective stress $\bar{\sigma}_n$ can be obtained as

$$\bar{\sigma}_n = \frac{\sum_{j=1}^N \sigma_{n_j}}{N}, \quad (3.6)$$

where N refers to the number of peaks and σ_{n_j} refers to the r-node stress of the j th peak. Using the expression given in equation (3.5), the limit load of the structure is determined.

The r-node method has been applied to a number of two-dimensional mechanical components and structures such as frames, arches^{34,35} and shells.³⁴ Limit loads of three-dimensional non-symmetric plate structures subjected to a variety of loading is made possible by plotting r-node stress surfaces.³⁶ The limit load estimates obtained using this method are found to compare well

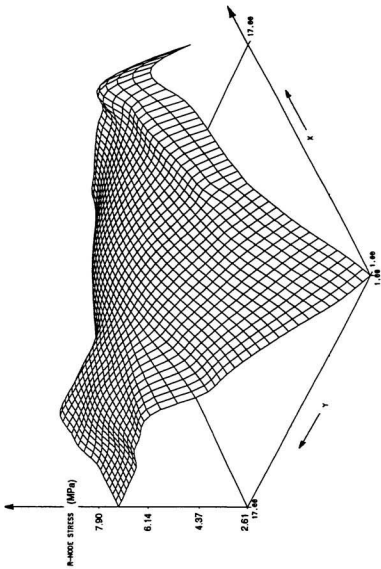


Figure 3.3: Spline Interpolated R-Node Stress Surface of the Square Plate Simply Supported on All Sides

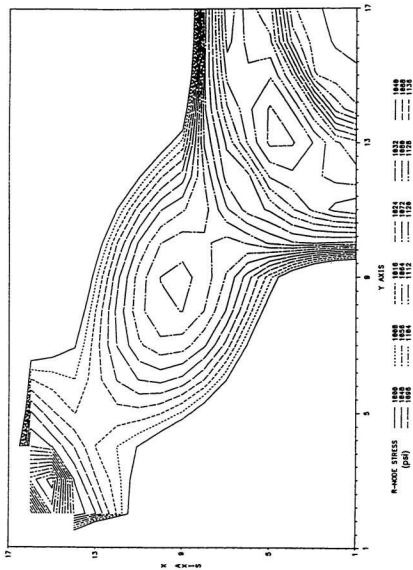


Figure 3.4: Iso R-Node Stress Contour of the Square Plate Simply Supported on All Sides

with analytical and inelastic finite element analysis results. Although the r-node method has been consistently giving conservative estimates of limit loads, rigorous guidelines for ensuring that the limit loads obtained are lower bounds would be of immense use for practicing engineers. In this thesis such guidelines are proposed and the properties and the usefulness of the r-nodes are investigated in detail.

3.4 The Elastic Compensation Method

The procedure proposed by Mackenzie et al.⁶ (Section 2.6.3) is based on the classical lower bound theorem of limit analysis and a number of linear elastic iterations. An initial linear elastic finite element analysis of the discretized structure is carried out. This analysis is usually designated as the zeroth iteration. Based on this, the elastic moduli of all the elements are modified by following the procedure suggested by Seshadri.⁵ A number of linear elastic iterations are carried out, similar to the procedure suggested by Marriott,⁴ until any further iteration does not decrease the value of the maximum equivalent stress in the component significantly. After every iteration, the new values of elastic moduli are determined for the subsequent iteration based on equation (3.3) as:

$$[E_{(i)}]_r = \left[\frac{\sigma_{arb}}{(\sigma_e^2)_{(i-1)}} \right] [E_{(i-1)}]_r, \quad (3.7)$$

where i is the iteration number, and r is the element number in the discretized component or structure. Since the elastic moduli are modified for the entire

component and the analyses are linear in nature, the value of the applied load, P , can be arbitrary. The stress distribution having the least maximum stress among the given set of iterations is selected to be the required statically admissible stress field. The final limit load can be determined as a linearly scaled value of the applied load such that the maximum stress in the component corresponds to the yield stress. The limit load is given by the expression:

$$P_{LC} = P \frac{\sigma_y}{(\sigma_e)_M} \quad (3.8)$$

where σ_y is the yield stress, $(\sigma_e)_M$ is the maximum von Mises equivalent stress for any given elastic iteration and P is the applied load.

3.5 The Theorem of Nesting Surfaces

It was explained in Section 2.7 that the reference stress, being independent of the creep exponent, should be a unique point through which the stress distributions corresponding to any value of n should pass.^{45,46} Since the solution for an infinite creep exponent corresponds to perfect plasticity, Sim proposed that the reference stress can be obtained from equation (2.70) which, obviously, requires prior knowledge of limit loads. The combined r-node stress obtained using the r-node method is one way of directly determining the reference stress. Alternately, the task of direct determination of reference stress using linear elastic stress distributions can be accomplished by using the "theorem of nesting surfaces".¹⁷ In this section, finite element implementation of the theorem of nesting surfaces is carried out for $n = 1$ so

as to enable direct determination of the reference stress from linear elastic analyses stress distributions.

The reference stress, using the theorem of nesting surfaces, can be expressed as

$$\sigma_R = \left[\frac{1}{\bar{V}} \int_V \sigma_e^{n+1} dV \right]^{\frac{1}{n+1}}. \quad (3.9)$$

For linear elastic analyses, $n = 1$ and therefore,

$$\sigma_R = \left[\frac{1}{\bar{V}} \int_V \sigma_e^2 dV \right]^{\frac{1}{2}}. \quad (3.10)$$

In terms of the finite element discretization scheme, equation (3.10) can be written as

$$\sigma_R = \sqrt{\frac{\sum_{i=1}^n \sigma_{ei}^2 \Delta V_i}{V}}. \quad (3.11)$$

Thus the stress distributions obtained from linear elastic finite element analyses can be used for directly determining the reference stress.

3.6 The Extended Lower Bound Theorem

Mura et al.¹⁶ applied their proposed extended lower bound theorem for determining the limit load of a tension specimen and obtained good limit load estimates. However, real life structures are more complicated in nature and hence warrant a procedure that is generic. The methods based on modified elastic moduli are viable alternatives since they provide statically admissible stress distributions. The implementation of the extended lower bound theorem so as to enable direct determination of limit loads by using stress

distributions obtained from linear elastic finite element analysis is discussed in this section.

In equation (2.56), the linear elastic stress distribution s_{ij}^o corresponds to an applied traction, $m^o P$. If \bar{s}_{ij}^o is a statically admissible stress distribution corresponding to an applied traction P , then $m^o \bar{s}_{ij}^o$ would correspond to $m^o P$.

It is therefore clear that

$$s_{ij}^o = m^o \bar{s}_{ij}^o. \quad (3.12)$$

Thus equation (2.48) can be written as

$$F = m^o - \int_{V_T} \mu^o \left[\frac{1}{2} (m^o)^2 \bar{s}_{ij}^o \bar{s}_{ij}^o - k^2 + (\phi^o)^2 \right] dV. \quad (3.13)$$

The factors m^o , μ^o and ϕ^o can be determined by rendering the functional, F , stationary, leading to the following set of equations:

$$\frac{\partial F}{\partial m^o} = 0; \quad \frac{\partial F}{\partial \mu^o} = 0; \quad \frac{\partial F}{\partial \phi^o} = 0. \quad (3.14)$$

The von Mises equivalence for uniaxial state of stress can be written as follows:

$$\frac{1}{2} \bar{s}_{ij}^o \bar{s}_{ij}^o = \frac{(\sigma_x^o)^2}{3} \quad (3.15)$$

and

$$k^2 = \frac{\sigma_y^o}{3}. \quad (3.16)$$

Equation (3.13) becomes

$$F = m^o - \int_{V_T} \frac{\mu^o}{3} \left[\{ (m^o)^2 (\sigma_x^o)^2 - \sigma_y^o \} + 3(\phi^o)^2 \right] dV. \quad (3.17)$$

Applying equation (3.14) in conjunction with equation (3.17), we get

$$\phi^o = 0 \quad (3.18)$$

and

$$m^o = \frac{\sigma_y \sqrt{V_T}}{\sqrt{\sum_{k=1}^N (\sigma_{ek}^o)^2 \Delta V_k}} \quad (3.19)$$

where the quantities σ_{ek}^o and ΔV_k are the von Mises equivalent stresses and volumes of respective elements in the FEA discretization scheme.

Comparing the expressions for m^o , as obtained from equation (3.19), and the reference stress, as obtained from the theorem of nesting surfaces [equation (3.11)], it can be seen that

$$m^o = \frac{\sigma_y}{\sigma_R}. \quad (3.20)$$

Thus a monotonic increase in the value of the reference stress implies a monotonic decrease in the value of m^o , with increasing n . Since equation (2.79) gives a lower bound on the reference stress for $n = 1$, m^o corresponding to $n = 1$ is an upper bound multiplier for limit loads.

Equation (2.56) can be simplified further using equations (3.15) and (3.16) as

$$m' = \frac{2m^o \sigma_y^2}{\sigma_y^2 + (m^o)^2 (\sigma_e^o)_M^2} \leq m. \quad (3.21)$$

Equations (3.19) and (3.21) can be readily obtained on the basis of linear elastic FEA. $(\sigma_e^o)_M$ is the maximum equivalent stress in a component or

structure for a prescribed load, P . The lower bound limit load can therefore be expressed as:

$$P_{LM} = m'P. \quad (3.22)$$

Combining equations (3.20) and (3.21), the limit load can be bounded as follows:

$$m' \leq m \leq m^o. \quad (3.23)$$

3.7 Closure

The finite element implementation of the available methods for determining the limit loads has been discussed in this chapter. An alternate method for determining lower bound limit loads, proposed by Mura et al., has been implemented. By invoking the theorem of nesting surfaces it has been shown that the multiplier m^o defined by Mura is actually an upper bound on the safety factor.

In the next chapter, the advantages and limitations of the methods discussed in this chapter are investigated. An improved method for obtaining lower and upper bound limit loads, based on the extended variational theorem, is also presented.

Chapter 4

Improved Lower Bound Limit Load Estimates: The m_α -method

4.1 Introduction

The robust methods of limit analysis are attractive alternatives over analytical methods and inelastic finite element analysis since they are relatively easy to implement and make use of statically admissible stress distributions obtained from linear elastic analyses. However, the use of classical lower bound theorem requires a number of linear elastic iterations in order to obtain reasonable limit load estimates. Restricting the number of iterations to a few may often lead to overly conservative results. A robust method is one which has the ability to give acceptable results at minimum cost and effort. Hence any method aimed towards reducing the number of elastic iterations without compromising on the quality of results would be of definite

significance.

An in-depth study into the extended lower bound theorem, the notion of integral mean of yield and its relationship with the theorem of nesting surfaces offers sufficient motivation towards developing methods for obtaining improved lower and upper bound limit loads. In this chapter a method is proposed for determining lower bound limit loads on the basis of two linear elastic analyses. The method, designated as the m_α -method, invokes the notion of reference volume to account for localized collapse and the technique of “leap-frogging” to a limit state. These concepts are used in conjunction with the elastic modulus adjustment technique, described by Seshadri and Fernando,³⁴ for obtaining improved lower and upper bound limit load estimates. The advantages and limitations of the existing robust methods are also investigated in this chapter from an engineering stand-point.

4.2 Advantages and Limitations of the Existing Robust Limit Analysis Techniques

4.2.1 Classical Limit Theorems

The classical lower and upper bound theorems of limit analysis offer a practical way to avoid the severe limitations in estimating the limit loads by analytical methods. By choosing statically admissible stress fields and kinematically admissible velocity fields in an appropriate manner, reasonable

estimates of the bounds can be obtained. However, application of classical lower and upper bound methods is limited to simple geometric configurations and loading patterns. Coming up with the appropriate statically admissible stress distribution or kinematically admissible strain distribution is not a trivial task. Furthermore, the construction of generalized yield surfaces in terms of stress and moment resultants and the manipulations involving strain-rate vectors can be cumbersome and unwieldy.

Mackenzie et al.⁶ extracted statically admissible stress fields by performing linear elastic FEA and applied the classical lower bound theorem. Their repeated elastic analyses procedure and the elastic modulus adjustment scheme is essentially an adaptation of the methods proposed by Marriott⁴ and Seshadri.⁵

It is worthwhile carrying out repeated elastic iterations provided the stress distributions obtained progressively approach limit type. There is no assurance, however, that the stress distributions would approach limit type even after many iterations. This problem can be illustrated by considering the example of a torispherical head subjected to internal pressure (Figure 4.1) where the maximum stress does not converge; rather it fluctuates with successive elastic iterations as shown in Figure 4.2.

Performing repeated elastic analyses by modifying the elastic moduli leads to softening in some regions and hardening in the other regions of the structure. In some cases, the difference between the magnitudes of elastic moduli during this process can become large. For instance, in a compact tension

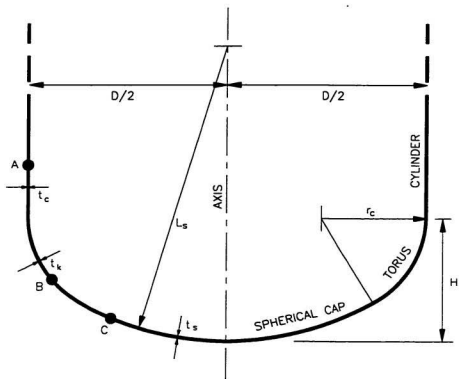
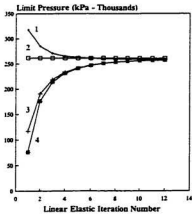


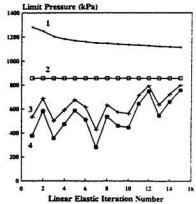
Figure 4.1: Dimensions of a Torispherical Head

Thick Cylinder Subjected to Uniform Internal Pressure



Class I Structure

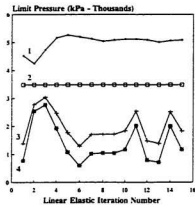
Torispherical Head Subjected to Uniform Internal Pressure



Class I (First Two Iterations)

Class II (Beyond the Second Iteration)

Rectangular Plate Partially Fixed and Partially Simply Supported



Class I (First Two Iterations)

Class III (Beyond the Second Iteration)

1 - $m P^*$	(Upper bound)
2 - $m P$	(Exact)
3 - P	(Lower bound - classical)
4 - $m P$	(Lower bound - Mura's)

Figure 4.2: Typical Response of Structures to Repeated Elastic Iterations

Table 4.1: Values of Elastic Moduli of Two Elements in a Compact Tension Specimen - Elastic Iteration Number 6 ($q = 1$)

Element Number	Elastic Modulus Value (Pa)
8	958.73
31	2.43×10^{12}

specimen, after the sixth iteration the range of values of elastic moduli in the structure was found to be quite high. The elastic moduli values of two typical elements are given in Table 4.1 as representative cases. Such situations lead to what is referred to as ill-conditioning⁵² of the stiffness matrix in the finite element formulation which can severely affect the accuracy of the stress values obtained. Also, there is no prescribed procedure to determine the value of the arbitrary stress in equation (3.3). This aspect is problematic since an improper selection of the arbitrary number during every elastic analysis may cause the elastic moduli values to progressively assume either very large or negligibly small values, thus falling out of the range of numerical accuracy of the FEA software.

4.2.2 Extended Lower Bound Theorem

The main advantage in using the extended lower bound theorem lies in the fact that both upper (m^o) and lower bound (m') limit load multipliers can be determined for any given stress distribution. It should be noted that the factor m^o is an upper bound multiplier only if the corresponding stress distribution satisfies the theorem of nesting surfaces.

The extended lower bound theorem of limit analysis, however, has its own limitations. In the classical method of determining lower bound limit load, the maximum equivalent stress value is all that is needed from a statically admissible stress field. However, determination of Mura's lower bound multiplier (m') requires, in addition to the entire stress field, the volume associated with every element in order to calculate the parameter m^o . The factor m^o can thus assume very large values in case of problems where the collapse is local.

It can also be shown that the magnitude of lower bound limit load determined using Mura's method is always less than that obtained using classical limit load and hence, as such, has no advantage. The relationship between the classical lower bound limit load,

$$P_{LC} = P \frac{\sigma_y}{(\sigma_\epsilon)_{max}}, \quad (4.1)$$

the upper bound limit load,

$$P_U = m^o P, \quad (4.2)$$

and Mura's lower bound limit load,

$$P_{LM} = \frac{2m^o\sigma_y^2}{\sigma_y^2 + (m^o)^2(\sigma_\epsilon)_{\max}^2} \quad (4.3)$$

can be expressed as:

$$P_{LM} = \frac{2P_U P_{LC}^2}{P_{LC}^2 + P_U^2} \quad (4.4)$$

Let

$$\frac{P_U}{P_{LC}} = \omega. \quad (4.5)$$

Therefore,

$$\frac{P_{LC}}{P_{LM}} = \frac{1 + \omega^2}{2\omega}, \quad (4.6)$$

Since $\omega \geq 1$, as per equation (4.6),

$$\frac{P_{LC}}{P_{LM}} \geq 1. \quad (4.7)$$

Therefore, for any elastic stress distribution, the limit load value determined using equation (4.1) will always be equal to or greater than the one evaluated using equation (4.3).

The lower bound limit load values given by equations (4.1) and (4.3) were determined for a number of structural components such as a thick-walled cylinder subjected to uniform pressure, spherical pressure vessel with a cylindrical nozzle subjected to uniform pressure, beams and torispherical heads. to mention a few. Equations (3.23) and (4.7) were validated for a number of linear elastic stress distributions. For the purpose of illustration, some typical limit load estimates are plotted in Figure 4.2 for a number of elastic iterations.

4.2.3 Theorem of Nesting Surfaces

The theorem of nesting surfaces was proposed by Calladine and Drucker¹⁷ as a method for determining the reference stress based on the nesting surfaces of energy dissipation in creep. The reference stress is given by the expression

$$\sigma_{ref} = \sqrt{\frac{\sum_{i=1}^N \sigma_{ei}^2 \Delta V_i}{V}} \quad (4.8)$$

The maximum and the minimum values of the reference stress correspond to $n \rightarrow \infty$ and $n = 1$ respectively. The stress distributions relating to the various values of n can be simulated by performing a number of elastic analyses in conjunction with elastic modulus modification after every iteration (of course, assuming that all these iterations progressively lead to limit type state for an arbitrarily applied external load). Thus a limit type stress distribution can be identified with the stress distribution corresponding to $n \rightarrow \infty$. Assuming the external load applied to be equal to the exact limit load and limit stress distribution, for a structure that completely becomes plastic at collapse, $\sigma_{ref} = \sigma_y$ and otherwise $\sigma_{ref} < \sigma_y$. Thus in general,

$$\sigma_{ref} \leq \sigma_y \quad (4.9)$$

The reference stress formula due to Sim^{45,46} given by equation (2.70) can be expressed as

$$P_{L1} = P_L \frac{\sigma_y}{\sigma_{ref}} \quad (4.10)$$

where P_L is the applied load which, in this case, is taken to be the exact limit load. From equations (4.9) and (4.10), $P_{L1} \geq P_L$. The unconservative

nature of the limit load obtained using the theorem of nesting surfaces is therefore not useful for pressure component design. Since the stress distributions correspond to linear elastic analysis and can be scaled linearly, the aforementioned relationships are valid even if the applied load is of any arbitrary value. As the collapse of structures becomes more local, the reference stress, which is determined on the basis of the total volume of the structure, becomes increasingly smaller than the actual. The concept of reference volume to be discussed in Section 4.4 offers a convenient way to overcome this problem.

4.3 Robustness of Structural Behavior during Repeated Elastic Iterations

It was seen in Section 4.2.1 that performing a number of elastic analyses may not necessarily lead to a limit type of stress distribution and may even cause unstable structural response such as fluctuation of maximum stress. Therefore, it becomes useful to understand the requirements for a valid stress distribution and the ways and means for obtaining it.

The factor m^o is one of the parameters that is useful in assessing whether or not limit stress distribution is being approached during successive elastic iterations. As the number of iterations increase, m^o should monotonically decrease and converge. Should this not occur, i.e., if there is an increase in the value of m^o as compared to its value during the previous iteration, then

the theorem of nesting surfaces would be violated* implying that the stress distributions are not on a redistribution path leading to limit type.

The structural behavior would be considered robust and stable if the sequence of equivalent stresses described below and their relative locations are preserved during the linear elastic finite element analyses., i.e., the sequence

$$\sigma_{e1} \geq \sigma_{e2} \geq \dots \geq \sigma_{eN}.$$

holds good.

An iteration variable ζ is introduced, such that both m^o and $(\sigma_e)_{Mf}$ are functions of ζ . A change in the secant modulus $[(E_s)_j$ in equation (3.3)] by an infinitesimal amount will imply a change $\Delta\zeta$ in the iteration variable. The criteria for a lower bound limit load is the concurrent satisfaction of the following:

$$(1) \quad m_l^o \geq m_{lI}^o \quad \text{or} \quad \frac{dm^o}{d\zeta} \leq 0.$$

This requirement ensures satisfaction of the theorem of nesting surfaces which assures that there is a progressive increase in the internal energy dissipation, for a given value of applied load, as the stress field becomes closer to the limit type. (4.11)

*While carrying out repeated elastic iterations, assume that limit type stress distribution is obtained at the n th iteration. Any stress distribution corresponding to a preceding iteration (say, iteration number r) should be on a path leading to the final limit state. One of the requirements for this is that the inequality

$$m_l^o \geq \dots \geq m_r^o \geq \dots \geq m_n^o$$

is satisfied. Otherwise, the "theorem of nesting surfaces" is considered to be violated.

$$(2) \quad (\sigma_M^o)_I \geq (\sigma_M^o)_{II} \quad \text{or} \quad \frac{d\sigma_M^o}{d\zeta} \leq 0, \quad (4.12)$$

This stipulation aims at a flatter stress distribution approaching a limit type stress field.

$$(3) \quad \text{The relative locations of the set of stresses } \sigma_{e1} > \sigma_{e2} > \dots > \sigma_{eN} \text{ are invariant.}$$

This requirement ensures that successive distributions are perturbed states about the initial pseudoelastic stress distributions with the r-node equivalent stress being invariant. (4.13)

The requirements stipulated by equations (4.11) to (4.13) ensure that the resulting stress distributions belong to a family of distributions: i.e., are intermediate stress distributions leading to one of limit type.

4.3.1 Class I, II and III Components and Structures

Repeated elastic FEA enables an analyst to obtain insight into both local⁵ as well as global³⁴ behavior of components and structures. The global structural behavior can be assessed by plotting m^o , m' and σ_M as a function of the iteration variable ζ . In practical terms, there is little advantage in carrying out a large number of iterations just to find out if the global behavior would degenerate. This would very much depend on the geometry and loading on a given component configuration, and on the elastic modulus modification scheme. However, it is sufficient for the purpose of ascertaining the bounds to determine the trend based on the first and second linear elastic FEA. It is therefore useful to categorize the behavior as follows:

Class I: These are components and structures that are characterized by a monotonic convergent behavior. The m_o estimates obtained are reliable. For Class I components and structures

$$\left. \begin{aligned} \frac{dm^o}{d\zeta} &\leq 0 \\ \frac{dm'}{d\zeta} &\geq 0 \\ \frac{d\sigma_M^o}{d\zeta} &\leq 0 \end{aligned} \right\} \quad (4.14)$$

and the maximum stress location is also more or less invariant.

A thick-walled cylinder subjected to a uniform internal pressure and an indeterminate beam under a uniformly distributed load are examples of Class I components and structures.

Class II: Successive iterations of modulus softening may sometimes result in an increase in the magnitude of the maximum equivalent stress. This type of behavior is usually associated with thin structures without a re-entrant corner*. The criteria for Class II components and structures are:

$$\left. \begin{aligned} \frac{dm^o}{d\zeta} &\leq 0, \\ \frac{dm'}{d\zeta} \\ \frac{d\sigma_M^o}{d\zeta} \end{aligned} \right\} \text{fluctuate.} \quad (4.15)$$

The maximum stress location may also fluctuate for this type of structure.

Typical problems that fall under this category are thin torispherical heads subjected to a uniform internal pressure.

Class III: The criteria for these class of components and structures can be expressed as

$$\left. \begin{aligned} \frac{dm^o}{d\zeta} &> 0, \\ \frac{dm'}{d\zeta} \\ \frac{d\sigma_M^o}{d\zeta} \end{aligned} \right\} \text{fluctuate.} \quad (4.16)$$

*The presence of re-entrant corners in components such as a spherical pressure vessel with a cylindrical nozzle and a compact tension specimen enable stable positioning of the maximum equivalent stress location.

The maximum stress location fluctuates and the theorem of nesting surfaces is violated, and therefore the results are invalid.

Figure 4.2 shows the typical behavior of the three classes of structures during linear elastic iterations based on a modulus-softening index of $q = 1$.

The modulus softening scheme given by equation (3.3) is modified as:

$$(E_s)_j = \left[\frac{\sigma_{arb}}{\sigma_{\sigma_j}^0} \right]^q E_{\sigma}. \quad (4.17)$$

Should the component or structure exhibit Class II or III behavior, then using $q < 1$ (say, 0.5 or 0.25) instead of 1.0 may stabilize the structural behavior of pressure components by weakening the extent of elastic moduli modification and thereby transforming their behavior to Class I.

4.4 Local Plastic Collapse - Notion of Reference Volume (V_R)

If plastic collapse occurs over a localized region of the mechanical component or structure, m° will be significantly overestimated if it is calculated on the basis of the total volume, V_T . Furthermore, the corresponding m' will be underestimated [equation (4.7)].

The reference volume concept is introduced here to identify the “kinematically active” portion of the component or structure that participates in plastic action. If V_T is the total volume and V_R is the reference volume, then $V_R \leq V_T$. During local collapse, plastic action is confined to a sub-region of

the total volume (Figure 4.3). The magnitude of the upper bound multiplier (m°) would therefore depend on the sub-volume, V_β , where

$$V_\beta = \sum_{k=1}^{\beta} (\Delta V_k). \quad (4.18)$$

In order to carry out the various summations, we consider the following sequence, i.e.,

$$(\sigma_{e1}^\circ)^2 \Delta V_1 > (\sigma_{e2}^\circ)^2 \Delta V_2 > \dots > (\sigma_{eN}^\circ)^2 \Delta V_N. \quad (4.19)$$

When $\beta = 1$, equation (3.19) degenerates to the classical lower bound value, i.e.

$$m^\circ = \frac{\sigma_y}{\sigma_{e1}^\circ}. \quad (4.20)$$

An iteration variable ζ is introduced next in such a way that infinitesimal changes to the element elastic modulus of the various elements during the second and subsequent linear elastic FEA would induce a corresponding change $\Delta\zeta$. The magnitude of $\Delta\zeta$ would, of course, depend on the nature of the modulus-adjustments.

For the degenerate case, m° would increase with ζ thereby violating the nesting surface theorem. It is implied here that the second linear elastic FEA would lead to a "flatter" distribution of stress. On the other hand, m° evaluated on the basis of the total volume would decrease with increasing ζ . Therefore, for some volume V_R , where $\Delta V_1 < V_R \leq V_T$ corresponding to $\beta = \alpha$, the multiplier m° would be invariant, i.e., $m_I^\circ = m_{II}^\circ$. In other words, the theorem of nesting surfaces would be just satisfied. The schematic of vari-

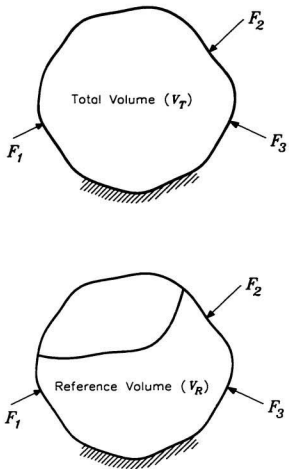


Figure 4.3: Total and Reference Volumes

ation of m^o and m' with the iteration variable, ζ , is shown in Figure 4.4. The procedure for determining the reference volume is illustrated in Figure 4.5.

4.5 The m_α -method

In this section, Mura's variational formulation is extended to provide improved lower bound limit loads for symmetric as well as nonsymmetric components and structures. Using a modulus-adjustment scheme akin to the R-Node method, the multiplier m_α can be obtained on the basis of two linear elastic FEA by "leap-frogging" to a near asymptotic limit state. The first linear elastic FEA corresponds to the conventional linear elastic analysis, while the second linear elastic FEA involves modifications to the elastic-modulus of all the elements according to equation (4.17). In equation (4.17) the element numbers vary from $k = 1$ to $k = N$ and q is the "modulus-adjustment index" which is nominally taken to be equal to unity as in the R-Node method.³⁴ A value of $q < 1$ can be used to stabilize the structural behavior of "sensitive" pressure components.

On the basis of the results of the first and second linear elastic FEA, and making use of the expression given by equation (3.19), the values of m_I^o and m_{II}^o can be determined. The average surfaces of dissipation¹⁷ can now be expressed as:

$$\left. \begin{aligned} m_1^o &= c_1 \\ m_2^o &= c_2 \end{aligned} \right\} \quad (4.21)$$

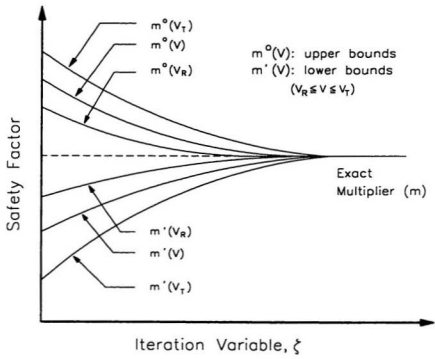


Figure 4.4: Variation of m° and m' with Elastic Iterations

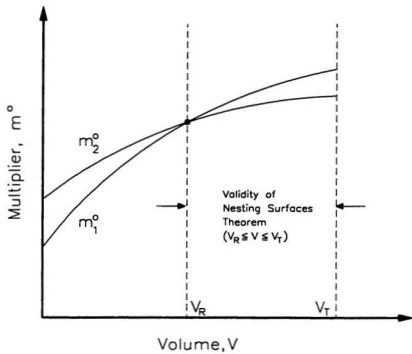


Figure 4.5: Determination of Reference Volume

where c_1 and c_2 are constants. In equation (3.19), $V_R \leq V \leq V_T$. The theorem of nesting surfaces essentially asserts that $m_i^o \geq m_{II}^o \geq m$, where m is the exact factor of safety.

As ζ increases with successive linear elastic FEA iterations beyond two, m^o and m' would eventually converge to the exact value of the factor of safety, m . Whether or not the convergence is monotonic was discussed in Section 4.3.1.

Mura's lower bound multiplier can be expressed as:

$$m'(\zeta) = \frac{2m^o(\zeta)\sigma_y^2}{\sigma_y^2 + [m^o(\zeta)]^2[\sigma_M^o(\zeta)]^2} \quad (4.22)$$

where $\sigma_M^o(\zeta) = (\sigma_e^o)_{\max}$ is the maximum equivalent stress at iteration number "i". The quantities m' , m^o and σ_M are all functions of ζ .

Differentiating both sides of equation (4.22) with respect to ζ , we get

$$\frac{dm'}{d\zeta} = \frac{\partial m'}{\partial m^o} \frac{dm^o}{d\zeta} + \frac{\partial m'}{\partial \sigma_M^o} \frac{d\sigma_M^o}{d\zeta}. \quad (4.23)$$

In terms of finite differences, equation (4.23) can be expressed as:

$$\Delta m' = \left. \frac{\partial m'}{\partial m^o} \right|_{\zeta=\zeta_i} (\Delta m^o) + \left. \frac{\partial m'}{\partial \sigma_M^o} \right|_{\zeta=\zeta_i} (\Delta \sigma_M^o). \quad (4.24)$$

Although equation (4.24) is valid for any given iteration, in the proposed m_α -method only two iterations are required. If $\frac{dm^o}{d\zeta} < 0$, then $m^o > m'$.

The following quantities are defined next:

$$\left. \begin{aligned} \Delta m' &= m_\alpha - m'_i \\ \Delta m^o &= m_\alpha - m_i^o \\ \text{and } \Delta \sigma_M^o &= \frac{\sigma_y}{m_\alpha} - \sigma_{Mi}^o \end{aligned} \right\} \quad (4.25)$$

where the subscript i refers to the iteration number.

If we insist that $\sigma_{M\infty}^o = \frac{\sigma_y}{m_\alpha}$ when $m^o \rightarrow m_\alpha$ and $m' \rightarrow m_\alpha$, then it is clear from equation (2.56) that m_α would be a lower bound.

Making use of equations (4.22), (4.24) and (4.25), and carrying out the necessary algebraic manipulations, the following quadratic equation can be obtained:

$$Am_\alpha^2 + Bm_\alpha + C = 0 \quad (4.26)$$

where

$$\begin{aligned} A &= (m_i^o)^4 (\bar{\sigma}_{Mi}^o)^4 + 4(m_i^o)^2 (\bar{\sigma}_{Mi}^o)^2 - 1, \\ B &= -8(m_i^o)^3 (\bar{\sigma}_{Mi}^o)^2, \\ C &= 4(m_i^o)^3 (\bar{\sigma}_{Mi}^o), \\ \text{and } \bar{\sigma}_{Mi}^o &= \frac{\sigma_{Mi}^o}{\sigma_y}. \end{aligned}$$

The coefficients A , B and C can be evaluated from the results of any linear elastic FEA.

To ensure real roots for equation (4.26), the discriminant must be greater than zero, i.e.,

$$(m_i^o)(\bar{\sigma}_{Mi}^o) \leq (1 + \sqrt{2}). \quad (4.27)$$

While it is possible to evaluate m_α on the basis of the results of the first linear elastic FEA provided equation (4.27) is satisfied, the introduction of reference volume in conjunction with two linear elastic FEA enables much improved estimates of m_α . Furthermore, since m is bounded by m^o and m_α , the

use of reference volume would narrow the spread. The phrase “ m_α -method” therefore refers to the use of α elements in the finite element discretization scheme that pertains to the identification of an appropriate reference volume [equations (4.18) and (4.19)]. The “leap-frogging” of intermediate iterations is schematically illustrated in Figure 4.6.

4.6 Illustrative Example - Torispherical Head

The step-by-step implementation of the m_α -method is explained in this section by considering the example of a torispherical head subjected to uniform internal pressure (Figure 4.1). The dimensions of the head are $L_s/D=0.8$, $r/D=0.12$, $H/D=0.2360$ and a thickness of 2.54×10^{-2} m (1 in.). The Young's modulus and the yield stress of the material are respectively 206.85×10^6 kPa (30×10^6 psi) and 206.85×10^3 kPa (30×10^3 psi). The Poisson's ratio is assumed to be 0.3. For performing the analyses, an arbitrary uniform pressure of 200 kPa (29 psi) is applied.

Determination of Reference Volume

The following are the steps that are necessary for determining the reference volume:

- The elements are arranged in the descending order of energy dissipation corresponding to the first linear elastic analysis by following the sequence given by equation (4.19).

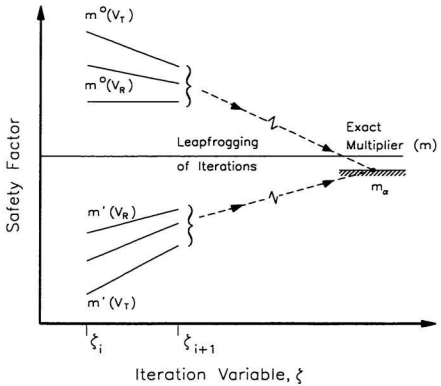


Figure 4.6: Leap-frogging of Elastic Iterations to a Limit State

- In the same order, the dissipations corresponding to the second linear elastic analysis are listed.
- The values of m^o are determined by progressively increasing the volume; starting with the element having the largest dissipation and following the sequence given by equation (4.19) for the entire volume.
- The volume corresponding to the two linear analysis having the same value of m^o is identified as the reference volume.

Computational Procedure:

Applied Pressure,	P	=	200 kPa
Elastic modulus softening index,	q	=	1
Value of yield stress,	σ_y	=	206850 kPa
Upper bound multiplier			
linear elastic analysis, I	m_I^o	=	6.41
linear elastic analysis, II	m_{II}^o	=	6.23

Maximum equivalent stress (nodal stresses interpolated)

linear elastic analysis, I	$[(\sigma_e)_M]_I$	=	82195.59 kPa
linear elastic analysis, II	$[(\sigma_e)_M]_{II}$	=	63351.79 kPa

Location of maximum equivalent stress (element number)

linear elastic analysis, I		=	553
------------------------------	--	---	-----

linear elastic analysis, *II*

= 541*

The classical limit load corresponding to
the second elastic iteration,

$$\begin{aligned}(P_{LC})_{II} &= P \frac{\sigma_y}{(\sigma_e)_{max}} \\ &= 200 \times \frac{206850}{63351.79} \\ &= 653.02 \text{ kPa}\end{aligned}$$

Upper bound multiplier based on the ref-
erence volume,

$$m_R^0 = 6.19$$

Therefore the upper bound limit load,

$$\begin{aligned}P_U &= m_R^0 P = 6.19 \times 200 \\ &= 1238.0 \text{ kPa}\end{aligned}$$

Normalized maximum stress,

$$\begin{aligned}\bar{\sigma}_{Mi}^0 &= \frac{\sigma_{Mi}^0}{\sigma_y} = \frac{63351.79}{206850} \\ &= 306.3 \times 10^{-3}.\end{aligned}$$

Next, the coefficients *A*, *B* and *C* of equation (4.26) are determined as follows:

$$\begin{aligned}A &= (m_i^0)^4 (\bar{\sigma}_{Mi}^0)^4 + 4(m_i^0)^2 (\bar{\sigma}_{Mi}^0)^2 - 1, \\ &= 6.19^4 \times (306.3 \times 10^{-3})^4 + 4 \times 6.19^2 \times (306.3 \times 10^{-3})^2 - 1 = 26.30 \\ B &= -8(m_i^0)^3 (\bar{\sigma}_{Mi}^0)^2, \\ &= -8 \times 6.19^3 \times (306.3 \times 10^{-3})^2 = -178.01\end{aligned}$$

*Element numbers 553 and 541 lie very close to one another in the finite element mesh and are given here just to illustrate that the maximum stress location has not changed appreciably between the first and the second elastic iterations.

$$\begin{aligned}
C &= 4(m_i^0)^3(\bar{\sigma}_{Mi}), \\
&= 4 \times 6.19^3 \times (306.3 \times 10^{-3}) = 290.59
\end{aligned}$$

Equation (4.26) therefore becomes

$$26.3m_\alpha^2 - 178.01m_\alpha + 290.59 = 0$$

leading to $m_{\alpha 1}=2.75$ and $m_{\alpha 2}=4.02$. Considering the larger of the two roots, the lower bound limit load estimate is given by, $P_L = m_{\alpha 2}P = 4.02 \times 200 = 804.0$ kPa (116.6 psi). The limit load estimate using inelastic analysis and the classical lower bound method are found to be 858.0 kPa (124.4 psi) and 651.0 kPa (94.4 psi), respectively.

It should be noted that, in general, it is not difficult to satisfy the conditions stipulated by equations (4.11) and (4.12) for generic structures. The third condition [equation (4.13)], however, places stringent requirements on the redistributed stress field and can be satisfied only if the elastic modulus modification scheme is capable of producing perturbations about the original stress field. This requires that the modulus modification scheme should be weak ($q < 1$) in case of sensitive structures so as not to cause any abrupt change in the elastic moduli values. However, in the m_α -method, the primary requirement is a statically admissible stress field that satisfies the two conditions given by equation (4.11) and (4.12). Therefore, ensuring that the maximum stress location does not show any unreasonable change would be sufficient for all practical purposes.

4.7 Numerical Examples

In this section, limit load estimates are determined for a number of structural components of practical interest. The benchmark problems considered here are torispherical heads, an indeterminate beam, a thick-walled cylinder, a spherical pressure vessel with a cylindrical nozzle, a pressure vessel support skirt, non-symmetric rectangular plates and a compact tension specimen (Tables 4.2 and 4.4). The materials used are assumed to be homogeneous, isotropic and elastic perfectly-plastic. All the problems are modeled using the ANSYS¹ software. Four-noded isoparametric quadrilateral elements are used in the finite element modeling of all the two dimensional problems with the exception of the compact tension specimen.

Non-symmetric plates are modeled using the three-dimensional eight-noded isoparametric solid elements while the compact tension specimen is modeled using the two-dimensional isoparametric six-noded triangular elements and the two-dimensional isoparametric eight-noded quadrilateral elements. The ANSYS commands listings of all the problems are given in Appendix C.

The upper bound limit load, $m^o P$, the improved lower bound limit load, $m_a P$, and the classical lower bound limit load, P_{LC} , for the second linear elastic analysis are determined for the aforementioned problems. These estimates are then compared with analytical and inelastic finite element analysis results. Based on the first two linear elastic FEA iterations, all the problems

analyzed in this paper can be classified as Class I.

4.7.1 Thick-Walled Cylinder

The thick-walled cylinder considered has an inner radius of 7.62×10^{-2} m (3 in.) and an outer radius of 22.86×10^{-2} m (9 in.). The yield stress of the material is assumed to be 206.85×10^3 kPa (30×10^3 psi), and the modulus of elasticity is 206.85×10^6 kPa (30×10^6 psi). The Poisson's ratio is assumed to be equal to 0.3. An arbitrary uniform internal pressure of 68.95×10^3 kPa (10×10^3 psi) is applied.

The thick-walled cylinder is modeled as an axisymmetric, plane strain problem. The analytical limit load for this problem, using the von Mises yield criterion, is given by the expression

$$P_{exact} = \frac{2}{\sqrt{3}} \sigma_y \ln Y, \quad (4.28)$$

where Y is the ratio of the outer radius to the inner radius of the cylinder. The limit load estimates are presented in Table 4.5.

4.7.2 Indeterminate Beam

The indeterminate beam of span 50.8×10^{-2} m (20 in.) and thickness 2.54×10^{-2} m (1 in.), shown in Figure 2.6, has end A built-in and end B simply supported. The beam is assumed to have unit width in the direction normal to the paper. The modulus of elasticity, the yield strength and the Poisson's ratio are assumed to be the same as in the previous problem. The

beam is modeled for the plane stress condition. A uniform arbitrary pressure of 172.4 kPa (25 psi) is applied.

When the first plastic hinge forms at end A , the structure becomes statically determinate. As the load intensity is increased further, an additional plastic hinge forms at point C resulting in the collapse of the beam. An expression for the collapse load⁸ is

$$P_{exact} = \frac{11.66M_p}{L^2}. \quad (4.29)$$

The variation of m^o , m' and m_o with volume is shown in Figure 4.7. Table 4.5 gives the limit load estimates for the structure.

4.7.3 Torispherical Heads

A considerable amount of technical research has been devoted to the design of torispherical heads. An approximate analysis of torispherical heads was carried out by Drucker and Shield.⁵³ Subsequently, additional work constituting improvements to the foregoing paper was also published.⁵⁴

The dimensions of the torispherical heads considered here (Figure 4.1) are presented in Table 4.2. The modulus of elasticity, yield strength and Poisson's ratio are assumed to have the same values as in the previous problems. The pressure vessels analyzed have a uniform thickness of 2.54×10^{-2} m (1 in.) through out. The ratio of the average diameter of the torispherical head (D) to the thickness of the shell (t) is taken to be equal to 300 (consistent with thin shell theory). An arbitrary internal pressure of 200 kPa (29 psi) is

Indeterminate Beam Subjected to Uniform Load

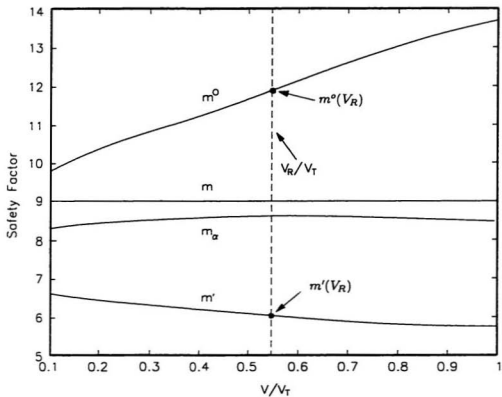


Figure 4.7: Variation of m^o , m' and m_α with Volume in an Indeterminate beam

Table 4.2: Dimensions of Torispherical heads

Case No.	Head Geometry Parameters		
	L_s/D	r/D	H/D
1	0.8	0.12	0.2360
2		0.14	0.2468
3		0.16	0.2577
4	0.7	0.12	0.2619
5		0.14	0.2710
6		0.16	0.2804
7	0.6	0.12	0.3068
8		0.14	0.3136
9		0.16	0.3207

applied. The variation of m^o , m' and m_o with volume is shown in Figure 4.8. The values of the limit loads are presented in Table 4.3.

4.7.4 Spherical Pressure Vessel with a Cylindrical Nozzle

Limit analysis of axisymmetric nozzles has been a topic of substantial interest since the 1960's. Analytical limit analyses of these structural components are available in a number of references.^{55,56} The nozzle-shell geometry parameters are as shown in Figure 4.9. To avoid any stress singularities, a fillet radius equal to $t/2$ has been provided at the re-entrant corner of the

Table 4.3: Limit Load Estimates of Torispherical Heads[†]

Case No. [‡]	Lower bounds		Inelastic FEA	Drucker & Shield ^{§§,54}	Upper bound $m_R^o P$
	$P_{LC}^†$	$m_o P$			
1	650.0 (567.7)*	804.0	858.0	803.3	1238.0
2	760.2 (662.3)	943.5	970.6	893.6	1326.9
3	863.4 (756.6)	1068.6	1100.0	983.9	1413.8
4	760.8 (657.6)	941.3	1002.0	947.4	1396.1
5	886.0 (780.8)	1098.4	1138.0	1050.1	1480.1
6	1024.2 (912.1)	1253.6	1288.0	1152.8	1560.8
7	933.2 (774.6)	1158.2	1260.0	1145.3	1635.1
8	1072.0 (913.6)	1321.0	1404.0	1263.9	1695.3
9	1240.0 (1081.9)	1488.0	1544.0	1382.4	1754.5

[†]All units in kPa

[‡]Refer Table 4.2 for shell geometries

[†] P_{LC} is the classical lower bound limit load obtained from the second linear elastic FEA.

*The quantities within the brackets correspond to $q = 0.25$ and those outside correspond to $q = 1$.

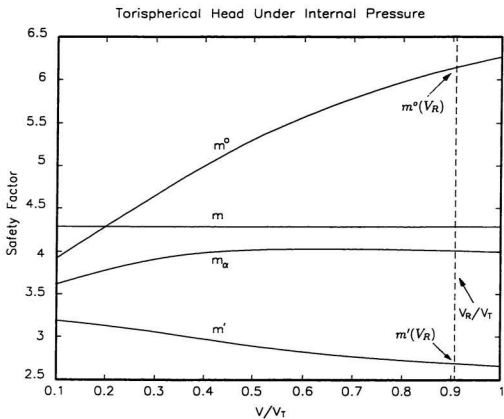


Figure 4.8: Variation of m^o , m' and m_α with Volume in a Torispherical Head

nozzle-shell intersection. The pressure vessel considered here has the values $R=1.0$ m (39.37 in.), $r=0.2$ m (7.87 in.) and $T=0.25$ m (9.84 in.). The nozzle thickness is determined by approximately sizing the pressure vessel based on the hoop stresses of the cylinder and the spherical shell expressible by the equation

$$t = \frac{2Tr}{R}. \quad (4.30)$$

The length of the nozzle is made greater than $5\sqrt{rt}$ to get away from the effects of stress discontinuities at the far end of the nozzle. The yield stress is assumed to be 300×10^3 kPa (43.51×10^3 psi) and the modulus of elasticity is taken to be 200×10^6 kPa (29×10^6 psi). The Poisson's ratio is taken to be the same value as for the previous problems. An arbitrary internal pressure of 200 kPa (29 psi) is applied. The results of the analyses are presented in Table 4.5.

4.7.5 Pressure Vessel Support Skirt

The pressure vessel support skirt shown in Figure 4.10 is a cylinder attached cone subjected to uniform axial load.⁵⁷ The top supporting ring is fixed to a rigid foundation. A blend radius is used at the cylinder-cone juncture. The sharp juncture notch and modeling singularity are eliminated because of the blend radius. The bottom of the cylinder has an axial load applied and it is free to deflect and rotate. The material yield strength is set at 275.8 MPa (40000.0 psi) and the Poisson's ratio is assumed to be 0.3. An axial pressure of 7736.2 kPa (1122.0 psi) is applied. This problem is of

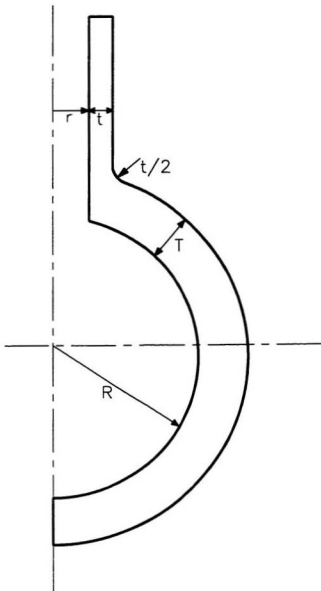


Figure 4.9: Dimensions of the Spherical Pressure Vessel with a Cylindrical Nozzle

interest since it serves as a bench-mark problem for developing stress classification procedures.⁵⁷ The limit load estimates for this problem are presented in Table 4.5.

4.7.6 Non-symmetric Rectangular Plate Structures

Plates form an important class of structural components since they are widely used as flat heads of pressure containments, internals of pressure vessels and heat exchangers, and various forms of closures. In this paper, the proposed methods are applied to non-symmetric plate structures with complex boundary conditions. The dimensions of the non-symmetric plate structures analyzed in this paper are shown in Figure 4.11. The elastic modulus, yield stress and the Poisson's ratio of the plates are assumed to have the same values as for the thick-walled cylinder. The plates are subjected to an arbitrary uniform pressure loading of 172.38 kPa (25 psi). The complex boundary conditions have been chosen for these problems with the intention of investigating the versatility and robustness of the proposed methods.

By virtue of their complex boundary conditions, analytical solutions for these configurations are difficult to obtain. For example, for the problems discussed in this section, the geometry along with the boundary conditions can cause complex shear interactions during failure thus rendering an analytical elastic-plastic analysis intractable. Assuming an appropriate collapse mechanism and evaluating an upper bound limit load is difficult for these types of problems. Also, the boundary conditions pose difficulties in estimating a

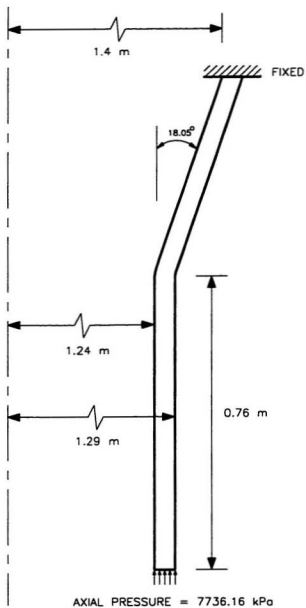
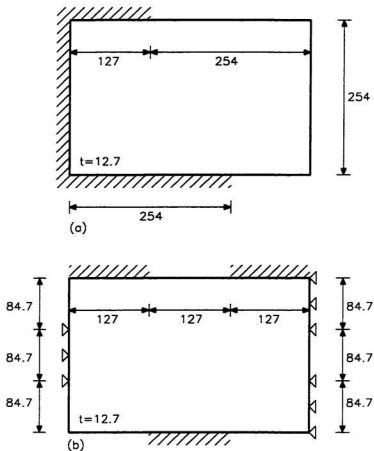


Figure 4.10: Pressure Vessel Support Skirt



- Note: (1) Figures not to scale
 (2) All dimensions in mm
 (3) Plates subjected to uniform pressure
 (4)  Simply supported edge
 Fixed Edge
 Free Edge

Figure 4.11: Non-symmetric Rectangular Plate Structures

lower bound limit load. The proposed methods, even for such complexities, provide a direct and systematic method for estimating the limit loads. The limit load estimates are given in Table 4.5.

4.7.7 Cracked Components

Determination of limit loads for cracked components is essential for the robust estimation of fracture parameters such as the J .^{58,59} For the present analysis, a compact tension specimen shown in Figure 4.12 is considered. The specimen is subjected to an arbitrary tensile force of 100 N (22.47 lbf). The material is assumed to exhibit elastic-perfectly plastic behavior. The elastic modulus of the material is assumed to be 211×10^6 kPa (30.6×10^6 psi) and the yield stress is taken to be 488.43×10^3 kPa (70.84×10^3 psi). The specimen is modeled as a plane stress problem with specified thickness.

It is necessary that the $(1/\sqrt{r})$ singularity of the strain field at the crack tip be generated when using linear elastic analysis. This is achieved most effectively by using an isoparametric six-noded triangular element with the mid-side nodes moved to quarter point.⁶⁰ This element exhibits strain singularity along the element boundaries as well as in the interior, and has finite strain energy and stiffness at all points within the element.

For the elastic perfectly-plastic behavior of the elements, Rice and Rosengren⁶¹ have shown the crack tip strain singularity to be of the order $(1/r)$. This is achieved by using an isoparametric eight-noded quadrilateral element that is degenerated into a triangle with mid-side nodes moved to the quarter

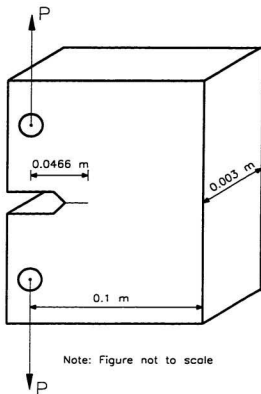


Figure 4.12: Compact Tension Specimen

Table 4.4: Configurations of Mechanical Components Analyzed

Case No.	Problem	Type of Loading
1	Thick Cylinder (Figure 2.2)	Uniform internal pressure
2	Indeterminate Beam (Figure 2.6)	Uniformly distributed load
3	Spherical Pressure Vessel (Figure 4.9)	Uniform internal pressure
4	Pressure Vessel Support Skirt (Figure 4.10)	Axial pressure
5	(a) Non-symmetric Plate (Figure 4.11a)	Uniform external pressure
	(b) Non-symmetric Plate (Figure 4.11b)	Uniform external pressure
6	Compact Tension Specimen (Figure 4.12)	Tensile load

point.⁶² It must be noted that the singular elements are used only around the crack tip, and these elements permit the use of a coarser mesh than is possible with ordinary elements. Because of the high stress gradients a third iteration is required in order to satisfy equation (4.27) for the m_α -method.

The limit loads obtained using the proposed methods are compared with inelastic finite element results (Table 4.5).

4.8 Closure

An improved method for determining lower bound limit loads of pressure components is presented in this chapter. The phrase m_α -method refers to the use of α elements in the finite element discretization scheme that pertains to the identification of an appropriate reference volume.

Table 4.5: Limit Load Estimates of Mechanical Components[†]

Case No. [‡]	Lower bounds		Inelastic FEA	Analytical Method	Upper bound m_R^*P
	P_{LC}^{\dagger}	$m_a P$			
1	180.1×10^3 (124.6×10^3)	220.5×10^3	261.6×10^3	262.4×10^3	272.6×10^3
2	1202.2 (882.6)	1490.2	1553.1	1507.3	2006.0
3	96.7×10^3 73.1×10^3	118.6×10^3	135.1×10^3	136.5×10^3	148.6×10^3
4	148.8×10^3 (119.6×10^3)	184.1×10^3	247.2×10^3	-	273.2×10^3
5a	453.4 (252.6)	561.3	707.7	-	827.1
5b	2691.2 (1644.3)	3219.0	3483.1	-	3770.0
6*	12.6 (3.5)	14.0	15.4	-	15.6

[†] All units in kPa unless otherwise specified

[‡] Refer Table 4.4 for respective configurations

[‡] P_{LC} is the classical lower bound limit load obtained from the second linear elastic FEA.

* The quantities within the brackets correspond to $q = 0.25$ and those outside correspond to $q = 1$.

* Units in kN

The multiplier m_{α} is obtained from the results of a linear elastic FEA by leap-frogging to a limit state. The numerical examples demonstrate that the method is accurate and versatile. A classification of components and structures into Class I, II and III categories is also provided so that insight into the behavior of sensitive structures is obtained.

Lower bounds obtained by the m_{α} -method are consistently better than the corresponding limit load estimates based on the classical lower bound theorem. The method can be applied to a wide range of symmetric and non-symmetric geometric configurations and complex loading conditions.

Chapter 5

In Search of the Redistribution Nodes

5.1 Introduction

The reference stress method attempts to correlate creep deformations in a structure with the results of a uniaxial creep test. The reference stress is relatively insensitive to material parameters characterizing creep behavior. The method has applications in the design and life assessment of nuclear and pressure components. Problems pertaining to creep growth, rupture damage, creep buckling, and more recently, elastic-plastic fracture are some specific cases where the method has been applied.

Determination of the reference stress is not always a simple task. An approximate method of its determination relies on the availability of limit load for the component. However, determination of limit load in itself is by no means an easy task. Seshadri⁵ introduced the r-node method in an attempt to directly determine the reference stress of generic structures and

hence the limit loads. R-Nodes are load-controlled locations in a mechanical component or a structure. As such, r-nodes lie on a distribution of stresses corresponding to primary stress as defined in the ASME codes and can be determined on the basis of two linear elastic analyses. On account of its load controlled nature, the “combined r-node equivalent stress” can be identified with the reference stress, which is widely used in integrity assessments of components and structures. The r-node method has been applied to a variety of mechanical components and structures³⁴⁻³⁶ and was found to provide good estimates of limit loads.

This chapter unifies the concepts of r-nodes, reference stress and the primary stress as defined in the ASME pressure vessels and piping codes. Aspects pertaining to lower bound limit loads are addressed because of their relevance in engineering design and practical guidelines are provided for analysts and designers.

5.2 R-Node Peaks and Collapse Mechanism

The r-node method for determining limit load estimates has been successfully used for estimating the limit loads for a variety of mechanical components and structures. The key to obtaining good estimates of limit loads using the r-node method lies in the proper identification of the r-node peaks.

In the case of certain structures, the r-node peaks are distinct and sufficiently spaced pointing to a “kinematically admissible” collapse mechanism. The problems that fall in this category are structures like beams, circu-

lar plates, arches, frames and symmetric three-dimensional rectangular plate configurations. Figure 2.6 and 5.1 show an indeterminate beam subjected to a uniform load and the corresponding collapse mechanism and r-node diagrams respectively. The plasticity spread at collapse as obtained from a detailed inelastic finite element analysis is also shown in Figure 5.1. It can be seen that the plastic hinge locations are well represented by the r-node diagram. However, in the case of structures such as an axisymmetric spherical pressure vessel with a cylindrical nozzle subjected to uniform internal pressure, detailed inelastic analysis reveals that a clear failure mechanism does not form prior to collapse (Figure 5.2). Rather, the failure is by the gross spread of plasticity surrounding the re-entrant region of the structure. Therefore, the r-node diagram cannot be expected to point to a distinct kinematically admissible collapse mechanism for these types of problems. Figure 5.3 shows the r-node diagram for the pressure vessel. For this problem, the r-node peak number one acts as a plastic control center describing the collapse process. Although the r-node diagram consists of three peaks, only one peak (i.e., peak number one) is considered for limit load determination. The reasons for not considering the other two peaks are described in Section 5.4.

5.3 Virtual R-Node Peaks and Convergence of R-Node Stresses

As explained earlier, the presence of distinct r-node peaks points to the existence of a possible collapse mechanism for the structure under consid-

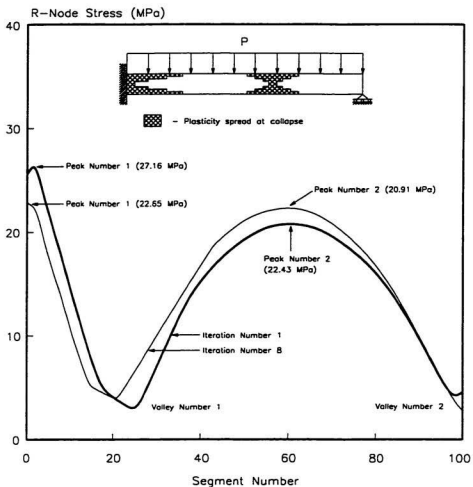


Figure 5.1: Indeterminate Beam subjected to Uniform Load - Dimensions and Convergence of Peak R-Node Stresses ($q = 1$)

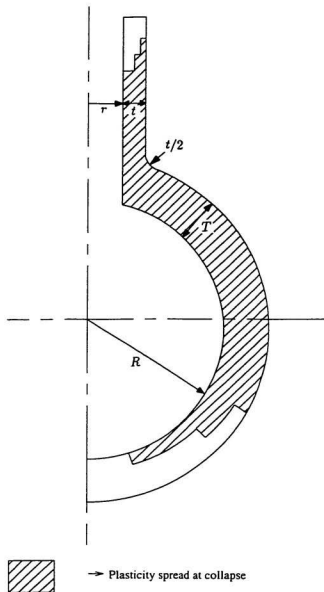


Figure 5.2: Spherical Pressure Vessel with a Cylindrical Nozzle subjected to Uniform Internal Pressure - Dimensions and Plasticity Spread at Collapse

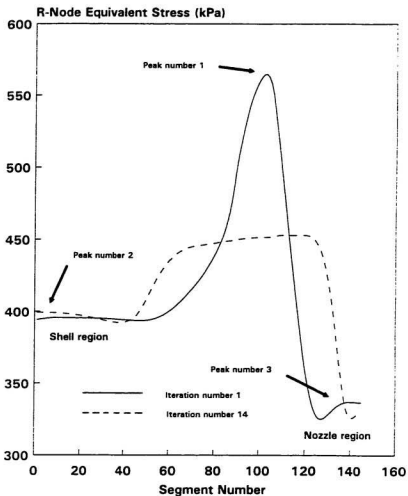
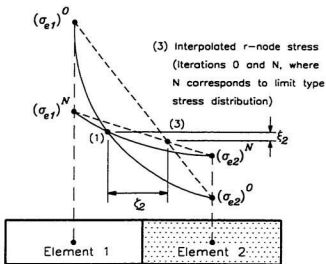
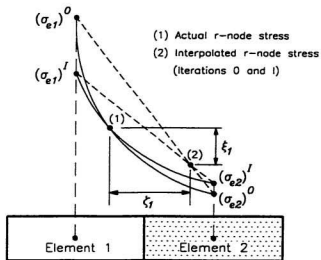


Figure 5.3: R-Node Diagrams of the Spherical Pressure Vessel with a Cylindrical Nozzle ($q = 1$)

eration. Some r-node peaks can be introduced due to errors arising out of interpolation of the stresses (Figure 5.4). These peaks, termed as “virtual r-node peaks”, should be ignored while estimating collapse loads.

The r-node method is a practical technique for determining limit loads based on the first and the second linear elastic finite element analyses. However, in order to illustrate the transient nature of the virtual r-nodes and to show that the real r-node stresses do converge to load-controlled limit type stresses, multiple successive elastic iterations are carried out. The first stress distribution corresponds to the initial elastic FEA and is designated as iteration number zero ($i = 0$). The modified stress distribution is obtained from one of the successive iterations and is indicated by the corresponding iteration number ($i = N$). As shown in Figure 5.4, the error in determining the r-node stress decreases as the modified stress distribution approaches limit type. The error involved in determining the r-node stress is shown as a consequence of the linear interpolation of the element centroidal stresses. Similar trends can be expected even if polynomial interpolations are used.

The presence of virtual r-node peaks can be demonstrated, for instance, by analyzing the r-node diagram of a torispherical head subjected to uniform internal pressure shown in Figure 4.1. The r-node diagrams corresponding to the first ($i = 0$) and the second ($i = 1$) linear elastic analyses, and the first and the third ($i = 2$) linear elastic analyses are shown in Figure 5.5. It can be observed from both the r-node plots that while peak number one is



ξ_1, ξ_2 - Interpolation errors pertaining to r -node stresses
 ζ_1, ζ_2 - Interpolation errors pertaining to r -node locations

Figure 5.4: Interpolation Errors while determining R-Nodes - Effect of Stress Distributions

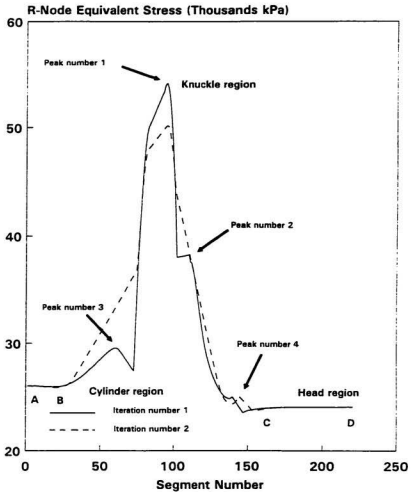


Figure 5.5: R-Node Diagram of a Torispherical Head subjected to Uniform Internal Pressure ($q = 1$)

real, peaks number two and three are virtual.

The convergence of the r-node stresses with elastic iterations can, for the purpose of illustration, be demonstrated by considering an indeterminate beam subjected to uniform load (Figure 2.6). It can be seen that the two distinct r-node peaks having different r-node stress magnitudes reach almost identical values after a number of linear elastic iterations as shown in Figure 5.1. Let σ_{n1} and σ_{n2} be the two r-node peak stresses of the indeterminate beam structure. The combined r-node stress $\bar{\sigma}_n$ is given by

$$\bar{\sigma}_n = \frac{\sigma_{n1} + \sigma_{n2}}{2}. \quad (5.1)$$

Here, the r-nodes are determined on the basis of initial elastic analysis, and the subsequent elastic results after the elastic moduli modification has been introduced. In order to verify the convergence of real r-node peaks, a number of elastic iterations can be carried out. When satisfactory stress convergence is achieved (say, at $i = r$), the r-nodes can be determined based on the stress distributions corresponding to the initial and the rth linear elastic analysis. The r-node stress of peak number one drops from its initial value of σ_{n1} to a value σ'_{n1} . Likewise, the r-node stress of peak number two increases from its original value of σ_{n2} to a value σ'_{n1} . The combined r-node stress is therefore given by

$$\bar{\sigma}_n = \frac{\sigma'_{n1} + \sigma'_{n1}}{2} = \sigma'_{n1}. \quad (5.2)$$

The real r-node peaks reach almost equal stress values after several iterations because, during collapse, the plastic hinges have the same stress value (equal

to yield stress).

In the above discussion, use of the initial elastic iteration for determining the r-node stresses (i.e., σ_{n1} , σ_{n2} and σ'_{n1}) is for reducing the interpolation errors pertaining to the r-node locations. This aspect is illustrated in Figure 5.4).

5.4 Identification of Real R-Node Peaks

It was explained earlier that virtual r-node peaks can exist in an r-node diagram because of interpolation errors. However, these virtual peaks progressively vanish as the modified linear elastic stress distribution approaches limit type. This of course requires a number of elastic iterations. However, the present objective is to obtain reasonably good lower bound limit load estimates based only on the first two linear elastic analyses. Therefore, practical guidelines for determining the real r-node peaks are provided as follows:

1. The r-node peaks that are present at simply supported edges are virtual. Every r-node peak is a potential plastic nucleation center. Since plastic moments cannot be developed along simply supported boundaries, r-node peaks at or in close proximity to these locations are virtual.
2. The uniform portion of an r-node diagram indicates the presence of membrane stress and absence of discontinuity stress in the region. Consider, for instance, the r-node diagram of a torispherical head (Figure 5.5). The portions AB and CD of the r-node diagram, being nearly

uniform, represent the regions where membrane stresses are dominant.

3. An r-node peak located in the vicinity of a boundary (other than simply supported; say, fixed or symmetric boundary for instance) can be identified as real if it is flanked by the boundary on one side and a valley on the other side. An r-node peak elsewhere in the structure can be recognized by the presence of valleys on its either sides. One stipulation while identifying a valley is that the minimum r-node valley stress should approximately correspond to the average membrane stress of the structure. Based on this criterion, peak number two of the torispherical head (Figure 5.5) can be readily identified as a virtual peak, since the valley to the left of it is much higher than the regions of uniform membrane stress represented by the lines *AB* and *CD*. Using the same argument, peak number one can be classified as real.
4. Examining Figure 5.6, which is the r-node diagram of a torispherical head corresponding to $q = 0.25$, it would seem at the immediate instance that there are two r-node peaks. However, a closer look would reveal that the so-called valley is comprised of only a single low stressed r-node. If this r-node is not included, the r-node diagram presents an entirely different picture. A valley should consist of at least an acceptable number of r-nodes as could be seen, for instance, in Figure 5.1. Therefore it can be concluded that there is only one r-node peak in Figure 5.6.

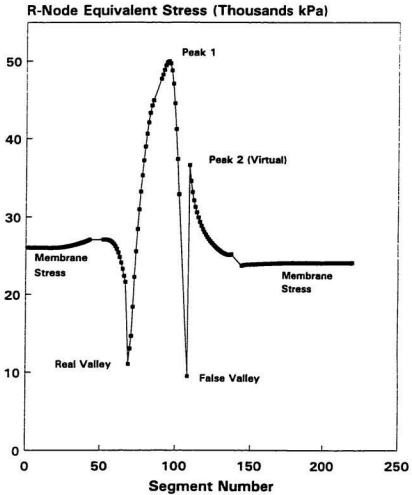


Figure 5.6: R-Node Diagram of a Torispherical Head ($q = 0.25$)

5. An r-node peak which is not distinct and located away from a "critical region" of the component or structure is a virtual peak. This can be demonstrated by analyzing the r-node diagram of the spherical pressure vessel with a cylindrical nozzle subjected to uniform internal pressure (Figure 5.3). The critical region for this structure is the region surrounding the re-entrant intersection of the nozzle and the shell (Figure 5.2). The r-node peaks number two and three are located far away from the re-entrant corner, at the extremities of the shell and nozzle portions. As seen in Figure 5.3, these regions of the shell and nozzle have uniform membrane stresses of low magnitudes and therefore are least likely to undergo failure. Thus the r-node peaks number two and three can be classified as virtual.

6. R-Node peaks along otherwise uniform r-node curves should be treated as virtual. This aspect can be illustrated by considering the example of the torispherical head shown in Figure 4.1. The region CD in the r-node diagram shown in Figure 5.5 has uniform membrane stress. The r-node peak number four has a stress value comparable to this membrane stress value. Therefore, in the likelihood of peak number four becoming plastic, the regions represented by AB and CD in Figure 5.5 should also become plastic. This would result in the entire structure becoming plastic at collapse. However, intuitively this is unlikely to happen since collapse would have occurred much earlier because of localized plasticity. Thus the r-node peak number four cannot be clas-

sified as a real peak.

While the guidelines proposed above are general, it is necessary to take precautions in order to rationally eliminate r-node peaks that are virtual. This is dependent on the specific component or structure that is being analyzed. In a situation where there is an uncertainty in deciding whether or not an observed r-node peak is virtual, it is prudent to consider only those r-node peaks that satisfy the above stated guidelines. The phrase “when in doubt leave it out” is useful for obtaining lower bound limit load estimates. In the extreme case where identification of r-node peaks become very difficult, to assure lower bounds it is suggested that the maximum r-node stress be used for calculating the limit load. Incidentally, the location and magnitude of the peak r-node stress are consistently found to be stable when compared to the maximum stress, with repeated elastic iterations. Two representative cases are presented in Tables 5.1 and 5.2 in order to illustrate the same.

5.5 Criteria for Lower-Bound Limit Loads

The main purpose of carrying out a number of elastic iterations in conjunction with systematic elastic moduli modification is to ensure that the resulting stress distributions progressively approach limit type. In other words, the stress fields should belong to a “family of distributions”, flanked by the distributions corresponding to the creep indices $n = 1$ and $n \rightarrow \infty$. This can be illustrated by considering a section of the indeterminate beam shown in Figure 2.6. A near limit type stress distribution is achieved in this case in

Table 5.1: Maximum Values of Equivalent and R-Node Stresses in a Torispherical Head* ($q = 1$)

Iteration No.	Maximum Equivalent Stress (kPa)		Maximum R-Node Stress (kPa)	
	Magnitude	Element Number	Magnitude	Element Number [†]
0	77564.00	553	-	-
1	59933.00	541	54167.91	567
2	82471.00	655	50190.78	568
3	69828.00	655	49127.14	569
4	60985.00	398	48647.28	569
5	67000.00	398	48373.66	569
6	96481.00	674	48214.06	569
7	65239.00	674	48168.21	574
8	71979.00	680	48085.51	580
9	73701.00	680	48070.41	580
10	57891.00	680	48046.12	580
11	51933.00	397	48004.39	580
12	65049.00	686	47980.21	580
13	57079.00	686	47964.33	580
14	51721.00	398	47948.00	569

*Case Number 1 in Table 4.2

[†]The element numbers are indicated only to illustrate the better locational stability of the highest stressed r-node as compared to the maximum stress location.

Table 5.2: Maximum Values of Equivalent and R-Node Stresses in a Pressure Vessel Support Skirt* ($q = 1$)

Iteration No.	Maximum Equivalent Stress (kPa)		Maximum R-Node Stress (kPa)	
	Magnitude	Element Number	Magnitude	Element Number [†]
0	2900.30	708	-	-
1	1734.20	708	1586.42	669
2	1595.40	708	1526.92	669
3	1509.30	708	1468.93	669
4	1632.50	1008	1418.79	668
5	1656.20	1008	1380.59	668
6	2044.80	1020	1352.88	668
7	2080.80	1020	1332.58	668
8	1946.30	1020	1317.30	668
9	1793.50	1020	1305.64	668
10	1644.80	1020	1296.44	668
11	1604.80	1032	1289.22	668
12	1622.20	1032	1284.00	668
13	1581.80	1032	1280.05	668
14	1513.70	444	1276.76	668

*Refer to Table 4.4 for details pertaining to this component

[†]The element numbers are indicated only to illustrate the better locational stability of the highest stressed r-node as compared to the maximum stress location.

the seventh linear elastic iteration as shown in Figure 5.7. The intermediate stress distributions lie in between the zeroth and the seventh iterations, in the order of increasing iterations. The conditions that are to be satisfied for ensuring this are given by equations (4.11) to (4.13), viz.,

$$\left. \begin{aligned}
 (1) \quad & \frac{dm^o}{d\zeta} \leq 0 \\
 (2) \quad & \frac{d\sigma_M^o}{d\zeta} \leq 0 \\
 (3) \quad & \text{The relative locations of the set of stresses} \\
 & \sigma_{e1} > \sigma_{e2} > \dots > \sigma_{eN} \text{ are invariant.}
 \end{aligned} \right\} \quad (5.3)$$

For a structure that is sensitive to elastic moduli modifications, leading to violation of equations (5.3), a lower value of q , say $q = 0.25$ or 0.5 , would improve the stability. The effect of the modulus adjustment index, q , on the stress distributions for a thick cylinder subjected to internal pressure is shown in Figure 5.8. The values of m^o , the maximum von Mises equivalent stresses and the corresponding locations are shown in Table 5.3. It can be seen that the stress distributions corresponding to $q \leq 1$ are valid since all the requirements stipulated by equations (5.3) are satisfied.

For generic structures it is not difficult to satisfy the first two conditions given by equation (5.3). The third condition, however, places very stringent requirements on the redistributed stress fields. Choosing a very small value of q , although effectively attenuates this problem, can lead to errors in determining the r-node stresses similar to those shown in Figure 5.4. Since the maximum stress in pressure components occurs mostly because of geometric

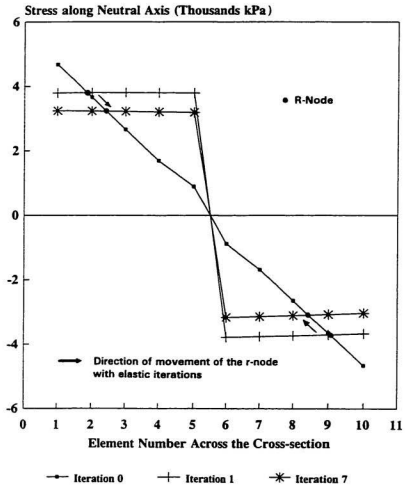


Figure 5.7: Stress Distribution across the Thickness of an Indeterminate Beam

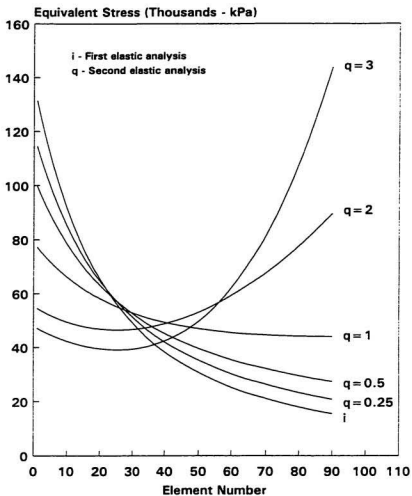


Figure 5.8: Influence of q for a Thick-Walled Cylinder analyzed in Section 4.7.1

Table 5.3: Values of $(\sigma_e)_{max}$, m° and Maximum Stress Location for the Cylinder considered in Figure 5.8

q	m°	$(\sigma_e)_{max}$ (MPa)	Maximum Stress Location (Element Number)
II Linear Analysis			
0.25	4.573	114.50	1
0.50	4.478	99.81	1
1.00	4.135	77.33	1
2.00	3.307	89.50	90
3.00	2.702	143.83	90
I Linear Analysis			
	4.605	131.47	1

discontinuities and secondary effects, it is quite sensitive to elastic iterations and redistributes readily. To achieve a practical compromise between the satisfaction of the third condition in equation (5.3) and an acceptable value of q , it would be sufficient to at least make sure that the maximum stress location does not vary with elastic iterations.

For explaining the conservative nature of the r-node stress, the stress distributions across a section of a beam are considered as shown in Figure 5.7. In this case, since limit type stress distribution is reached in the seventh elastic iteration, the value of the r-node stress $[(\sigma_{r-node})_{0-VII}]$ determined based on the zeroth and the seventh iterations, should correspond to the exact value. Since the remaining stress distributions are nested by these distributions, the r-node stresses determined using the remaining distributions should be such

that

$$(\sigma_{r-node})_{0-I} \geq (\sigma_{r-node})_{0-II} \geq \dots \geq (\sigma_{r-node})_{0-VII}. \quad (5.4)$$

Thus the limit load based on the first two iterations is always less than or equal to the exact limit load in this case. In case of generic structures which fail due to the formation of multiple hinges or hinge contours, equation (5.4) can be expressed as

$$(\bar{\sigma}_n)_{0-I} \geq (\bar{\sigma}_n)_{0-II} \geq \dots \geq (\bar{\sigma}_n)_{0-N} \quad (5.5)$$

where $(\bar{\sigma}_n)_{0-I}, (\bar{\sigma}_n)_{0-II}, \dots, (\bar{\sigma}_n)_{0-N}$ are the combined r-node stresses corresponding to the iteration pairs 0-I, 0-II, \dots , 0-N. In practice, since the r-nodes are determined based on the zeroth and the first elastic iterations, the corresponding stress value should be an upper bound. It is not, however, necessary to perform a number of elastic iterations in order to confirm the inequality given by equation (5.5). It would be sufficient to determine r-nodes based on the first two linear elastic analysis, provided that the first two conditions given by equation (5.3) and the invariance of the maximum stress location are satisfied by the stress distributions.

The aforementioned explanation can be illustrated by considering the indeterminate beam shown in Figure 2.6. The r-node peak stress values and the combined r-node stress values are given in Table 5.4. It can be seen that as the stress distribution approaches the limit type, the r-node peak stresses and the combined r-node stress also converge to a stable value.

Table 5.4: Variation of R-Node Peak Stresses with Elastic Iterations in an Indeterminate Beam

Elastic Iteration Pair	R-Node Peak Stress (MPa)		Combined R-Node Stress (MPa)	Maximum von Mises Equivalent Stress (MPa)
	σ_{n1}	σ_{n2}	$\bar{\sigma}_n = \frac{\sigma_{n1} + \sigma_{n2}}{2}$	
0-I	27.16	20.91	24.04	44.98
0-II	25.02	21.62	23.32	27.61
0-III	24.07	21.95	23.01	25.43
0-IV	23.49	22.15	22.82	24.23
0-V	23.12	22.27	22.69	23.64
0-VI	22.87	22.35	22.61	23.29
0-VII	22.73	22.40	22.57	23.03
0-VIII	22.65	22.43	22.55	22.83
Reference Stress (MPa): Inelastic = 22.98; Theory = 23.72				

5.6 Illustrative Example - Pressure Vessel Support Skirt

The systematic procedure for calculating the lower bound limit load of a Pressure Vessel Support Skirt is explained in this section. The dimensions of the pressure vessel and the pertinent details are given in Section 4.7.5 and Figure 4.10. Figure 5.9 shows the r-node diagram for this problem. The following are the calculation steps involved in determining the limit loads:

Applied axial pressure,	P	=	7736.2 kPa
Softening index,	q	=	1
Yield stress,	σ_y	=	275800 kPa
Upper bound multiplier			
linear elastic analysis, <i>I</i>	m_I^o	=	36.79
linear elastic analysis, <i>II</i>	m_{II}^o	=	36.05

Maximum equivalent stress (nodal stresses interpolated)

linear elastic analysis, <i>I</i>	$[(\sigma_e)_M]_I$	=	239.8 MPa
linear elastic analysis, <i>II</i>	$[(\sigma_e)_M]_{II}$	=	143.4 MPa

Location of maximum equivalent stress (element number)*

linear elastic analysis, <i>I</i>		=	708
-----------------------------------	--	---	-----

*The element numbers are given here just to illustrate that the maximum stress location has not changed between the two elastic iterations.

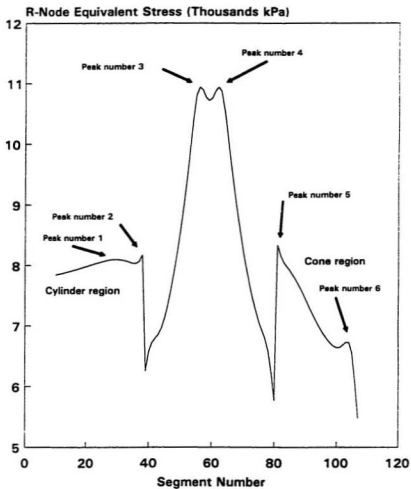


Figure 5.9: R-Node Diagram for a Pressure Vessel Support Skirt ($q = 1$)

linear elastic analysis, <i>II</i>	= 708
Number of r-node peaks	= 6

Virtual r-node peaks	
Peak Number	Reason
1	No distinct valleys
4	No distinct valley to the left - peaks 3 and 4 can coalesce into a single peak
6	No distinct valley on the left; part of an otherwise smooth curve

R-Node stresses of valid r-node peaks	
Peak Number	R-Node Stress (kPa)
2	8178.68
3	10938.33
5	8335.83

$$\text{Combined r-node stress, } \bar{\sigma}_n = \frac{8178.68 + 10938.33 + 8335.83}{3} = 9150.95 \text{ kPa}$$

$$\text{Limit load, } P_L = \frac{\sigma_y P}{\bar{\sigma}_n} = \frac{275800}{9150.95} \times 7736.19 = 233.16 \text{ MPa.}$$

The inelastic limit load estimate for this problem is 247.20 MPa and the classical lower bound limit load corresponding to the second linear elastic finite element analysis is 148.80 MPa.

5.7 Numerical Examples

In this section, the r-node method is used for determining the limit loads of mechanical components and structures analyzed in Section 4.7. Typical r-node diagrams for an indeterminate beam, a spherical pressure vessel with a cylindrical nozzle, torispherical heads and non-symmetric plate structures are shown in Figures 5.1, 5.3, 5.5, Figures 5.6 to 5.11 and Figures 5.12 to 5.15. The r-node diagram for the pressure vessel support skirt is shown in Figure 5.9. Figure 5.16 shows the stress distributions for a compact tension specimen. All the components are analyzed for two different values of q , viz., $q = 1$ and $q = 0.25$, and the limit load estimates are tabulated in Tables 5.5 and 5.6.

5.8 Closure

The conservative aspect of the r-node method is demonstrated in this chapter. A proper understanding of the underlying rationale behind the r-node method and the attributes of the r-nodes are important for analysts of practical engineering components in order to effectively implement the technique. This chapter provides a systematic approach for the determination of the r-node peaks that are relevant to lower bound limit loads.

Various investigators^{34-36,63} have successfully obtained good limit loads for a variety of problems such as frames, arches, pressure vessel heads and non-symmetric structures. The limit load estimates obtained using the method

Table 5.5: Limit Loads of Torispherical Heads using the R-Node Method⁵

Case No. [†]	1	2	3	4	5
Limit Load	763.7 (735.2)*	850.6 (827.9)	948.4 (929.2)	891.8 (859.1)	994.9 (971.0)

Case No.	6	7	8	9
Limit Load	1118.6 (1098.5)	1089.3 (1051.0)	1205.4 (1175.2)	1348.6 (1325.9)

⁵All units in kPa unless otherwise specified

[†]Refer Table 4.2 for shell geometries and Table 4.3 for limit load estimates using conventional methods

*The quantities within the brackets correspond to $q = 0.25$ and those without brackets correspond to $q = 1$.

are consistently lower than the inelastic finite element analysis results in all the cases - a feature one would expect since the formulation is based on equilibrium considerations alone. This conservative feature of the method is significant from the standpoint of engineering design.

Table 5.6: Limit Loads of Mechanical Components using the R-Node Method[‡]

Case No. [†]	1	2	3	4
Limit Load	261.3×10 ³ (232.0×10 ³) [*]	1483.3 (1383.2)	106.3×10 ³ (102.8×10 ³)	233.2×10 ³ (184.7×10 ³)

Case No.	5a	5b	6
Limit Load	651.9 (502.7)	3253.1 (2812.0)	11.9 (11.5) [*]

[‡]All units in kPa unless otherwise specified

[†]Refer Table 4.4 for respective configurations and Table 4.5 for limit load estimates using conventional methods

^{*}The quantities within the brackets correspond to $q = 0.25$ and those without brackets correspond to $q = 1$.

^{*}Units in kN

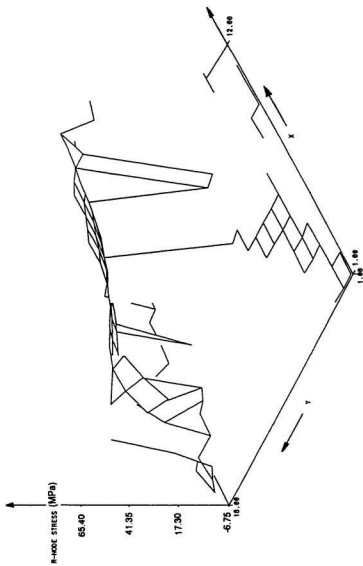


Figure 5.10: R-Node Stress Surface for the Non-Symmetric Plate Structure shown in Figure 4.11a

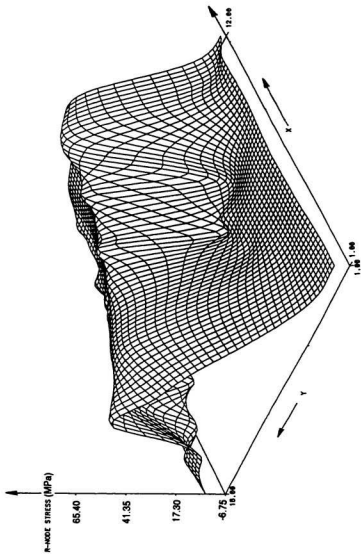


Figure 5.11: Spline Interpolated R-Node Stress Surface for the Non-Symmetric Plate Structure shown in Figure 4.11a

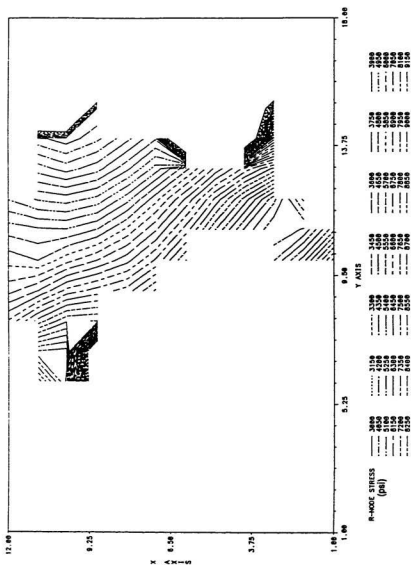


Figure 5.12: Iso R-Node Stress Contour for the Non-Symmetric Plate Structure shown in Figure 4.11a

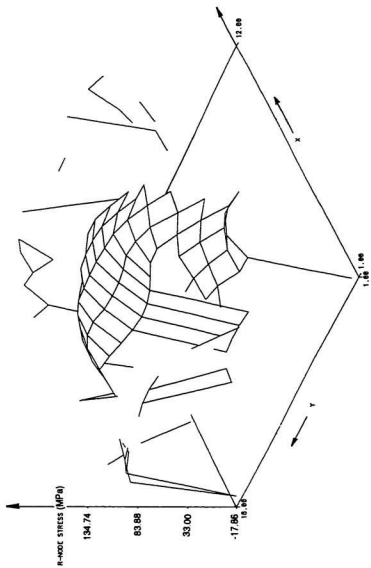


Figure 5.13: R-Node Stress Surface for the Non-Symmetric Plate Structure shown in Figure 4.11b

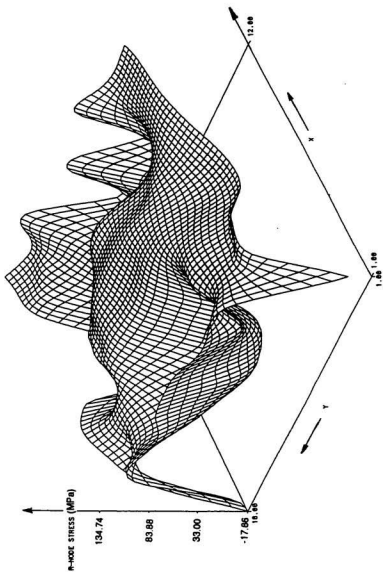


Figure 5.14: Spline Interpolated R-Node Stress Surface for the Non-Symmetric Plate Structure shown in Figure 4.11b

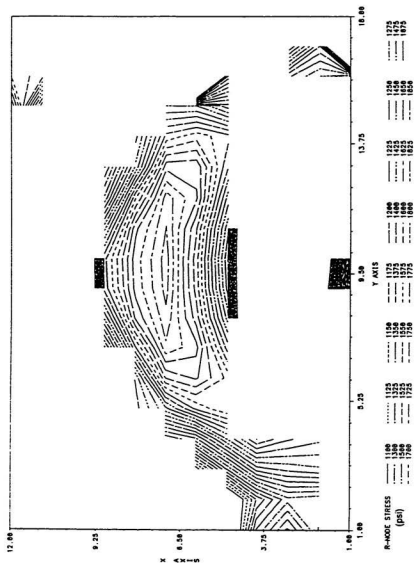


Figure 5.15: Iso R-Node Stress Contour for the Non-Symmetric Plate Structure shown in Figure 4.11b

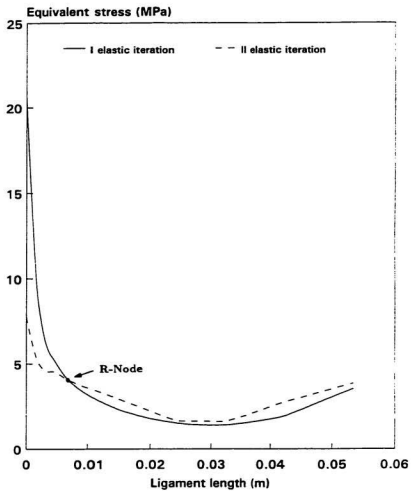


Figure 5.16: Stress Distributions for a Compact Tension Specimen

Chapter 6

Limit Loads of Layered Beams and Layered Cylindrical Shells using the R-Node Method

6.1 Introduction

The importance of built-in anisotropy in engineering design such as reinforced structures and composites is well known on account of their superior strength-to-weight characteristics. A knowledge of limit load of components fabricated from these materials is therefore important from a design standpoint. The r-node method of limit load determination has been found to give good estimates of lower bound limit loads for isotropic components. This success has provided the impetus to extend the method to laminated structures.

In this chapter, the r-node method is extended to two-layered beams and two-layered axisymmetric cylindrical shells. Each layer is assumed to be

made out of a homogeneous, isotropic and elastic perfectly-plastic material. While the formulations for the beam problems are developed by considering the theory of bending, the theorem of nesting surfaces of dissipation^{17,18} is invoked in the case of cylindrical shells. The limit load estimates are compared with inelastic finite element analysis results.

6.2 Limit Load Estimates of Two-Layered Beams subjected to Uniform Load

6.2.1 Elastic Modulus Modification Index based on Deformation Control ($q = 1$)

For an isotropic beam, the elastic modulus modification scheme given by equation (4.17) can be expressed as:

$$(E_s)_j = \left[\frac{\sigma_{arb}}{\sigma_{(z)}} \right]^q E_o \quad ; \quad 0 < q \leq 1 \quad (6.1)$$

where $\sigma_{(z)}$ is the stress in the direction of the neutral axis. For obtaining an expression similar to the above for a two-layered beam, one can invoke the theory of beam bending.

In this section, formulations for determining the limit load estimates of two-layered beams are presented for $q = 1$ in equation (6.1). The dimensions of a rectangular laminated beam subjected to pure bending is shown in Figure 6.1. The bending moment, M , at any cross-section of the beam can be expressed as

$$M = \int \sigma_{(z)} z \, dz$$

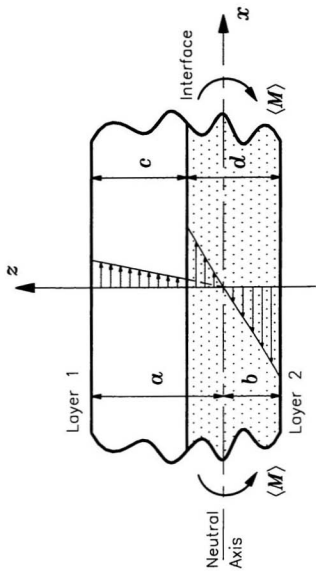


Figure 6.1: Two-Layered Beam under Pure Bending

$$= \int_{a-c}^a \sigma_{(z)} z \, dz + \int_0^{a-c} \sigma_{(z)} z \, dz + \int_{-b}^0 \sigma_{(z)} z \, dz \quad (6.2)$$

where $\sigma_{(z)}$ is the normal stress in the x direction. Assuming k to be the curvature of the beam for the second elastic analysis and considering that $\sigma_{(z)} = \epsilon_{(z)} E_{(z)}$, where $\epsilon_{(z)} = kz$, equation (6.2) can be rewritten as

$$M = \int_{a-c}^a E_{(z)1} k z^2 \, dz + \int_0^{a-c} E_{(z)2} k z^2 \, dz + \int_{-b}^0 E_{(z)2} k z^2 \, dz. \quad (6.3)$$

The subscripts "1" and "2" stand for material numbers one and two respectively.

The quantities $E_{(z)1}$ and $E_{(z)2}$ can be determined, in a manner similar to the expression given by equation (6.1), as

$$E_{(z)1} = E_1 \frac{(\sigma_{arb})_1}{[\sigma_{(z)1}]_I} \quad ; \quad E_{(z)2} = E_2 \frac{(\sigma_{arb})_2}{[\sigma_{(z)2}]_I} \quad (6.4)$$

where the subscript I stands for first linear elastic analysis.

The elastic stress distributions along the direction of the neutral axis can be expressed as.⁶⁵

$$\left. \begin{aligned} [\sigma_{(z)1}]_I &= \frac{MzE_1}{E_1I_1 + E_2I_2} \\ [\sigma_{(z)2}]_I &= \frac{MzE_2}{E_1I_1 + E_2I_2} \end{aligned} \right\} \quad (6.5)$$

where I_1 and I_2 are the corresponding moments of inertia of the layers.

Substituting equations (6.4) and (6.5) into equation (6.3) and simplifying, the expression for strain can be obtained as:

$$[\epsilon_{(z)}]_{II} = \frac{M^2 z}{[E_1I_1 + E_2I_2][\beta_1(\sigma_{arb})_1 + \beta_2(\sigma_{arb})_2]} \quad (6.6)$$

where

$$\beta_1 = \int_{a-c}^a z \, dz \quad \text{and} \quad \beta_2 = \int_{-b}^{a-c} z \, dz.$$

The subscript “II” in equation (6.6) stands for second linear analysis.

The expression for the stress in the first layer for the second linear analysis can be given by

$$[\sigma_{(z)1}]_{II} = E_{(z)1} [\epsilon_{(z)}]_{II}. \quad (6.7)$$

Substituting the first of equations (6.4) and equation (6.6) into equation (6.7) and simplifying,

$$[\sigma_{(z)1}]_{II} = \frac{(\sigma_{arb})_1 M}{\beta_1 (\sigma_{arb})_1 + \beta_2 (\sigma_{arb})_2}. \quad (6.8)$$

Similarly, the stress in the second layer for the second linear analysis is:

$$[\sigma_{(z)2}]_{II} = \frac{(\sigma_{arb})_2 M}{\beta_1 (\sigma_{arb})_1 + \beta_2 (\sigma_{arb})_2}. \quad (6.9)$$

From equations (6.8) and (6.9) it can be seen that the stress distributions after modifying the elastic moduli are independent of z . In other words, the stress distribution pertains to a limit type of distribution.

The condition for net-section yielding can be obtained from Figure 6.2 using similar triangles. As the applied load, P , is increased to P_1 so as to cause net-section yield, i.e., $P \rightarrow P_1$, then

$$\left. \begin{aligned} [\sigma_{(z)1}]_{II} &= \sigma_{n1} \rightarrow \sigma_{y1} \\ \text{and } [\sigma_{(z)2}]_{II} &= \sigma_{n2} \rightarrow \sigma_{y2} \end{aligned} \right\} \quad (6.10)$$

where σ_{n1} and σ_{n2} are the r-node stresses in the respective layers. If

$$P = \gamma P_1, \quad (6.11)$$

where γ is a scaling factor, equation (6.10) becomes

$$\left. \begin{aligned} [\sigma_{(z)1}]_{II} &= \gamma \sigma_{y1} \\ \text{and } [\sigma_{(z)2}]_{II} &= \gamma \sigma_{y2}. \end{aligned} \right\} \quad (6.12)$$

Equations (6.8), (6.9) and (6.12) lead to

$$\frac{[\sigma_{(z)1}]_{II}}{[\sigma_{(z)2}]_{II}} = \frac{(\sigma_{arb})_1}{(\sigma_{arb})_2} = \frac{\sigma_{y1}}{\sigma_{y2}}. \quad (6.13)$$

Therefore, a relationship between $(\sigma_{arb})_1$ and $(\sigma_{arb})_2$ can be obtained as

$$(\sigma_{arb})_2 = \frac{\sigma_{y2}}{\sigma_{y1}} (\sigma_{arb})_1. \quad (6.14)$$

Assuming $E_1(\sigma_{arb})_1 = C_1$ and $E_2(\sigma_{arb})_2 = C_2$, from equation (6.14) we obtain

$$C_2 = \left[\frac{\sigma_{y2}}{\sigma_{y1}} \right] \left[\frac{E_2}{E_1} \right] C_1 \quad (6.15)$$

and the corresponding secant moduli can be expressed as:

$$\begin{aligned} E_{(z)1} &= \frac{C_1}{[\sigma_{(z)1}]_I} \\ E_{(z)2} &= \frac{C_2}{[\sigma_{(z)2}]_I}. \end{aligned}$$

By taking C_1 to be any arbitrary positive value, C_2 can be determined thus enabling the second linear elastic analysis to be carried out. The quantities $[\sigma_{(z)1}]_I$ and $[\sigma_{(z)2}]_I$ can be determined from the first linear elastic analysis.

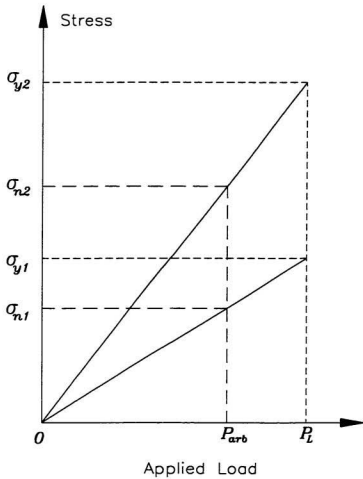


Figure 6.2: Relationship between R-Node Stresses and Yield Stresses in a Two-Layered Beam

The combined r-node stresses $\bar{\sigma}_{n1}$ and $\bar{\sigma}_{n2}$ for both the layers are determined separately. Ideally, the ratio of these values should correspond to the ratio of the corresponding yield stresses. However, the finite element mesh and interpolation can cause some numerical inaccuracies. Therefore, to be on the conservative side, the lower of $\sigma_{y1}/\bar{\sigma}_{n1}$ and $\sigma_{y2}/\bar{\sigma}_{n2}$ is taken to be the limit load multiplier. The limit load can then be expressed as:

$$P_L = P \left[\min \left(\frac{\sigma_{y1}}{\bar{\sigma}_{n1}}, \frac{\sigma_{y2}}{\bar{\sigma}_{n2}} \right) \right] \quad (6.16)$$

where P is the applied load, which is arbitrary.

6.2.2 General Elastic Modulus Modification Scheme ($0 \leq q \leq 1$)

Equation (6.15) was derived for a specific case of $q = 1$. In this section, the procedure is extended for the general case of $0 \leq q \leq 1$.

The moment, M , for the second linear analysis can be expressed in a manner similar to equation (6.3) as

$$M = \int_{a-c}^a E_{(z)1} k z^2 dz + \int_0^{a-c} E_{(z)2} k z^2 dz + \int_{-b}^0 E_{(z)2} k z^2 dz \quad (6.17)$$

where

$$\left. \begin{aligned} E_{(z)1} &= E_1 \left[\frac{(\sigma_{arb})_1}{[\sigma_{(z)1}]_f} \right]^q \\ E_{(z)2} &= E_2 \left[\frac{(\sigma_{arb})_2}{[\sigma_{(z)2}]_f} \right]^q \end{aligned} \right\} \quad 0 \leq q \leq 1. \quad (6.18)$$

Applying equations (6.5) and (6.18) in equation (6.17) and simplifying,

$$[\epsilon_z]_{II} = \frac{M^{(q+1)} z}{(E_1 I_1 + E_2 I_2)^q [\beta_1 (\sigma_{arb})_1^q + \beta_2 (\sigma_{arb})_2^q]} \quad (6.19)$$

where

$$\beta_1 = E_1^{(1-q)} \int_a^{a-c} z^{(2-q)} dz$$

$$\text{and } \beta_2 = E_2^{(1-q)} \int_{-b}^{a-c} z^{(2-q)} dz.$$

Considering that $[\sigma_{(z)}]_{II} = [\epsilon_{(z)}]_{II} E_{(z)}$, the following expressions can be obtained for the stresses

$$[\sigma_{(z)1}]_{II} = \frac{E_1^{(1-q)} (\sigma_{arb})_1^q M z_1^{(1-q)}}{\beta_1 (\sigma_{arb})_1^q + \beta_2 (\sigma_{arb})_2^q}; \quad (a-c) \leq z_1 \leq a \quad (6.20)$$

and

$$[\sigma_{(z)2}]_{II} = \frac{E_2^{(1-q)} (\sigma_{arb})_2^q M z_2^{(1-q)}}{\beta_1 (\sigma_{arb})_1^q + \beta_2 (\sigma_{arb})_2^q}; \quad -b \leq z_2 \leq (a-c) \quad (6.21)$$

At the interface, $z_1 = z_2$. Therefore,

$$\frac{[\sigma_{(z)1}]_{II}}{[\sigma_{(z)2}]_{II}} = \left[\frac{E_1}{E_2} \right]^{(1-q)} \left[\frac{(\sigma_{arb})_1}{(\sigma_{arb})_2} \right]^q. \quad (6.22)$$

Next, the two extreme cases, $q = 1$ and $q = 0$ are considered. For $q = 1$, equation (6.22) becomes

$$\left. \frac{[\sigma_{(z)1}]_{II}}{[\sigma_{(z)2}]_{II}} \right|_{q=1} = \frac{(\sigma_{arb})_1}{(\sigma_{arb})_2}. \quad (6.23)$$

Comparing equations (6.13) and (6.23), the relationship

$$\left. \frac{[\sigma_{(z)1}]_{II}}{[\sigma_{(z)2}]_{II}} \right|_{q=1} = \frac{\sigma_{y1}}{\sigma_{y2}} \quad (6.24)$$

can be obtained. For $q = 0$, the stress ratio given by equation (6.22) degenerates to the ratio of the elastic moduli, i.e.,

$$\left. \frac{[\sigma_{(z)1}]_{II}}{[\sigma_{(z)2}]_{II}} \right|_{q=0} = \frac{E_1}{E_2}. \quad (6.25)$$

Assuming the stress ratio to be a linear function of q ,

$$\frac{[\sigma_{(z)1}]_{II}}{[\sigma_{(z)2}]_{II}} = \omega_1 q + \omega_2, \quad (6.26)$$

and substituting equations (6.24) and (6.25) in equation (6.26) we obtain

$$\frac{[\sigma_{(z)1}]_{II}}{[\sigma_{(z)2}]_{II}} = \left[\frac{\sigma_{y1}}{\sigma_{y2}} - \frac{E_1}{E_2} \right] q + \frac{E_1}{E_2}. \quad (6.27)$$

Equations (6.22) and (6.27) together lead to the expression

$$C_2 = \frac{C_1}{\psi^q \{(\zeta - \psi)q + \psi\}} \quad (6.28)$$

where

$$\begin{aligned} C_1 &= \text{an arbitrary value,} \\ [E_{(z)}]_1 &= \frac{C_1}{[\sigma_{(z)1}]_I^q}, \\ [E_{(z)}]_2 &= \frac{C_2}{[\sigma_{(z)2}]_I^q}, \\ \psi &= \frac{E_1}{E_2}, \\ \text{and } \zeta &= \frac{\sigma_{y1}}{\sigma_{y2}}. \end{aligned}$$

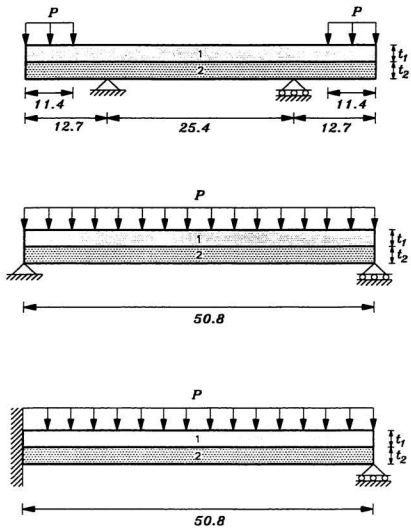
For $q = 1$, equation (6.28) reduces to the expression given by equation (6.14). For isotropic materials, $\zeta = \psi = 1$ leading to the equation $(\sigma_{arb})_1 = (\sigma_{arb})_2$. The absence of β_1 and β_2 in equation (6.28) implies that the position of the neutral axis has no effect in the elastic moduli modification scheme. The cross-sectional dimensions of the beam also do not have any significance with regards to equation (6.28).

6.2.3 Numerical Examples

Three different configurations of two-layered beams under different support conditions, as shown in Figure 6.3, are considered. These problems are analyzed for various values of q and elastic moduli ratios. The yield stresses are taken to be 68.95×10^3 kPa (10×10^3 psi) and 206.85×10^3 kPa (30×10^3 psi) respectively, for both the materials. The Poisson's ratio is assumed to be the same for both the materials, having a value of 0.3.

The beams, modeled for plane stress conditions using the ANSYS¹ software, are assumed to have unit width in the direction normal to the paper. The four noded iso-parametric quadrilateral elements are used for creating the finite element mesh. An arbitrary external load of 172.4 kPa (25 psi) is applied in all the three cases as shown in Figure 6.3.

The stress distributions for typical sections are shown in Figures 6.4 and 6.5. The r-node diagrams for an indeterminate beam is shown in Figure 6.6. The results obtained are compared with those obtained using inelastic finite element analyses and are presented in Tables 6.1 to 6.4. The inelastic results are, of course, independent of the elastic moduli ratios. A typical beam bending problem is characterized by the presence of an r-node on each side of the neutral axis.³⁴ However, for the ratios of E_1/E_2 equal to three and ten, only one r-node is present across the cross-section. The other r-node, although satisfying the requirement given by equation 6.13, is present outside the boundary of the structure and hence cannot be taken into consideration. Therefore, the corresponding results are also not valid



All dimensions in cm.

Figure 6.3: Dimensions of the Two-Layered Beams Analyzed

and are presented just for the purpose of illustration.

6.3 Limit Load Estimates of Two-Layered Axisymmetric Cylindrical Shells under Uniform Internal Pressure

It is well-known that the elastic properties of materials such as the Young's modulus and the Poisson's ratio have little influence on the limit load of any structure. However, while performing elastic analysis of layered structures, the relative elastic moduli values may give misleading indication as though these represent the relative strengths of the layers. Thus, the material with a higher elastic modulus would seem stronger, even though it might be having a lower value of yield strength than the remaining layers, thus leading to inaccurate magnitudes of the r-node stresses. In this section, formulations for the layered cylinder problem are carried out by determining the elastic material properties based on the magnitude of the reference stresses in the respective layers.

6.3.1 Formulations for Layered-Cylinder Problem

The theory of bending was used to carry out the formulations in the case of two-layered beam problems. However, since membrane stresses are dominant in a two-layered cylinder, a different formulation is necessary. One way of approaching this problem is by stipulating that the ratio of the reference stress values, calculated on the basis of the elastic properties, is equal to the

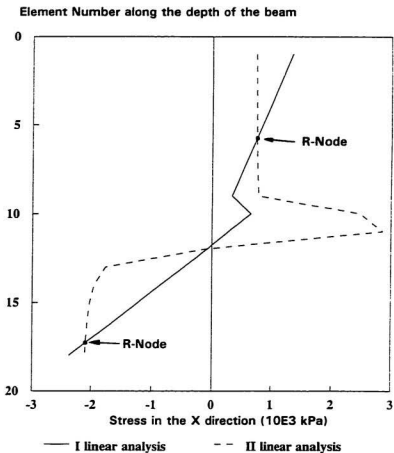


Figure 6.4: Stress Distribution in a Typical Section - Two-Layered Beam subjected to Pure Bending ($t_1 = t_2 = 1.27$ cm., $\psi = 1/3$ and $q = 1$)

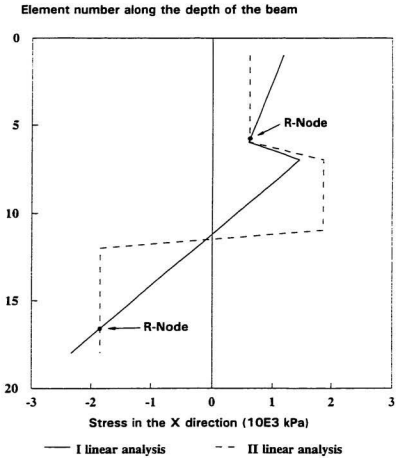


Figure 6.5: Stress Distribution in a Typical Section - Two-Layered Beam subjected to Pure Bending ($t_1 = 0.84$ cm, $t_2 = 1.70$ cm., $\psi = 1/3$ and $q = 1$)

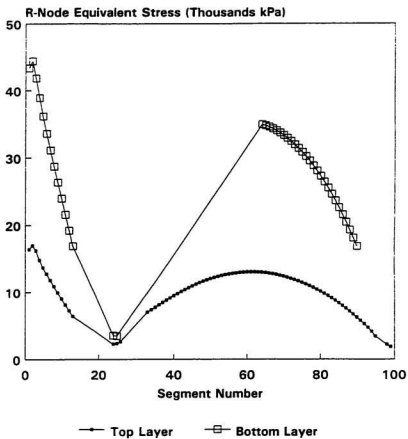


Figure 6.6: R-Node Diagram of a Two-Layered Indeterminate Beam subjected to Uniform Loading ($t_1 = t_2 = 1.27$ cm., $\psi = 1/3$ and $q = 1$)

Table 6.1: Limit Loads for a Two-Layered Beam subjected to Pure Bending[†] ($t_1 = t_2 = 1.27$ cm.)

Ratio of Elastic Moduli (kPa/kPa) $\psi = \frac{E_1}{E_2}$	Modulus adjustment index, q			
	1.00	0.75	0.50	0.25
$\frac{68.95 \times 10^6}{206.85 \times 10^6}$	2281.35	2169.37	2067.05	1976.93
$\frac{68.95 \times 10^6}{689.50 \times 10^6}$	2229.08	2237.50	2029.34	2382.50
$\frac{208.85 \times 10^6}{68.95 \times 10^6}$	1755.67	1357.63	1180.70	1077.14
$\frac{689.50 \times 10^6}{68.95 \times 10^6}$	1425.13	861.05	723.77	659.30

[†]Limit loads in kPa

Yield stress of the first layer, $\sigma_{y1} = 68.95 \times 10^3$ kPa

Ratio of yield stress values, $\zeta = 1/3$

Limit load estimate based on inelastic analysis, $(P_L)_{\text{Inelastic}} = 2327.06$ kPa

In the analyses pertaining to the last two rows of results, there is a significant shift in the neutral axis between the two linear elastic iterations. This introduces errors in the elastic modulus modification process and hence the results are not valid.

Table 6.2: Limit Loads for a Two-Layered Beam subjected to Pure Bending[†] ($t_1 = 0.846$ cm.; $t_2 = 1.694$ cm.)

Ratio of Elastic Moduli (kPa/kPa) $\psi = \frac{E_1}{E_2}$	Modulus adjustment index, q			
	1.00	0.75	0.50	0.25
$\frac{68.95 \times 10^6}{206.85 \times 10^6}$	2789.72	2670.78	2564.39	2467.24
$\frac{68.95 \times 10^6}{689.50 \times 10^6}$	2743.73	2723.87	2709.18	2704.01
$\frac{206.85 \times 10^6}{68.95 \times 10^6}$	2580.25	1430.57	1162.63	1057.49
$\frac{689.50 \times 10^6}{68.95 \times 10^6}$	2049.68	1129.61	757.48	622.07

[†]Limit loads in kPa

Yield stress of the first layer, $\sigma_{y1} = 68.95 \times 10^3$ kPa

Ratio of yield stress values, $\zeta = 1/3$

Limit load estimate based on inelastic analysis, $(P_L)_{\text{Inelastic}} = 2744.21$ kPa

The results in the last two rows are not valid for the same reason as mentioned in Table 6.1.

Table 6.3: Limit Loads for a Two-Layered Simply Supported Beam subjected to Uniform Pressure[†] ($t_1 = t_2 = 1.27$ cm.)

Ratio of Elastic Moduli (kPa/kPa) $\psi = \frac{E_1}{E_2}$	Modulus adjustment index, q			
	1.00	0.75	0.50	0.25
$\frac{68.95 \times 10^6}{206.85 \times 10^6}$	562.98	535.53	510.44	488.37
$\frac{68.95 \times 10^6}{206.85 \times 10^6}$	550.36	552.56	501.20	578.63
$\frac{206.85 \times 10^6}{68.95 \times 10^6}$	436.11	335.86	291.59	265.73
$\frac{689.50 \times 10^6}{68.95 \times 10^6}$	349.58	212.02	178.37	162.58

[†]Limit loads in kPa

Yield stress of the first layer, $\sigma_{y1} = 68.95 \times 10^3$ kPa

Ratio of yield stress values, $\zeta = 1/3$

Limit load estimate based on inelastic analysis, $(P_L)_{\text{Inelastic}} = 572.29$ kPa

The results in the last two rows are not valid for the same reason as mentioned in Table 6.1.

Table 6.4: Limit Loads for a Two-Layered Indeterminate Beam subjected to Uniform Pressure[†] ($t_1 = t_2 = 1.27$ cm.)

Ratio of Elastic Moduli (kPa/kPa) $\psi = \frac{E_1}{E_2}$	Modulus adjustment index, q			
	1.00	0.75	0.50	0.25
$\frac{68.95 \times 10^6}{206.85 \times 10^6}$	792.72	751.97	716.67	685.09
$\frac{68.95 \times 10^6}{689.50 \times 10^6}$	783.62	790.17	801.75	821.75
$\frac{206.85 \times 10^6}{68.95 \times 10^6}$	556.43	452.04	402.74	371.36
$\frac{689.5 \times 10^6}{68.95 \times 10^6}$	378.19	290.49	251.53	232.09

[†]Limit loads in kPa

Yield stress of the first layer, $\sigma_{y1} = 68.95 \times 10^3$ kPa

Ratio of yield stress values, $\zeta = 1/3$

Limit load estimate based on inelastic analysis, $(PL)_{\text{Inelastic}} = 861.88$ kPa

The results in the last two rows are not valid for the same reason as mentioned in Table 6.1.

ratio of the yield stress values. For a two-layered cylinder shown in Figure 6.7 this can be written as

$$\frac{(\sigma_{R1})_I (E_1, E_2, \nu, P, r_1, r_2, r_3)}{(\sigma_{R2})_I (E_1, E_2, \nu, P, r_1, r_2, r_3)} = \frac{\sigma_{y1}}{\sigma_{y2}} \quad (6.29)$$

The reference stress can be conveniently determined by using the "theorem of nesting surfaces"^{17,39} as:

$$\left. \begin{aligned} (\sigma_{R1})_I &= (\sigma_{ref1})_I = \sqrt{\frac{\int_{V_1} (\sigma_{eqv1})_I^2 dV}{V_1}} \\ \text{and} \\ (\sigma_{R2})_I &= (\sigma_{ref2})_I = \sqrt{\frac{\int_{V_2} (\sigma_{eqv2})_I^2 dV}{V_2}} \end{aligned} \right\} \quad (6.30)$$

where σ_{e1} and σ_{e2} are the von Mises equivalent stress values, obtained from linear elastic analysis, given by

$$\sigma_{eqv} = \frac{1}{\sqrt{2}} [(\sigma_\theta - \sigma_r)^2 + (\sigma_r - \sigma_z)^2 + (\sigma_z - \sigma_\theta)^2]^{1/2} \quad (6.31)$$

and σ_{ref} is the lower bound reference stress determined using the theorem of nesting surfaces.

If the vessel is subjected to a uniform internal pressure, P , then assuming plane-strain conditions, the expressions for the hoop, radial and longitudinal stresses can be given by the Lamé's equations as:⁶⁶

$$\left. \begin{aligned} [(\sigma_\theta)_i]_I &= \frac{P}{R_1^2 - 1} \left(1 + \frac{r_2^2}{r^2} \right) - \frac{P_{int} R_1^2}{R_1^2 - 1} \left(1 + \frac{r_1^2}{r^2} \right) \\ [(\sigma_r)_i]_I &= \frac{P}{R_1^2 - 1} \left(1 - \frac{r_2^2}{r^2} \right) - \frac{P_{int} R_1^2}{R_1^2 - 1} \left(1 - \frac{r_1^2}{r^2} \right) \\ [(\sigma_z)_i]_I &= \nu \{ [(\sigma_r)_i]_I + [(\sigma_\theta)_i]_I \} ; \quad r_1 \leq r \leq r_2 \end{aligned} \right\} \quad (6.32)$$

for the inner cylinder and

$$\left. \begin{aligned} [(\sigma_\theta)_2]_I &= \frac{P_{int}}{R_2^2 - 1} \left(1 + \frac{r_3^2}{r^2} \right) \\ [(\sigma_r)_2]_I &= \frac{P_{int}}{R_2^2 - 1} \left(1 + \frac{r_3^2}{r^2} \right) \\ [(\sigma_z)_2]_I &= \nu \{ [(\sigma_r)_2]_I + [(\sigma_\theta)_2]_I \} \quad ; \quad r_2 \leq r \leq r_3 \end{aligned} \right\} \quad (6.33)$$

for the outer cylinder.

In the above expressions, r_1 , r_2 and r_3 refer to the inside, interface and the outside radii respectively, and $R_1 = r_2/r_1$ and $R_2 = r_3/r_2$.

The displacements at the interface are given by the expressions:

$$\begin{aligned} [u_1(r_2)]_I &= - \frac{r_2 (-r_2^2\nu + r_2^2 - 2r_2^2\nu^2 - r_1^2\nu - r_1^2) P_{int}}{E_1 (-r_1^2 + r_2^2)} \\ &\quad - \frac{r_2 (2r_1^2\nu^2 + 2r_1^2\nu) P}{E_1 (-r_1^2 + r_2^2)} \end{aligned} \quad (6.34)$$

and

$$[u_2(r_2)]_I = \frac{r_2 (r_2^2\nu - r_2^2 + 2r_2^2\nu^2 + r_3^2\nu + r_3^2) P_{int}}{E_2 (r_2^2 - r_3^2)} \quad (6.35)$$

The term P_{int} refers to the interface pressure which can be determined by equating $u_1(r_2)$ and $u_2(r_2)$.

The equivalent stresses σ_{eqv1} and σ_{eqv2} can be determined by substituting equations (6.32) and (6.33) into equation (6.31). These equivalent stress expressions are then substituted into equation (6.30) for determining the respective reference stresses $(\sigma_{ref1})_I$ and $(\sigma_{ref2})_I$, taking into account equations (6.34) and (6.35). The condition given by equation (6.29) can therefore

be expressed as

$$\frac{(\sigma_{ref1})_I}{\sigma_{y1}} = \frac{(\sigma_{ref2})_I}{\sigma_{y2}} \quad (6.36)$$

The ratio of the yield stress and the reference stress values as given by equation (6.36) is denoted as m^o [equation (3.19)]. Therefore, equation (6.36) can be expressed as:

$$(m_1^o)_I = (m_2^o)_I \quad (6.37)$$

Equation (6.37) gives the necessary and sufficient condition for ensuring that the elastic properties selected result in stress values that point to the strengths of the cylinders in terms of their respective yield values.

The elastic constants E_1 , E_2 and ν should be selected such that equation (6.37) is satisfied. The foregoing computations can be easily performed by using any of the available symbolic mathematical softwares such as Maple.¹⁹

The elastic modulus softening is carried out by using the relations

$$E_{s1} = E_1 \left[\frac{(\sigma_{ref1})_I}{\sigma_{e1}} \right]^q$$

and

$$E_{s2} = E_2 \left[\frac{(\sigma_{ref2})_I}{\sigma_{e2}} \right]^q$$

where σ_{e1} and σ_{e2} correspond to the equivalent stress values of the elements in the respective layers, which can be obtained from the first linear elastic analysis.

Equation (6.37) can be readily extended for an “ N -layered” cylinder as

$$[m_1^o]_I = [m_2^o]_I = \dots = [m_N^o]_I \quad (6.38)$$

6.3.2 Numerical Examples

A variety of configurations of two-layered thick cylindrical shells are analyzed in this section. The dimensions, material properties and the limit load estimates are presented in Tables 6.5 and 6.6. The cylinders are modeled using four-node axisymmetric isoparametric elements under plane strain conditions. For performing the r-node analysis, an arbitrary uniform internal pressure of 50000 kPa is applied. Typical plots of stress distributions across the thickness are shown in Figures 6.8 and 6.9.

6.4 Closure

Anisotropic materials such as reinforced structures and composites play an important role in engineering design on account of their superior strength-to-weight characteristics. The main objective of this chapter is to demonstrate that the r-node method can be applied for determining the limit loads of layered structures. The formulations and the underlying theory for determining the r-nodes, at this stage, is not generic as in the case of isotropic structures.

The formulations that are presented in this paper are suitable for no more than two-linear elastic finite element analyses. The fact that the r-node method requires only two linear elastic analyses makes the method attractive for determining the limit loads.

The numerical examples demonstrate that the method is easy to implement and the results compare well with those obtained using inelastic finite

element analysis. Since the formulations for the beam problem are based on the theory of bending, these can also be extended for determining the limit loads of two-layered symmetric and non-symmetric plate structures.

Table 6.5: Limit Load Estimates for a Two-Layered Cylinder - Configuration 1[‡]

Case No.	Ratio of the yield strengths (kPa/kPa)	Ratio of Elastic Moduli (kPa/kPa)	Poisson's Ratio ν	Limit Pressure (kPa)	
	$\zeta = \frac{\sigma_{y1}}{\sigma_{y2}}$	$\psi = \frac{E_1}{E_2}$		R-Node [†]	Inelastic Analysis
1	$\frac{68.95 \times 10^3}{206.85 \times 10^3}$	91.87×10^{-3}	0.48	173999.96 (169537.42) [165347.17]	174170.00
2	$\frac{68.95 \times 10^3}{689.50 \times 10^3}$	7.57×10^{-3}	0.48	488393.86 (475391.87) [463234.06]	492330.00
3	$\frac{206.85 \times 10^3}{68.95 \times 10^3}$	1.04	0.48	161358.37 (158032.50) [154939.09]	160830.00
4	$\frac{689.50 \times 10^3}{68.95 \times 10^3}$	3.54	0.48	432077.64 (423586.11) [415703.42]	431560.00

[‡] $r_1 = 8$ cm., $r_2 = 13$ cm., $r_3 = 23$ cm., and $P = 50000$ kPa

[†]The numbers within the ordinary parenthesis and square brackets correspond to $q = 0.5$ and $q = 0.01$ respectively and those without the brackets correspond to $q = 1$.

Table 6.6: Limit Load Estimates for a Two-Layered Cylinder - Configuration 2[†]

Case No.	Ratio of the yield strengths (kPa/kPa) $\zeta = \frac{\sigma_{y1}}{\sigma_{y2}}$	Ratio of Elastic Moduli (kPa/kPa) $\psi = \frac{E_1}{E_2}$	Poisson's Ratio ν	Limit Pressure (kPa)	
				R-Node [‡]	Inelastic Analysis
1	$\frac{68.95 \times 10^3}{206.85 \times 10^3}$	91.60×10^{-3}	0.48	150701.95 (147140.36) [143674.01]	151670.00
2	$\frac{68.95 \times 10^3}{689.50 \times 10^3}$	11.67×10^{-3}	0.48	371599.79 (364928.77) [358207.42]	377160.00
3	$\frac{206.85 \times 10^3}{68.95 \times 10^3}$	1	0.48	197716.18 (191047.12) [184985.29]	197500.00
4	$\frac{689.50 \times 10^3}{68.95 \times 10^3}$	3.38	0.48	584330.75 (563049.82) [543765.77]	583340.00
5	$\frac{68.95 \times 10^3}{68.95 \times 10^3}$	318.80×10^{-3}	0.48	87442.12 (85003.86) [82713.93]	87282.00

[†] $r_1 = 10$ cm., $r_2 = 20$ cm., $r_3 = 30$ cm., and $P = 50000$ kPa

[‡]The numbers within the ordinary parenthesis and square brackets correspond to $q = 0.5$ and $q = 0.01$ respectively.

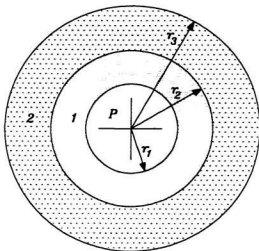


Figure 6.7: Two-Layered Cylinder under Internal Pressure

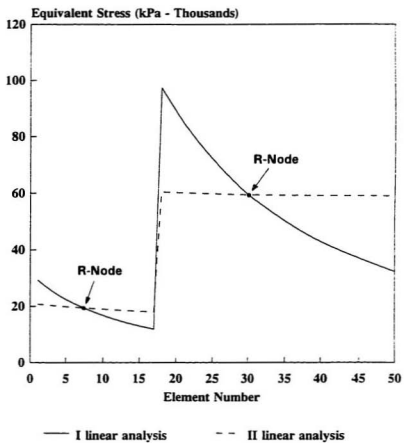


Figure 6.8: Typical Stress Distributions across a Layered Cylinder
 - Configuration 1, Case No. 1 ($q = 1$)

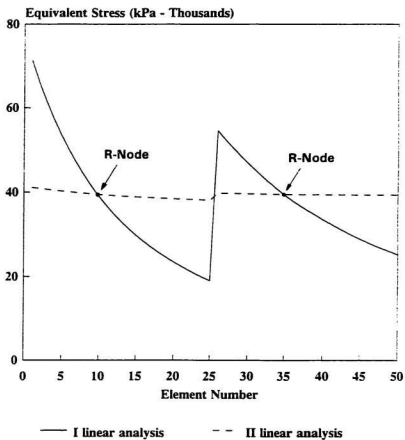


Figure 6.9: Typical Stress Distributions across a Layered Cylinder - Configuration 2, Case No. 5 ($q = 1$)

Chapter 7

Minimum Weight Design of Pressure Components using the Iso R-Node Stress Concept

7.1 Introduction

Limit load determination of mechanical components and structures using the r-node method^{5,34} involves identification of r-nodes as load-controlled locations. The r-node peaks and their corresponding equivalent stress values can characterize the nature of plastic collapse that is likely to occur. For instance, distinct r-node peaks could represent well-defined plastic hinge locations and suggest a kinematically admissible collapse mechanism. The non-peak r-nodes which in many cases represent a large volume of the structure, although load-controlled, may not always lead to cross-sectional plasticity.

While designing mechanical components and structures, in addition to the knowledge of limit loads, it is useful to know whether it is possible to

obtain an optimum shape that can perform the intended function with the minimum weight. The component design obtained as a consequence of such an objective, even if not practical due to various constraints, can still offer valuable insights. In many engineering applications such as structural designs for space projects, weight reduction with minimal loss of strength is of significant interest. For homogeneous materials, the minimum weight configuration coincides with minimum volume, and therefore, conventional studies^{10,67,68} have focused on the problem of minimizing the volume.

Although conventional analysis methods offer insight into the aspect of minimum weight, solutions are available only for simple geometric descriptions. The structures that are used in practice are much more complex, and therefore warrant procedures that are more general, simple and efficient. The r-node method offers a simple and systematic alternative for minimizing the weight of mechanical components and structures without significant loss of strength. The method invokes the load-controlled nature of the r-nodes and utilizes the r-node concept for structural optimization. In essence, the invocation of a minimum weight concept is tantamount to the finding of a "primary stress" structure.

7.2 Minimum Weight Design based on the Iso R-Node Stress Concept

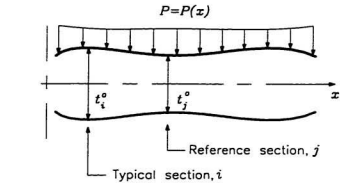
In any mechanical component or structure, distinct r-node peaks could represent well-defined plastic hinge locations or hinge contours depending on

the type of component or structure analyzed. The remaining r-nodes present in the structure, although load-controlled, may or may not lead to cross-sectional plasticity. It can therefore be inferred that if there is a structure with equal r-node stresses throughout, then such a structure would become entirely plastic at collapse. A thick cylinder subjected to uniform internal pressure is an example for such a case. In other words, if the geometry of a structure* is suitably modified so that the r-node stresses are of equal magnitude throughout, collapse would occur as a result of gross plasticity rather than by the formation of discrete plastic zones. The process of removal of material from a mechanical component or structure for the purpose of achieving uniform r-node stresses is the basis for minimum weight design using the r-node concept.

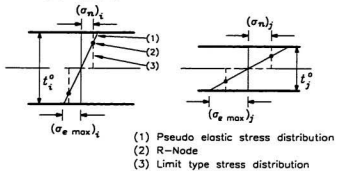
The procedure for minimizing the weight of structures using the r-node method can be illustrated by considering a simple structure (Figure 7.1) of an arbitrary length and of varying cross-section that is subjected to some prescribed loading such that the structure undergoes bending. Minimum weight design is achieved by modifying the geometry such that the entire structure would undergo concurrent yielding.

The r-nodes are assumed to be potential plastic hinge locations. It is reasonable to postulate that the cross-section of the structure with the highest r-node stress value would reach plasticity first, followed by another inde-

*that would have otherwise undergone collapse due to the formation of distinct plastic hinges



ORIGINAL STRUCTURE



FINAL OPTIMIZED STRUCTURE

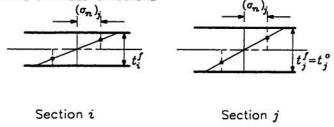


Figure 7.1: An Arbitrary Beam of Varying Cross-section - Application of the Iso R-Node Stress Concept

pendent plastic zone in the cross-section containing the next highest r-node peak. This process would continue until a kinematically admissible collapse mechanism leading to collapse of the component develops.

Let t_i be the thickness of any given cross-section, i , of the original structure as shown in Figure 7.1, and $(\sigma_n)_i$ the corresponding r-node equivalent stress. Unlike the elastic stresses which vary linearly across the cross-section, the r-node stresses, by virtue of being load-controlled, represent the entire cross-section (Figure 7.1). Therefore, for any section i containing an r-node or r-nodes, the limit type moment can be expressed as

$$(\bar{M}_p)_i = \frac{(\sigma_n)_i (t_i^o)^2}{4}, \quad (7.1)$$

where the superscript "o" stands for "original structure".

For the section, j , which contains the r-node with the highest equivalent stress, the moment for a fully plastic-type distribution can be expressed as:

$$(\bar{M}_p)_j = \frac{(\sigma_n)_j (t_j^o)^2}{4}. \quad (7.2)$$

When $(\sigma_n)_j$ approaches σ_y ; $(\bar{M}_p)_j$ approaches M_p , where σ_y and M_p stand for the material yield stress and the plastic moment, respectively.

From equations (7.1) and (7.2), for every cross-section of the structure to reach the plastic state simultaneously, the corresponding thickness t_i^o should be modified such that, as t_i^o approaches t_i^f ; $(\sigma_n)_i$ approaches $(\sigma_n)_j$, where the superscript "f" stands for "final optimized structure". This would be possible if the moment corresponding to limit type distribution, which is

primarily due to loading and boundary conditions, is stipulated to have the same value before and after optimizing the structure, i.e.,

$$\frac{(\sigma_n)_i (t_i^o)^2}{4} = \frac{(\sigma_n)_j (t_i^f)^2}{4} \quad (7.3)$$

from which the final thickness of any cross-section, i , can be obtained as,

$$t_i^f = \left(\sqrt{\frac{(\sigma_n)_i}{(\sigma_n)_j}} \right) t_i^o. \quad (7.4)$$

The expression for determining the section thickness corresponding to minimum weight design as given by equation (7.4) has been derived for a beam type structure where the failure is caused by bending stresses. However, practical mechanical components or structures are subjected to complex stress distributions, making it difficult for the analyst to guess 'a priori' the optimal configuration.

The main purpose of equation (7.4) is to establish a relationship between the cross-sectional dimensions of a structure subjected to bending and the r-node stress, in light of minimum weight design. It is not necessary, however, that similar specific expressions be derived for practical pressure components. The expression given by equation (7.4) is not unique for minimizing the weight of a beam structure. Any convenient empirical expression can be used for arriving at the final thickness, t_i^f . With a number of r-node iterations*, the dimensions of the original structure progressively undergo changes such that the final optimized structure is the one with equal r-node

*Every iteration consists of an r-node analysis, i.e., two sets of linear elastic finite element analyses.

stresses. Since bending is one of the dominant actions in many thin-walled or slender components, equation (7.4) is found to perform adequately.

In essence the minimum weight design as described by equation (7.4) implies that it is not necessary for any cross-section, i , of a structure to have a thickness t_i^0 in order to withstand the given load; indeed the structure would serve the intended purpose even if the thickness is reduced to t_i^f .

7.3 Minimum Weight Design - Another Perspective

The theorem of nesting surfaces^{17,18} (Section 2.8) can also be invoked for relating the concepts of reference stress and minimum weight. In designing for minimum weight under prescribed loading conditions, the geometry of a structure should be such that the entire volume undergoes plasticity at collapse. This aspect can be readily verified by examining the nesting surfaces for the two bar structure shown in Figure 2.8.

The nesting surfaces shown in Figure 2.8 have points where the surfaces corresponding to $n = 1$ and $n \rightarrow \infty$ are coincident. The intersecting of all Q_e at such points can be attributed to the situation where all the material in the structure has the same absolute value of stress. This is precisely the condition for 'minimum weight' design of the structure under a given loading. When a structure satisfies the minimum weight criterion for a given set of loads, all the surfaces Q_e are coincident on the the load-space. Minimum weight is both a necessary and sufficient condition for the exact coincidence

of all Q_e .¹⁷ The shaded portions of the nesting surfaces (Figure 2.8) is an indication of the extent of deviation from the minimum weight state for a set of prescribed loading conditions. The limitation of this approach is its dependency on the state of the applied load and its applicability only to simple structures.

7.4 Step-by-step Procedure for Minimizing the Weight of Structures using the R-Node Method

The methodology described in Section 7.2 can be presented as a step-by-step procedure so that mechanical components and structures can be configured for minimum weight conditions, as follows:

1. The given component is suitably discretized and linear elastic analyses are performed. The r-nodes are then determined by following the procedure proposed by Seshadri and Fernando.³⁴
2. The section with the highest r-node stress is identified as section j and, based on this r-node stress value, the thickness of the rest of the structure is determined by using equation (7.4).
3. R-Node analysis is performed for the modified component so obtained, and equation (7.4) is once again applied and improved cross-sectional dimensions are obtained.

4. The design improvement procedure explained in step number three can be repeated a few times (typically five to six times) until there is no further change in the r-node stresses with iterations or until a stage where any further iteration might lead to practically unworkable designs. Of course, the analyst might wish to terminate the iteration even after two linear elastic runs (say), and get "closer" to the optimal configuration.

It should be noted, however, that the reference section j determined in step number two should always be maintained as the reference section throughout the iteration process.

5. While performing the r-node analysis, it is not necessary that all sections contain r-nodes. Standard interpolation techniques can be used for determining the r-node stresses at these missing locations.

The resulting structure would have large zones with more or less equal r-node stress values indicating that these zones would entirely undergo plastic deformations at collapse rather than narrow cross-sections (or plastic hinges).

The procedure described opens up a wide range of application possibilities in engineering designs such as minimum weight design of mechanical components, design for reducing stress concentrations and thereby increasing the fatigue life of structures and for designing reinforcements at the re-entrant corner of a nozzle shell intersection, to mention a few.

7.5 Numerical Examples

In this section, the r-node concept for minimizing the weight of structures is applied for minimizing the weight of structural components of practical interest. The problems considered here are an indeterminate beam subjected to uniform load and a spherical pressure vessel with a cylindrical nozzle subjected to uniform internal pressure. For the first problem, a uniform rectangular beam is considered and an optimum shape for which the weight is minimum is determined. In the case of the spherical pressure vessel, the nozzle and the reinforcement at the nozzle shell intersection are designed. The problems are modeled using the ANSYS¹ software. The four-noded isoparametric quadrilateral elements are used for finite element modeling. Limit loads are evaluated by using inelastic finite element analysis and the r-node method.

7.5.1 Indeterminate Beam subjected to Uniform Load

The indeterminate beam of span 50.8×10^{-2} m (20 in.) and thickness 2.54×10^{-2} m (1 in.), shown in Figure 2.6, has end *A* built in and end *B* simply supported. The beam is assumed to have unit width in the direction normal to the paper. A uniform arbitrary pressure of 172.4 kPa (25 psi) is applied. The yield stress of the material is assumed to be 208.85×10^3 kPa (30×10^3 psi) and the modulus of elasticity is 206.85×10^6 kPa (30×10^6 psi). The Poisson's ratio is assumed to be equal to 0.3. The collapse mechanism of the structure and the associated r-node multi-bar model³⁴ are shown in

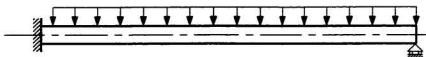
Figure 2.6. Minimum volume problems of this kind have been solved by Kodiyalam and Vanderplaats⁶⁹ by expanding the nodal forces in a Taylor series with respect to the shape variations.

The minimum weight structure after six iterations is shown in Figure 7.2. It can be seen that the final structure has 22 percent less volume as compared to the original one. The results of the analyses are given in Table 7.1. In this case, the limit load of the optimized structure is more than that of the original structure because, during optimization the maximum thickness of the final structure was increased by ten percent as compared to the original structure. The plasticity spread at collapse for the original structure and for the final optimized structure is shown in Figure 7.3 and the corresponding r-node diagrams are shown in Figure 7.4, respectively.

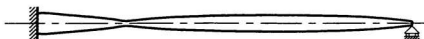
At the point of contraflexure of the beam and at the simply supported edge, since the bending moment values are equal to zero, the computed thicknesses should ideally be equal to zero. In actual cases, however, the thickness value determined depends not only on the required bending strength, but also on the shear strength necessary to transmit the shear force.

7.5.2 Design of Reinforcement and Nozzle of an Axisymmetric Spherical Pressure Vessel with a Cylindrical Nozzle subjected to Internal Pressure

Design of reinforcements for axisymmetric nozzles has been a topic of substantial interest since the 1960's. Proper design of nozzles and reinforce-



(a) ORIGINAL STRUCTURE



(b) MINIMUM WEIGHT STRUCTURE

Figure 7.2: Discretized Indeterminate Beams



(a) ORIGINAL STRUCTURE



(b) MINIMUM WEIGHT STRUCTURE

Figure 7.3: Plasticity Spread at Collapse for the Indeterminate Beams

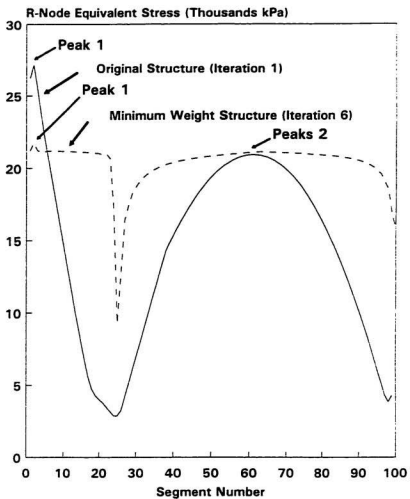


Figure 7.4: R-Node Diagrams for the Indeterminate Beams

Table 7.1: Comparison of a Uniform Indeterminate Beam with an Optimized Beam

Structure	Limit Load - Inelastic FEA (kPa)	Limit Load Estimate - R-Node Method (kPa)	Volume of the Plastic Region ($\times 10^{-6} \text{ m}^3$)	Total volume of the structure ($\times 10^{-6} \text{ m}^3$)
Original	1551.38	1483.32	95.70	327.74
Optimized	1639.29	1640.67	190.75	254.33

ments ensures that the resulting pressure vessel has an adequately robust design and a low stress concentration factor.⁷⁰

To demonstrate the design procedure, a spherical pressure vessel (Figure 7.5) with equal nozzle and shell thickness of 0.25 m (9.84 in.) is considered. The yield stress is assumed to be 300×10^3 kPa (43.51×10^3 psi) and the modulus of elasticity is taken to be 200×10^6 kPa (29×10^6 psi). The Poisson's ratio is assumed to have a value of 0.3. An arbitrary internal pressure of 200 kPa (29 psi) is applied. A fillet radius of 0.125 m (4.92 in.) is provided at the re-entrant corner of the nozzle-shell intersection. The section number one, as indicated in Figure 7.5, is assumed to be the reference section based on which the thickness of the remaining sections are determined. The pro-

Table 7.2: Comparison of Optimized Pressure Vessel Design with Conventional Pressure Vessel Design

Type of Pressure vessel	Minimum thickness of the nozzle (m)	Minimum thickness of the shell (m)	Limit Load - Inelastic FEA (MPa)	Limit Load Estimate - R-Node Method (MPa)	Volume of Pressure vessel (m ³)	Maximum Equivalent Stress (kPa)
Reinforced (using the r-node method, Figure 7.6)	0.090	0.255	153.300	143.755	3.386	840.110
Unreinforced (Figure 7.7)	0.090	0.250	149.400	121.017	3.320	944.530

cedure described in Section 7.4 is applied for this structure and two r-node iterations are carried out. The resulting component is shown in Figure 7.6.

An unreinforced pressure vessel having uniform shell and nozzle thickness as shown in Figure 7.7 is considered for the purposes of comparison. The results of the analyses are presented in Table 7.2 and the corresponding r-node diagrams are shown in Figure 7.8.

It can be seen from Table 7.2 that while the volume of material required for the proposed design (Figure 7.2) is only two percent more than that required for the conventional design, the limit load is increased by about three percent and the maximum equivalent stress is reduced by eleven percent.

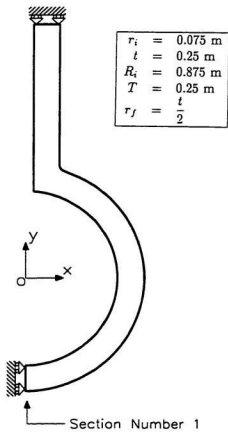


Figure 7.5: Spherical Pressure Vessel with Equal Nozzle and Shell Thickness

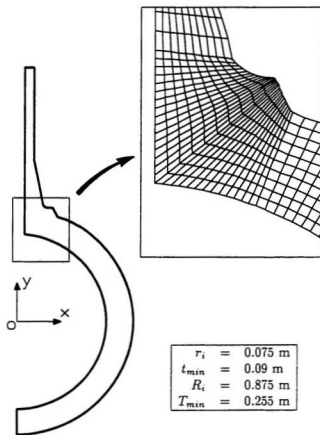


Figure 7.6: Reinforced Spherical Pressure Vessel

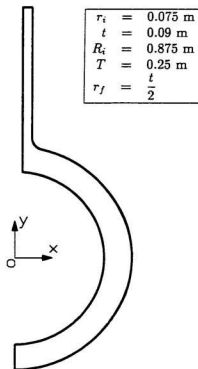


Figure 7.7: Unreinforced Spherical Pressure Vessel

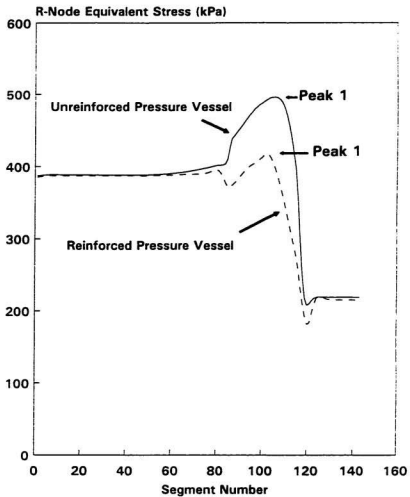


Figure 7.8: R-Node Diagrams for the Spherical Pressure Vessels

Table 7.3: Limit Load Estimates based on the R-Node Method - Indeterminate Beam

Structure	No. of R-Node Peaks	R-Node Stress ($\times 10^3$ kPa)	Combined R-Node Stress, $\bar{\sigma}_n = (\sigma_{n1} + \sigma_{n2})/2$ ($\times 10^3$ kPa)	Limit Load Estimate based on Equation (3.5) (kPa)
Original Beam	2	$\sigma_{n1}=27.16$ $\sigma_{n2}=20.91$	24.03	1483.32
Optimized Beam	2	$\sigma_{n1}=21.73$ $\sigma_{n2}=21.10$	21.42	1640.67

Table 7.4: Limit Load Estimates based on the R-Node Method - Spherical Pressure Vessel with a Cylindrical Nozzle

Structure	No. of R-Node Peaks	R-Node Stress (kPa)	Limit Load Estimate based on Equation (3.5) ($\times 10^3$ kPa)
Reinforced Pressure Vessel	1	$\bar{\sigma}_n=417.38$	143.76
Unreinforced Pressure Vessel	1	$\bar{\sigma}_n=495.80$	121.02

7.6 Closure

A simple and systematic procedure based on the r-node concept has been proposed for minimizing the weight of mechanical components and structures. The usefulness of the method has been demonstrated by way of carrying out size optimizations for mechanical components and structures of practical interest.

In the context of this chapter, the aim is designing a component or structure to make it, as far as possible, equally strong all over such that when loaded, the component or structure would collapse simultaneously, if at all.

Chapter 8

Conceptual Models for Understanding the Role of R-Nodes in Plastic Collapse

8.1 Introduction

In the r-node method of limit load determination, the combined r-node stress, which can be identified with the reference stress in creep, can be directly determined from the r-node diagram by identifying the r-node peaks with equivalent uniaxial multi-bar models. The bars represent the sequence of formation of independent plastic zones in the component.

The multi-bar models enable one to obtain an expression for the combined r-node stress, by invoking equilibrium considerations. However, multi-bar models only represent the r-node peaks in a structure and do not provide a physical representation of the underlying collapse process in terms of the entire structure. Therefore, it would be useful to provide simple models

which, along with the bar models, would characterize the stress redistribution and the collapse thereof.

8.2 Idealization of an R-Node

In Section 2.6.2, the r-node has been identified with a uniaxial bar model. The stress in the bar, which is designated as the r-node peak stress, is directly proportional to the applied load such that, when this stress reaches the elastic limit, a plastic hinge can be construed to have developed in the structure. For an elastic-perfectly plastic material, the uniaxial bar and hence the r-node can therefore be represented by a mechanical model. In Figure 8.1, the stress in the bar is proportional to the applied load until the elastic limit is reached. Any additional load beyond this results in the friction-device to move indefinitely, thereby causing collapse. This basic unit can be put together with other simple mechanical units for creating an analogous system that would represent the collapse of the entire structure.

8.3 Analogous Systems that Depict Plastic Collapse

In this section, simple analogous systems that depict the plastic collapse process are developed. The problems considered are a thick cylinder subjected to uniform internal pressure and a uniformly loaded indeterminate beam. Limit loads for these problems using the r-node method have already been determined in Chapter 5.

8.3.1 Thick Cylinder subjected to Uniform Internal Pressure

A thick-walled cylinder subjected to uniform internal pressure, as shown in Figure 8.2, is considered. The r-node for this component can be determined as the location in which the stress is invariant to elastic moduli changes. The uniaxial bar model for location A , which is the lone r-node for this structure, is shown in Figure 8.2. The analogous model depicting the stress redistribution and collapse is shown in Figure 8.3.

The analogous model essentially consists of a mechanical model which represents the r-node and a pair of tanks interconnected by a pipe (AB) which depicts the structure. The rollers provided maintain a uniaxial state of stress and strain by avoiding any possible lateral movement of the system. The spring constant, k , the damping coefficient, c , the density of the liquid, the dimensions of the tank, the reservoir and the pipes are component specific quantities that depend on the geometry, loading and boundary conditions of the structure that is being analyzed.

The externally applied load can be symbolized by means of a reservoir containing liquid. All the components of the analogous model with the exception of the liquid are assumed to be weightless. The correspondence between the actual structure and the analogous system during collapse is illustrated in Table 8.1.

8.3.2 Indeterminate Beam subjected to Uniformly distributed Load

The two bar model for an indeterminate beam, representing the r-nodes, is shown in Figure 2.6 and the r-node diagram is shown in Figure 5.1. Although a number of r-nodes are present along the length of the beam, consideration of only the two r-node peaks as per the guidelines offered in Chapter 5 simplifies the analogous model to a great extent. The two r-node peaks are represented by two mechanical models. Pipe AB is at a lower level than pipe CD implying that the formation of a plastic hinge at the location A precedes the occurrence of the same at the location B (Figure 2.6). The liquid level reaching the pipe AB corresponds to the mechanical model number one reaching its elastic limit.

8.4 Closure

An r-node has been idealized as a mechanical model. Based on this model, a conceptual characterization of the collapse process has been suggested by considering some practical configurations. It is hoped that the proposed models along with the existing r-node multi-bar models would assist in the better understanding of the r-nodes and their functioning during collapse.

Table 8.1: Correspondence between the Actual Structure and the Analogous System for a Thick Cylinder subjected to Uniform Internal Pressure

Actual Structure	: Analogous System
Applied Traction	: Liquid in the reservoir
Structure	: Tanks 1 and 2
R-Node	: Mechanical model and pipe (AB)
Stress in the structure	: Weight of the liquids in the tanks
Onset of yield at some portion of the structure	: Liquid level in one of the tanks (say, tank 1) just reaching the pipe level
Additional loading causes stress redistribution about the r-node	: Additional liquid input into tank 1 only gets redistributed through the pipe AB into tank 2
The r-node by itself does not get involved in stress redistribution	: The pipe AB serves only as a conduit for the transfer of liquid from tank 1 to tank 2 without actually being affected by the redistribution process
R-Node stress is proportional to the applied load and is insensitive to the material constitutive relationship	: The spring extends strictly in proportion to the weight of the liquid in the tanks irrespective of the distribution of liquids in the tanks
When the r-node stress reaches the yield stress, the plasticity becomes uncontained thereby causing collapse	: When the liquid level in tank 2 reaches the pipe level, even an infinitesimal additional inflow causes the friction-device to move, thereby causing collapse

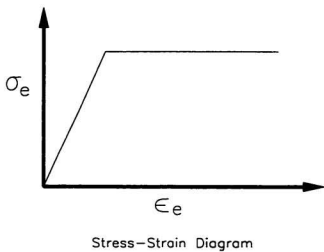
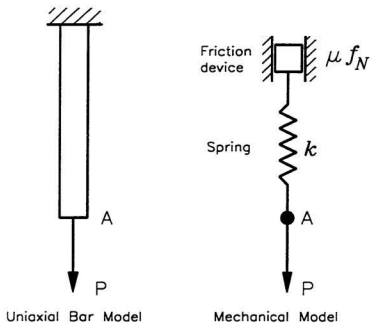


Figure 8.1: Idealization of an R-Node

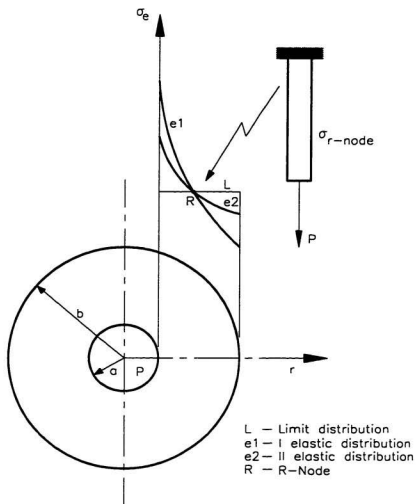


Figure 8.2: Determination of R-Node in a Thick Cylinder Subjected to Uniform Internal Pressure

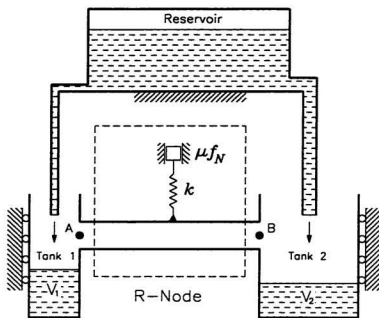


Figure 8.3: Analogous Model for a Thick Cylinder Subjected to Uniform Internal Pressure

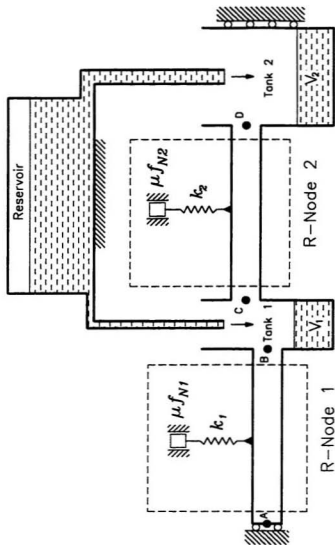


Figure 8.4: Analogous Model for an Indeterminate Beam Subjected to Uniform Loading

Chapter 9

Conclusions and Future Research

9.1 Conclusions

Interest in limit load determination originated with the primary purpose of capitalizing on the reserve strength of structures. However, a relationship between limit loads and reference stress has substantially widened the scope of applicability of limit analysis results.

Duly recognizing the underlying difficulties of conventional methods, this thesis presents simple techniques for estimating reference stress and limit loads. The r-node method and the m_σ -method are the robust techniques that are developed herein in the aforementioned vein. The concepts of load control, primary stress and reference stress form the basis of the r-node method. The m_σ -method is based on the extended lower bound limit load theorem in conjunction with the concepts of reference volume and leap-frogging to a near limit state. It is demonstrated that reasonable upper and lower bound

limit load estimates can be determined on the basis of two linear elastic finite element analyses. The r-node method is also used for determining the limit loads of laminated beams and laminated cylindrical shells. Given the usefulness of composites and reinforced structures in engineering, the proposed method should serve as a starting point for further research in this area.

Useful concepts such as the reference volume, leap-frogging and iso r-nodes are introduced in an attempt to elicit valuable physical insights into the problem. The reference volume concept, for instance, enables identification of the “kinematically active” regions in a component or structure. The idea of leap-frogging is introduced in order to reach the limit state rapidly in comparison to repeated elastic iterations. The notion of iso r-node stress utilizes the aspect of load-control for minimizing the weight of mechanical components. Useful designs from a standpoint of increased fatigue life through reduced stress concentrations are also possible through this approach. In order to provide the analyst with a guide to the response of structures to elastic iterations, mechanical components are classified into three distinct categories. Recommendations are also provided for ensuring convergence to lower bound values and related numerical stability issues.

Through numerical examples, the proposed methods have been demonstrated to be accurate, easy to implement and less expensive. The methods are general and can be applied to a variety of component configurations. It is intended that the techniques developed would be useful for practicing engineers, especially during the preliminary stages of design and during condition

assessment exercises.

The time consuming aspect of the conventional analysis techniques is a distinct disadvantage in highly competitive environments where rapid and reliable methods are essential for evolving newer designs or upgrading the existing ones. It is hoped that the methods proposed in this thesis would adequately bridge the gaps between accuracy, speed, simplicity and cost of analysis.

9.2 Future Research

The advantages offered by the robust techniques proposed in this thesis amply indicate that further research in this direction would be rewarding. The r-node method and the m_a -method have been applied to a number of bench mark problems and the results obtained are found to be encouraging. Further research should concentrate on applying these methods to more complex structures such as three-dimensional nozzle-shell intersections. Development of reduced modulus methods for determining the limit loads of generic composite structures would be another research area worth pursuing.

The proposed minimum weight design procedure using iso r-nodes is found to effectively attenuate the discontinuity stresses in pressure components. It would be worthwhile to direct future efforts by incorporating design constraints in the method so as to evolve workable configurations that are suitable for manufacturing units.

Bibliography

- [1] *ANSYS Engineering Analysis System User's Manual*, Rev. 5. Swanson Analysis Systems Inc., Houston, Pa., 1992.
- [2] Burgreen, D., *Design Methods for Power Plant Structures*, First Edition, C. P. Press, New York, 1975.
- [3] Seshadri, R., and Marriott, D. L., "On Relating the Reference Stress. Limit Load and the ASME Stress Classification Concepts," *International Journal of Pressure Vessels and Piping*, Vol. 56, pp. 387-408, 1993.
- [4] Marriott, D. L., "Evaluation of Deformation or Load Control of Stresses under Inelastic Conditions using Elastic Finite Element Stress Analysis." *Proceedings of the ASME-PVP Conference*, Pittsburgh, Vol. 136, 1988.
- [5] Seshadri, R., "The Generalized Local Stress Strain (GLOSS) Analysis - Theory and Applications," *Transactions of the ASME: Journal of Pressure Vessel Technology*, Vol. 113, pp. 219-227, 1991.

- [6] Mackenzie, D., and Boyle, J. T., "A Method for Estimating Limit Loads by Iterative Elastic Analysis. I-Simple Examples," *International Journal of Pressure Vessels and Piping*, Vol. 53, pp. 77-95, 1993.
- [7] Hodge, P. G., *Plastic Analysis of Structures*, McGraw Hill Book Company, New York, 1959.
- [8] Mendelson, A., *Plasticity: Theory and Application*, The Macmillan Company, New York, 1968.
- [9] Prager, W., and Hodge, P. G., *Theory of Perfectly Plastic Solids*, Dover Publications, Inc., New York, 1951.
- [10] Save, M. A., and Massonet, C. E., *Plastic Analysis and Design of Plates, Shells and Disks*, Vol. II, North-Holland Publishing Company, Amsterdam, 1972.
- [11] *ASME Boiler and Pressure Vessel Code*, American Society of Mechanical Engineers, 1989.
- [12] Kalnins, A., and Updike, D. P., "Role of Plastic Limit and Elastic-Plastic Analyses in Design," *ASME Pressure Vessels and Piping Conference*, San Diego, Vol. 210-2, pp. 135-142, 1991.
- [13] Hibbitt, Karlsson & Sorenson Inc., *ABAQUS User Manuals*, Vol. 1-4, 1994.

- [14] Marriott, D. L., *Beyond Finite Element Analysis*, Professional Development Session 3, 11th Symposium on Engineering Applications of Mechanics, University of Regina, Regina, May, 1992.
- [15] Mura, T., and Lee, S. L., "Application of Variational Principles to Limit Analysis," *Quarterly of Applied Mathematics*, Vol. 21, No. 3, pp. 243-248, 1963.
- [16] Mura, T., Rimawi, W. H., and Lee, S. L., "Extended Theorems of Limit Analysis," *Quarterly of Applied Mathematics*, Vol. 23, No. 2, pp. 171-179, 1965.
- [17] Calladine, C. R., and Drucker, D. C., "A Bound Method for Creep Analysis of Structures: Direct use of Solutions in Elasticity and Plasticity," *Journal of Mechanical Engineering Science*, Vol. 4, No. 1, pp. 1-11, 1962.
- [18] Boyle, J. T., "The Theorem of Nesting Surfaces in Steady Creep and its Application to Generalized Models and Limit Reference Stresses." *Res Mechanica*, Vol. 4, pp. 275-294, 1982.
- [19] Char, B. W., Geddes, K. O., Gonnet, G. H., Leong, B. L., Monagan, M. B., and Watt, S. M., *The Maple V Language Reference Manual*, Springer-Verlag, 1991.
- [20] Berak, E. G., and Gerdeen, J. C., "A Finite Element Technique for Limit Analysis of Structures," *Transactions of the ASME: Journal of Pressure Vessel Technology*, Vol. 112, pp. 138-144, May, 1990.

- [21] Jones, G. L., and Dhalla, A. K., "Classification of Clamp Induced Stresses in Thin-walled Pipe," *Proceedings of the ASME-PVP Conference*, New York, Vol. 81, pp. 1-10, 1981.
- [22] Dhalla, A. K., and Jones, G. L., "ASME Code Classification of Pipe Stresses: A Simplified Elastic Procedure," *International Journal of Pressure Vessel and Piping*, Vol. 26, pp. 145-166, 1986.
- [23] Blake, A., *Practical Stress Analysis in Engineering Design*, Second Edition, Marcell Dekker Inc., New York, 1990.
- [24] Fernando, C. P. D., *Limit Loads of Mechanical Components and Structures using the GLOSS R-Node Method*, M.Sc. Thesis, Industrial Systems Engineering Department. University of Regina, Canada, 1992.
- [25] Calladine, C. R., *Engineering Plasticity*, Pergamon Press, Oxford. 1969.
- [26] Dhalla, A. K., "Verification of an Elastic Procedure to verify Follow-up." *Design of Elevated Temperature Piping*, Eds. Mallet, R. H.. and Mello, R. M., ASME, New York, pp. 81-96, 1984.
- [27] Severud, L. K., "A Simplified Method Evaluation for Piping Elastic Follow-up," *Proceedings of the 5th International Congress of Pressure Vessel Technology*, ASME, San Fransisco, pp. 367-387, 1984.
- [28] Dhalla, A. K., "A Simplified Procedure to Classify Stresses for Elevated Temperature Service," *Proceedings of the ASME-PVP Conference*, San Diego, Vol. 120, pp. 177-188, 1987.

- [29] Seshadri, R., "Simplified Methods for determining Multiaxial Relaxation and Creep Damage," *Proceedings of the ASME-PVP Conference*, San Diego, Vol. 210-2, pp. 173-180, 1991.
- [30] Vaidyanathan, S., Kizhatil, R. K., and Seshadri, R., "GLOSS Plot Validation and Application to Elevated Temperature Component Design," *Proceedings of the ASME-PVP Conference*, Honolulu, Vol. 161, pp. 25-31. 1989.
- [31] Seshadri, R., and Kizhatil, R. K., "Inelastic Analyses of Pressure Components using the 'GLOSS' Diagram," *Proceedings of the ASME-PVP Conference*, Nashville, Vol. 186, pp. 105-113, 1990.
- [32] Kizhatil, R. K., and Seshadri, R., "Inelastic Strain Concentration Factors and Low Cycle Fatigue of Pressure Components using GLOSS Analysis," *Proceedings of the ASME-PVP Conference*, San Diego, Vol. 210-2, pp. 149-154, 1991.
- [33] Seshadri, R., "Classification of Stress in Pressure Components using the 'GLOSS' Diagram." *Proceedings of the ASME-PVP Conference*, Nashville, Vol. 186, pp. 115-123, 1990.
- [34] Seshadri, R., and Fernando, C. P. D., "Limit Loads of Mechanical Components and Structures using the GLOSS R-Node Method," *Transactions of the ASME: Journal of Pressure Vessel Technology*, Vol. 114, pp. 201-208, 1992.

- [35] Fernando, C. P. D., and Seshadri, R., "Limit Loads of Framed Structures and Arches using the GLOSS R-Node Method," *Proceedings of the 11th Symposium on Engineering Applications of Mechanics*, pp. 236-242, 1992.
- [36] Mangalaramanan, S. P., *Robust Limit Loads of Plate Structures*, M. Sc. Thesis, Faculty of Engineering, University for Regina, Regina, 1993.
- [37] Nadarajah, C., Mackenzie, D., and Boyle, J. T., "A Method of Estimating Limit Loads by Iterative Elastic Analysis. II-Nozzle Sphere Intersection with Internal Pressure and Radial Load," *International Journal of Pressure Vessels and Piping*, Vol. 53, pp. 97-119, 1993.
- [38] Shi, J., Mackenzie, D., and Boyle, J. T., "A Method of Estimating Limit Loads by Iterative Elastic Analysis. III-Torispherical Heads under Internal Pressure," *International Journal of Pressure Vessel and Piping*, Vol. 53, pp. 121-142, 1993.
- [39] Boyle, J. T., "Fundamental Concepts in the Reference Stress Method for Creep Design," *Transactions of the 5th International Conference on Structural Mechanics in Reactor Technology*, International Congress Center, Berlin, pp. 1-7. L4/5, August, 1979.
- [40] Soderberg, C. R., "Interpretation of Creep Tests on Tubes," *Transactions of the ASME*, Vol. 63, pp. 737-748, 1941.

- [41] Schulte, C. A., "Predicting Creep Deflections of Beams," *Proceedings of the A.S.T.M.*, Vol. 60, pp. 895-904, 1960.
- [42] Marriott, D. L., and Leckie, F. A., "Some Observations on the Deflections of Structures during Creep," *Proceedings of the Institution of Mechanical Engineers*, Vol. 178, pt. 3L, pp. 115-125, 1963-64.
- [43] Anderson, R. G., Gardner, L. R. T., and Hodgkins, W. R., "Deformation of Uniformly Loaded Beams Obeying Complex Creep Laws," *Journal of Mechanical Engineering Sciences*, Vol. 5, pp. 238-244, 1963.
- [44] Mackenzie, A. C., "On the use of a Single Uniaxial Test to Estimate Deformation Rates in Some Structures Undergoing Creep," *International Journal of Mechanics and Sciences*, Vol. 10, pp. 441-443, 1968.
- [45] Sim, R. G., "Reference Stress Concepts in the Analysis of Structures During Creep," *International Journal of Mechanics and Sciences*, Vol. 12, pp. 561-573, 1970.
- [46] Sim, R. G., "Evaluation of Reference Stress Parameters for Structures Subject to Creep," *Journal of Mechanical Engineering Science*, Vol. 13, pp. 47-50, 1971.
- [47] Johnson, A., "An Alternative Definition of Reference Stress for Creep," *International Conference on Creep and Fatigue in Elevated Temperature Applications*, Institution of Mechanical Engineers, Conference Publication No. 13, Paper C205/73, Philadelphia, 1973.

- [48] *Recommended Practice in Elevated Temperature Design: A Compendium of Breeder Reactor Experiences (1970-1987)*, Welding Research Council Bulletin, Vol. II & Vol. IV, Preliminary Design and Simplified Methods, Edited by A. K. Dhalla, 1991.
- [49] R5, *Assessment Procedure for High Temperature Response of Structures*, Nuclear Electric, Berkeley Nuclear Laboratories, 1990.
- [50] R6, *Assessment of the Integrity of Structures Containing Defects*, Nuclear Electric, Berkeley Nuclear Laboratories, 1990.
- [51] Carter, K. F., and Ponter, A. R. S., "Calculation of Limit Loads and Shakedown Boundaries using the Modified Elastic Modulus Method," *Computational Plasticity: Fundamentals and Applications*, Part II, pp. 1597-1608, 1992.
- [52] Kreyszig, E., *Advanced Engineering Mathematics*, Fifth Edition. New Age International (P) Limited, Publishers, pp. 815, June, 1995.
- [53] Drucker, D. C., and Shield, R. T., "Limit Analysis of Symmetrically Loaded Thin Shells of Revolution," *Transactions of the ASME: Journal of Applied Mechanics*, Vol. 26, pp. 61-68, 1959.
- [54] Shield, R. T., and Drucker, D. C., "Design of Thin Walled Torispherical and Toriconical Heads," *Transactions of the ASME: Journal of Applied Mechanics*, Vol. 28, pp. 292-297, 1961.

- [55] Dinno, L. S., and Gill, S. S., "The Limit Analysis of a Pressure Vessel consisting of a Cylindrical and Spherical Shell," *International Journal of Mechanical Sciences*, Vol. 7, pp. 21-42, 1965.
- [56] Gill, S. S., *The Stress Analysis of Pressure Vessels and Pressure Vessel Components*. Pergamon Press, Vol. 3, 1970.
- [57] Hollinger, G. L., and Hechmer, J. L., "Three-Dimensional Stress Evaluation Guidelines Progress Report," *Recertification and Stress Classification Issues*, ASME PVP-Vol. 277, pp. 95-102, 1994.
- [58] Nuclear Electric, "Recommended Practice in Elevated Temperature Design," *A Compendium of Breeder Reactor Experiences (1970-1987)*, Vol. 4, Special Topics, 1991.
- [59] Wu, S., and Seshadri, R., "A Simplified Three-Dimensional Model for Analyzing Pressure Vessels and Piping Components with Defects." *Proceedings of the ASME Pressure Vessels and Piping Conference, Montreal*, Vol. 324, 1996.
- [60] Barsoum, R. S., "On the use of Isoparametric Finite Elements in Linear Fracture Mechanics," *International Journal for Numerical Methods in Engineering*, Vol. 10, pp. 25-37, 1976.
- [61] Rice, J. R., and Rosengren, G. F., "Plane Strain Deformation near a Crack Tip in a Power-Law Hardening Material," *Journal of the Mechanics and Physics of Solids*, Vol. 16, pp. 1-12, 1968.

- [62] Barsoum, R. S., "Triangular Quarter-Point Elements as Elastic and Perfectly-Plastic Crack Tip Elements," *International Journal for Numerical Methods in Engineering*, Vol. 11, pp. 85-98, 1977.
- [63] Muthukrishnan, J., *Analysis of Framed Structures using the GLOSS R-Node Method*, M.Sc. Thesis, Industrial Systems Engineering Department, University of Regina, Canada, 1992.
- [64] Seshadri, R., "In Search of the Redistribution Nodes," *Presented at the International Conference on Pipes & Pressure Vessels*, Singapore, 1995.
- [65] Gere, J. M., and Timoshenko, S. P., *Mechanics of Materials*, PWS-KENT Publishing Company, Third Edition, pp. 301-308, 1990.
- [66] Nichols, R. W., *Pressure Vessel Engineering Technology*, Applied Science Publishers Limited, London, 1971.
- [67] Foulkes, J., "Minimum Weight Design and the Theory of Plastic Collapse," *Quarterly of Applied Mathematics*, Vol. 10, pp. 347-358, 1953.
- [68] Drucker, D. C., "Design for Minimum Weight," *International Congress of Applied Mechanics*, Vol. 9, pp. 212-222, 1956.
- [69] Kodiyalam, S., and Vanderplaats, G. N., "Shape Optimization of Three-Dimensional Continuum Structures via Force Approximation Techniques," *AIAA Journal*, Vol. 27, No. 9, pp. 1256-1263, 1989.

- [70] Calladine, C. R., "On the Design of Reinforcements for Openings and Nozzles in Spherical Pressure Vessels," *Journal of Mechanical Engineering Sciences*, Vol. 8, No. 1, pp. 1-14, 1966.

Publications during the Course of the Ph.D Program

Journals

- [1] Mangalaramanan, S. P., and Seshadri, R., "Robust Limit Load of Plate Structures," *Transactions of the CSME*, Vol. 1, pp. 108-129, 1994.
- [2] Seshadri, R., and Mangalaramanan, S. P., "Lower Bound Limit Loads using Variational Concepts: The m_α -method," *To appear in the International Journal of Pressure Vessels and Piping*, 1997.
- [3] Mangalaramanan, S. P., and Seshadri, R., "Minimum Weight Design of Pressure Components using R-Nodes," *To appear in the ASME Journal of Pressure Vessel Technology*, 1997.
- [4] Mangalaramanan, S. P., "Conceptual Models for Understanding the Role of R-Nodes in Plastic Collapse," *To appear in the ASME Journal of Pressure Vessel Technology*, 1997.

International Conferences

- [1] Mangalaramanan, S. P., and Seshadri, R., "Robust Limit Loads of Plate Structures," *Proceedings of the CSME Forum*, Vol. 1, pp. 108-129. 1994.
- [2] Mangalaramanan, S. P., and Seshadri, R., "Extended Theorem of Limit Analysis - Finite Element Implementation," *Presented at the 15th Canadian Congress of Applied Mechanics*, 1995.
- [3] Mangalaramanan, S. P., and Seshadri, R., "Robust Limit Load Determination based on Extended Variational Principles," *3rd Annual Student Paper Competition, ASME/JSME Pressure Vessels and Piping Conference*, Honolulu, July, 1995.
- [4] Mangalaramanan, S. P., and Seshadri, R., "Minimum Weight Design of Pressure Components using R-Nodes," *Presented at the ASME Pressure Vessels and Piping Conference*, Montreal, July, 1996.
- [5] Mangalaramanan, S. P., and Seshadri, R., "Limit Loads of Layered Beams and Layered Cylindrical Shells using the R-Node Method," *Accepted for presentation in the ASME Pressure Vessels and Piping Conference. Orlando*, 1997.

Appendix A

Fortran Program for determining the R-Node Locations and Stresses

This program (rnode.for) determines the r-node equivalent stress values, their respective locations, the values of m^o , m' and the classical limit load values for both the linear elastic analyses. The input to be given are the equivalent stress and element volume listings, and the yield stress value.

PROGRAM GLOSS

PARAMETER(MEMO=1500)

INTEGER FLAG1,RSEG,ELELOC,COUNT,RSEGG

REAL M1,M2

CHARACTER*15 FNAME1,FNAME2,FNAME3,UNITS

DIMENSION SIG1(MEMO),SIG2(MEMO),NELE(MEMO)

DIMENSION RSTR(MEMO),RLOC(MEMO),RSEG(MEMO)

DIMENSION ELELOC(MEMO),RNO(MEMO),RSTR1(MEMO),

10

```

1 VOL(MEMO)
  DIMENSION RSTR2(MEMO),RSTR3(MEMO),ICOUNT(MEMO),
1 RSEGG(MEMO)

  DO K=1,30
  WRITE(*,*)
  END DO
  WRITE(*,*)'WELCOME TO THE R-NODE
1 PROGRAM - VERSION 5'
  WRITE(*,*)'
  WRITE(*,*)'
  WRITE(*,*)'ENTER THE NAME OF THE FIRST LINEAR ANALYSIS
1 INPUT FILE'
53  READ (*,'(A)')FNAME1
  OPEN(15,FILE=FNAME1,STATUS='OLD',ERR=56)
  WRITE(*,*)'ENTER THE NAME OF THE SOFTENED NTH LINEAR
1 ANALYSIS INPUT FILE'
54  READ (*,'(A)')FNAME2
  OPEN(16,FILE=FNAME2,STATUS='OLD',ERR=57)
  OPEN(UNIT=17,FILE='ZRSTRO.OUT',STATUS='UNKNOWN')
  * OPEN(UNIT=18,FILE='ZRSTRS.OUT',STATUS='UNKNOWN')

  WRITE(*,*)'ENTER THE NAME OF THE OUTPUT FILE FOR THE
1 HIGHEST R-NODE STRESS'
67  READ(*,'(A)')FNAME3
  OPEN(UNIT=19,FILE=FNAME3,STATUS='NEW',ERR=66)
  GOTO 68
66  WRITE(*,*)'OUTPUT FILE ALREADY EXISTING. ENTER ANOTHER
1 FILE NAME'

```

GOTO 67

* *DUMMY STATEMENT*

68 DUMMY=0.0

* *OPEN(UNIT=20,FILE='ZRSTR.AVG',STATUS='UNKNOWN')*

* *OPEN(UNIT=21,FILE='ZRSTR.SML',STATUS='UNKNOWN')*

OPEN(UNIT=22,FILE='ZSUMOF1.SQR',STATUS='UNKNOWN')

OPEN(UNIT=23,FILE='ZSUMOF2.SQR',STATUS='UNKNOWN') 50

OPEN(UNIT=24,FILE='ZMURA.RES',STATUS='UNKNOWN')

WRITE(*,*)'WHAT IS THE UNIT OF STRESS

1 (EG. PSI, N/SQ.M., PA, KPA ETC.)'

READ(*,*(A))UNITS

WRITE(*,*)'YIELD STRESS = ? ',UNITS

READ(*,*)SIGY

WRITE(*,*)'APPLIED LOAD = ? ',UNITS

READ(*,*)PAPP

20 **WRITE(*,*)'TOTAL NUMBER OF ELEMENTS = ?'** 60

READ(*,*)NELEM

WRITE(*,*)'NUMBER OF ELEMENTS PER SECTION = ?'

READ(*,*)NEPS

CALL CHKINP(NELEM,NEPS,FLAG1)

IF (FLAG1.EQ.1) THEN

GO TO 20

END IF

NSEG = NELEM/NEPS

CALL VINPUT(SIG1,SIG2,NELE,NELEM,VOL,SIGY, 70

1 PAPP,UNITS)

```

      CALL RNODE(SIG1,SIG2,NSEG,NELEM,NEPS,RSEG.
1 RSTR,RLOC,ELELOC,I)
      CALL RESULT(RSEG,RLOC,ELELOC,RSTR,NEPS,I)
      CALL CALCU(I,RSTR1,RSTR2,RSTR3,KJ,RSEG,RSTR,
1 ICOUNT,RSEGG)
      WRITE(19,*)'MAXIMUM R-NODE STRESS'
*   WRITE(20,*)'AVERAGE R-NODE STRESS'
*   WRITE(21,*)'MINIMUM R-NODE STRESS'
      BIG1=0.0
      DO 155 IPP=1,KJ
      WRITE(19,*) RSEGG(IPP),RSTR1(IPP)
      IF(RSTR1(IPP).GT.BIG1)BIG1=RSTR1(IPP)
*   WRITE(20,*) RSEGG(IPP),RSTR2(IPP)
*   WRITE(21,*) RSEGG(IPP),RSTR3(IPP)
155  CONTINUE
      WRITE(24,*)'THE HIGHEST R-NODE STRESS VALUE = ',
1 BIG1,' ',UNITS

      CLOSE(24)
      CLOSE(23)
      CLOSE(22)
*   CLOSE(21)
*   CLOSE(20)
      CLOSE(19)
*   CLOSE(18)
      CLOSE(17)
      CLOSE(16)
      CLOSE(15)
      GO TO 58

56  PRINT *,'THE FIRST INPUT FILE ',FNAME1,' IS NOT EXISTING.

```

```

1 RE-ENTER ANOTHER FILE NAME'
  GO TO 53
57 PRINT *, 'THE SECOND INPUT FILE ', FNAME2, ' IS NOT EXISTING .
1 RE-ENTER ANOTHER FILE NAME'
  GO TO 54
58 STOP
  END

* CHECK INPUT FOR CORRECTNESS 110

SUBROUTINE CHKINP(NELEM, NEPS, FLAG1)
INTEGER FLAG1
FLAG1=0
R = FLOAT(NELEM)
R1 = FLOAT(NEPS)
R2 = R/R1
I = NELEM/NEPS
R3 = FLOAT(I)
IF (R3.NE.R2) THEN 120
  FLAG1 = 1
  WRITE(*,21)
21 FORMAT(1X, 'INPUT ERROR: CHECK AND REINPUT TOTAL NUMBER
1 OF ELEMENTS ', /, 1X, 'OR NO. OF ELEMENTS PER SEGMENT. . . . .')
  END IF
  RETURN
  END

* READ INPUT FILE (STRS1.OUT AND STRS2.OUT) 130

SUBROUTINE VINPUT(SIG1, SIG2, NELE, NELEM, VOL,

```

```
1 SIGY,PAPP,UNITS)
  CHARACTER*(*) UNITS
  DIMENSION SIG1(NELEM),SIG2(NELEM),NELE(NELEM).
1 VOL(NELEM)
```

* *READ FIRST LINEAR ANALYSIS STRESS LISTING*

```
C READ(15,25)
C25 FORMAT(////////)
K = NELEM/41
J = NELEM - K * 41
I = 1
DO 30 K1 = 1,K
DO 35 K2 = 1,41
READ(15,*)NELE(I),SIG1(I)
35 I = I + 1
C READ(15,40)
C40 FORMAT(////////)
30 CONTINUE
DO 45 J1 = 1,J
READ(15,*)NELE(I),SIG1(I)
45 I = I + 1
```

* *READ SECOND LINEAR ANALYSIS STRESS LISTING*

```
C READ(16,50)
C50 FORMAT(////////)
I = 1
DO 55 K1 = 1,K
DO 60 K2 = 1,41
```

```

        READ(16,*)A,SIG2(I),VOL(I)
60     I = I + 1
      C   READ(16,65)
C65     FORMAT(////)
55     CONTINUE
        DO 70 J1 = 1,J
          READ(16,*)A,SIG2(I),VOL(I)
70     I = I + 1

```

```

        SUMM = 0.0
        SUMX = 0.0
        VOLU = 0.0

```

170

- * *TO FIND THE BIGGEST OF THE SECOND*
- * *LINEAR ANALYSIS STRESS VALUE*

```

        BIGG = 0.0
        BIGG1 = 0.0
        DO K = 1,NELEM
          IF(SIG2(K).GT.BIGG)BIGG=SIG2(K)
        END DO
        DO K = 1,NELEM
          IF(SIG1(K).GT.BIGG1)BIGG1=SIG1(K)
        END DO

```

180

```

        DO K = 1,NELEM
          SUMN = (SIG2(K)**2)*VOL(K)
          SUMY = (SIG1(K)**2)*VOL(K)
          VOLU = VOLU + VOL(K)
          SUMM = SUMM + SUMN

```

190

```

SUMX = SUMX + SUMY
WRITE(22,*) SUMX,VOLU
WRITE(23,*) SUMM,VOLU
END DO
RMO = SIGY*SQRT(VOLU)/SQRT(SUMM)
DENOM = (SIGY**2 + (RMO*BIGG)**2)/(2.0*SIGY**2)
PLBOYL = SIGY/BIGG*PAPP
RMO1 = SIGY*SQRT(VOLU)/SQRT(SUMX)
DENOM1 = (SIGY**2 + (RMO1*BIGG1)**2)/(2.0*SIGY**2)
PLBOYL1 = SIGY/BIGG1*PAPP
WRITE(22,*) 'VALUE OF MO I LINEAR ANALYSIS = ',RMO1
WRITE(22,*) 'VALUE OF I LIN. ANALYSIS DENOMINATOR = ',
1 DENOM1
WRITE(22,*) 'BOYLES LIMIT LOAD I LINEAR ANALYSIS = ',
1 PLBOYL1,' ',UNITS
WRITE(22,*) 'HIGHEST STRESS OF I LINEAR ANALYSIS = ',
1 BIGG1,' ',UNITS
WRITE(22,*) 'MO X P = ',RMO1*PAPP,' ',UNITS
WRITE(22,*) 'MO X P/DENOM = ',RMO1*PAPP/DENOM1,
1 ' ',UNITS
WRITE(24,*) 'VALUE OF MO = ',RMO
WRITE(24,*) 'APPLIED PRESSURE = ',PAPP,' ',UNITS
WRITE(24,*) 'YIELD STRESS = ',SIGY,' ',UNITS
WRITE(24,*) 'VALUE OF MO X P = ',RMO*PAPP,' ',UNITS
WRITE(24,*) 'VALUE OF HIGHEST STRESS OF THE SOFTENED
1 LINEAR ANALYSIS = ',BIGG,' ',UNITS
WRITE(24,*) 'VALUE OF THE DENOMINATOR = ',DENOM
WRITE(24,*) 'VALUE OF MO X P / DENOMINATOR = ',
1 RMO*PAPP/DENOM,' ',UNITS
WRITE(24,*) 'VALUE OF LIMIT LOAD BY BOYLES METHOD = ',

```

200

210

220

```

1 PLBOYL, ' ',UNITS
  RETURN
  END

```

• *CALCULATE R-NODE STRESSES AND LOCATIONS*

```

  SUBROUTINE RNODE(SIG1,SIG2,NSEG,NELEM,NEPS,
1 RSEG,RSTR,RLOC,ELELOC,I)
  INTEGER RSEG,ELELOC
  REAL M1,M2
  DIMENSION SIG1(NELEM),SIG2(NELEM),RSEG(NELEM),
1 RSTR(NELEM),RLOC(NELEM),ELELOC(NELEM)

  I = 1
  DO 85 J = 1,NSEG
  DO 85 K = 1,NEPS-1
  IJK = (J - 1)*NEPS + K
  M1 = SIG1(IJK+1) - SIG1(IJK)
  M2 = SIG2(IJK+1) - SIG2(IJK)
  SLOPE = ABS(M1 - M2)
  IF (SLOPE.LE.0.00001) THEN
    GOTO 85
  END IF
  X = (SIG2(IJK) - SIG1(IJK))/(M1 - M2) + FLOAT(K) - 0.5
  Y = M1 * (SIG2(IJK) - SIG1(IJK))/(M1 - M2) + SIG1(IJK)
  RK = FLOAT(K) + 0.5
  RK1 = FLOAT(K) - 0.5
  IF(X.LE.RK.AND.X.GE.RK1) THEN
    RSTR(I) = Y

```

```

      RLOC(I) = X
      RSEG(I) = J
      ELELOC(I) = IJK
      I = I + 1
      END IF
85  CONTINUE
      RETURN
      END

```

260

* *DISPLAY RESULTS*

```

      SUBROUTINE RESULT(RSEG,RLOC,ELELOC,
1  RSTR,NEPS,I)
      INTEGER RSEG,ELELOC
      DIMENSION RSEG(I),RLOC(I),ELELOC(I),RSTR(I)
      WRITE(17,95)
95  FORMAT(1X,'SEGMENT NO      LOCATION          R-NODE STRESS')
      WRITE(17,100)
100 FORMAT(1X,'          R-NODE      ELEMENTS          ')
      DO 105 II = 1,I-1
      IE1 = RSEG(II)
      IE2 = ELELOC(II)
      IE3 = ELELOC(II) + 1
      WRITE(17,110) IE1,RLOC(II),IE2,IE3,RSTR(II)
110 FORMAT(1X,I4,2X,F9.5,2X,I5,2X,I5,2X,F13.5)
      * WRITE(18,111) IE1,RSTR(II)
*111 FORMAT(1X,I10,2X,F13.5)
105  CONTINUE
      RETURN
      END

```

280

- *CALCULATES THE HIGHEST, AVERAGE AND THE*
- *LOWEST R-NODE STRESSES*

```

SUBROUTINE CALCU(L,RSTR1,RSTR2,RSTR3,KJ,RSEG,
1 RSTR,ICOUNT,RSEGG)
  INTEGER RSEGG,RSEG,COUNT
  DIMENSION RSTR1(I),RSTR2(I),RSTR3(I),RSEG(I),
1 RSTR(I),ICOUNT(I)
  DIMENSION RSEGG(I)
  COUNT=1
  IJ=1
  KJ=1
  GOTO 125
130  IJ=IJ+1
125  INTA=RSEG(IJ)
  INTB=RSEG(IJ+1)
  IF(INTA.NE.INTB) GOTO 135
  COUNT=COUNT+1
  IF(IJ.EQ.I-1) GOTO 140
  GOTO 130
135  ICOUNT(KJ)=COUNT
  COUNT=1
  RSEGG(KJ)=RSEG(IJ)

  KJ=KJ+1
  IF(IJ.EQ.I-1) GOTO 140
  GOTO 130
140  ICOUNT(KJ)=1

```

```
MM=1
DO 145 IP=1,KJ
BIG=-1E20
AVG=0.0
SMALL=1E20
L=ICOUNT(IP)
DO 150 IQ=1,L
IF(RSTR(MM).GT.BIG) BIG=RSTR(MM)
AVG=RSTR(MM)+AVG
IF(RSTR(MM).LT.SMALL) SMALL=RSTR(MM)
150 MM=MM+1
RSTR1(IP)=BIG
RSTR2(IP)=AVG/L
RSTR3(IP)=SMALL
145 CONTINUE
RETURN
END
```

320

Appendix B

Fortran Program for determining the Minimum Weight Geometry of Mechanical Components and Structures

The following program (minwt.for) determines the r-nodes and the geometry of the minimum weight structure based on the iso r-node stress concept. The program automatically performs interpolation for sections that does not have r-nodes. The output of the program is nodal coordinates and element connectivity listings in an ANSYS readable format.

PROGRAM MINIMUM

PARAMETER(MEMO=1500)

CHARACTER*15 FNAME1,FNAME2,FNAME3,UNITS

INTEGER FLAG1,FLAG2,FLAG3,FLAG4,RSEG,

```

1 ELELOC,COUNT,RSEGG
  INTEGER FLAG5,FLAG6,FLAG7,FLAG8,FLAG9

REAL M1,M2

DIMENSION SIG1(MEMO),SIG2(MEMO),NELE(MEMO)
DIMENSION RSTR(MEMO),RLOC(MEMO),RSEG(MEMO)
DIMENSION ELELOC(MEMO),RNO(MEMO),
1 RSTR1(MEMO),VOL(MEMO)
  DIMENSION RSTR2(MEMO),RSTR3(MEMO),
1 ICOUNT(MEMO),RSEGG(MEMO)
  DIMENSION THICK(MEMO),ORSTR(MEMO),TRSEG(MEMO)
  DIMENSION NNUM(MEMO),XCORD(MEMO),YCORD(MEMO)
  DIMENSION TNSEC(MEMO),XCOORD(MEMO),
1 YCOORD(MEMO),STHK(MEMO)

CALL MESSAGE

WRITE(*,*)'ENTER THE NAME OF THE FIRST LINEAR
1 ANALYSIS INPUT FILE'
53 READ (*,'(A)')FNAME1
  OPEN(15,FILE=FNAME1,STATUS='OLD',ERR=56)
  WRITE(*,*)

WRITE(*,*)'ENTER THE NAME OF THE SOFTENED Nth LINEAR
1 ANALYSIS INPUT FILE'
54 READ (*,'(A)')FNAME2
  OPEN(16,FILE=FNAME2,STATUS='OLD',ERR=57)
  WRITE(*,*)

```

```

OPEN(UNIT=17,FILE='zrstr0.out',STATUS='UNKNOWN')
OPEN(UNIT=18,FILE='zrstrs.out',STATUS='UNKNOWN')

WRITE(*,*)'ENTER THE NAME OF THE OUTPUT FILE FOR THE
1 HIGHEST R-NODE STRESS'
67 READ(*, '(A)')FNAME3
OPEN(UNIT=19,FILE=FNAME3,STATUS='NEW',ERR=66)
WRITE(*,*)
GOTO 68

66 WRITE(*,*)'OUTPUT FILE ALREADY EXISTING. ENTER ANOTHER
1 FILE NAME'
WRITE(*,*)
GOTO 67

* DUMMY STATEMENT
68 DUMMY=0.0

OPEN(unit=20,file='zrstr.avg',status='unknown')
OPEN(unit=21,file='zrstr.sml',status='unknown')
OPEN(unit=22,file='zsumof1.sqr',status='unknown')
OPEN(unit=23,file='zsumof2.sqr',status='unknown')
OPEN(unit=24,file='zmura.res',status='unknown')
OPEN(unit=25,file='nlist',status='old')
OPEN(unit=26,file='nlist.new',status='unknown')
OPEN(unit=27,file='elist',status='old')
OPEN(unit=28,file='elist.new',status='unknown')

WRITE(*,*)'UNIT OF STRESS ? (eg. psi, N/sq.m., Pa,
1 kPa etc.)'

```

```

READ(*, '(A)')UNITS
WRITE(*,*)
WRITE(*,*)'YIELD STRESS = ? ',UNITS 70
READ(*,*)SIGY
WRITE(*,*)
WRITE(*,*)'APPLIED LOAD = ? ',UNITS
READ(*,*)PAPP
WRITE(*,*)
20 WRITE(*,*)'TOTAL NUMBER OF ELEMENTS = ?'
READ(*,*)NELEM
WRITE(*,*)
WRITE(*,*)'NUMBER OF ELEMENTS PER SECTION = ?'
READ(*,*)NEPS 80
WRITE(*,*)
701 WRITE(*,*)'FOR THICKNESS OF THE MINIMUM WEIGHT STRUCTURE'
WRITE(*,*)'CHOOSE ONE OF THE FOLLOWING OPTIONS:'
WRITE(*,*)'(*) Inner surface refers to the surface having'
WRITE(*,*)' the smaller set of node numbers in the node pairs'
WRITE(*,*)'(*) Outer surface refers to the surface having the'
WRITE(*,*)' larger set of node numbers in the node pairs'
WRITE(*,*)
WRITE(*,*)' 1 - PROBLEM WITH NEUTRAL AXIS'
WRITE(*,*)' e.g. beams' 90
WRITE(*,*)' 2 - PROBLEM WITH SMOOTH INNER SURFACE'
WRITE(*,*)' (such as the inner surface of pressure vessels)'
WRITE(*,*)' 3 - PROBLEMS WITH SMOOTH OUTER SURFACE'
WRITE(*,*)' 4 - SYMMETRIC WITH SMOOTH INNER SURFACE'
WRITE(*,*)' (line of symmetry corresponds to neutral axis'
WRITE(*,*)' i.e., inner half of option # 1)'
WRITE(*,*)' 5 - SYMMETRIC WITH SMOOTH OUTER SURFACE'

```

```

WRITE(*,*)'      (line of symmetry corresponds to neutral axis'
WRITE(*,*)'      i.e., outer half of option # 1)'
READ(*,*)FLAG2
WRITE(*,*)
WRITE(*,*)
IF(FLAG2.EQ.1)THEN
GOTO 702
ELSE IF(FLAG2.EQ.2)THEN
GOTO 702
ELSE IF(FLAG2.EQ.3)THEN
GOTO 702
ELSE IF(FLAG2.EQ.4)THEN
GOTO 702
ELSE IF(FLAG2.EQ.5)THEN
GOTO 702
ELSE
  WRITE(*,*)'OPTION # ',FLAG2,' INVALID'
  GOTO 701
END IF
702 WRITE(*,*)'CHOOSE ONE OF THE FOLLOWING OPTIONS'
WRITE(*,*)'MINIMUM WEIGHT BASED ON:'
WRITE(*,*)
WRITE(*,*)'  1 - MAXIMUM R-NODE STRESS IN A SECTION'
WRITE(*,*)'  2 - MINIMUM R-NODE STRESS IN A SECTION'
WRITE(*,*)'  3 - AVERAGE R-NODE STRESS IN A SECTION'
READ(*,*)FLAG3
WRITE(*,*)
WRITE(*,*)
IF(FLAG3.EQ.1)THEN
GOTO 725

```

```

ELSE IF(FLAG3.EQ.2)THEN
GOTO 725
ELSE IF(FLAG3.EQ.3)THEN
GOTO 725
ELSE
WRITE(*,*)'OPTION # ',FLAG3,' INVALID'
GOTO 702
END IF
725 WRITE(*,*)'During optimization some sections may become
1 impracticably thin.'
WRITE(*,*)'Therefore it becomes necessary to
1 prescribe the minimum'
WRITE(*,*)'thickness as "ASPECT" times the
1 maximum thickness'
718 WRITE(*,*)'VALUE OF ASPECT RATIO i.e., MINIMUM THICKNESS/
1 MAXIMUM THICKNESS (<1)'
READ(*,*)ASPECT
IF(ASPECT.GT.1.0)THEN
WRITE(*,*)'"ASPECT" MUST BE LESS THAN 1'
GOTO 718
END IF
WRITE(*,*)
WRITE(*,*)
723 WRITE(*,*)'CHOOSE ONE OF THE FOLLOWING OPTIONS'
WRITE(*,*)'SHAPE OPTIMIZATION BASED ON:'
WRITE(*,*)' 1 - BASED ON THE MAXIMUM R-NODE STRESS - Not
1 Recommended'
WRITE(*,*)
WRITE(*,*)' 2 - BASED ON THE R-NODE STRESS OF A PRESCRIBED
1 SECTION - Recommended'

```

```

READ(*,*)FLAG4
IF(FLAG4.EQ.1)THEN
    GOTO 727
ELSE IF(FLAG4.EQ.2)THEN
    GOTO 727
ELSE
    WRITE(*,*)'OPTION # ',FLAG4,' IS NOT VALID'
    GOTO 723
END IF
727  FLAG9=0
    IF(FLAG4.EQ.2)THEN
808  WRITE(*,*)'SECTION NUMBER CORRESPONDING TO REFERENCE
1 R-NODE STRESS'
    READ(*,*)FLAG9
    IF(FLAG9.GT.(NELEM/NEPS))THEN
        WRITE(*,*)'SECTION NUMBER ',FLAG9,' IS NOT VALID. SHOULD BE'
        WRITE(*,*)'LESS THAN ',NELEM/NEPS
        GO TO 808
    END IF
END IF
WRITE(*,*)
WRITE(*,*)
WRITE(*,*)'CHOOSE ONE OF THE FOLLOWING OPTIONS'
WRITE(*,*)' 1 - MAXIMUM THICKNESS OF THE ORIGINAL STRUCTURE'
WRITE(*,*)'      CANNOT BE EXCEEDED ANY WHERE DURING
1 OPTIMIZATION'
WRITE(*,*)' 2 - MAXIMUM THICKNESS CAN BE EXCEEDED IN SOME'
WRITE(*,*)'      PARTS OF THE STRUCTURE DURING OPTIMIZATION'
WRITE(*,*)' Option # 2 results in better design than
1 option # 1'

```

```

WRITE(*,*)' 3 - MAXIMUM THICKNESS OF THE ORIGINAL STRUCTURE'
WRITE(*,*)' CANNOT BE EXCEEDED ANY WHERE DURING
1 OPTIMIZATION'
WRITE(*,*)' BUT THE THINNER SECTIONS ARE GIVEN AN'
WRITE(*,*)' ADDITIONAL THICKNESS ALLOWANCE'
READ(*,*)FLAG5
IF(FLAG5.EQ.1)THEN
  GOTO 726
ELSE IF(FLAG5.EQ.2)THEN
  GOTO 726
ELSE IF(FLAG5.EQ.3)THEN
  GOTO 726
ELSE
  WRITE(*,*)'OPTION # ',FLAG5,' IS INVALID'
  GOTO 727
END IF
190

726 IF(FLAG5.EQ.1.AND.FLAG4.EQ.2)THEN
  WRITE(*,*)'OPTION # 1 IS NOT VALID SINCE OPTIMIZATION
1 IS BASED ON MAXIMUM SECTION'
  WRITE(*,*)'THICKNESS OF THE ORIGINAL STRUCTURE. SOME
1 SECTIONS OF THE OPTIMIZED STRUCTURE'
  WRITE(*,*)'CAN BECOME THICKER THAN THE MAXIMUM THICKNESS
210
1 OF THE ORIGINAL STRUCTURE'
  WRITE(*,*)
  WRITE(*,*)'DO YOU WANT TO'
  WRITE(*,*)' 1 - WANT TO CHANGE OPTIONS'
  WRITE(*,*)' 2 - CONTINUE WITH OPTION # 2'
  READ(*,*)FLAG6
  IF(FLAG6.EQ.2)THEN

```

```

        FLAG5=2
        ELSE
        GOTO 723
        END IF
    END IF
724  WRITE(*,*)
    WRITE(*,*)
    WRITE(*,*) 'PERCENTAGE DIMENSIONAL SAFETY ALLOWANCE
1 (USUALLY 0-10%) '
    READ(*,*)PERCENT
    IF(PERCENT.GT.50.0)THEN
        WRITE(*,*) 'INPUT VALUE OF ',PERCENT,'% INVALID. SHOULD '
        WRITE(*,*) 'BE LESS THAN 50.0%'
        GOTO 724
    END IF

    WRITE(*,*)
    WRITE(*,*)
805  WRITE(*,*) 'DO YOU WANT TO FORCE SIMPLY SUPPORTED BOUNDARY
1 CONDITION?'
    WRITE(*,*) '(i.e., postulate that the r-node stress in the'
    WRITE(*,*) ' simply supported egde(s) is zero)'
    WRITE(*,*)
    WRITE(*,*) 'YES => 1           :           NO => 2'
    READ(*,*)FLAG7
    IF(FLAG7.EQ.1)THEN
        GOTO 804
    ELSE IF(FLAG7.EQ.2)THEN
        GOTO 804
    ELSE

```

```

WRITE(*,*)'OPTION # ',FLAG7,' IS INVALID'
GOTO 805
END IF
250
804 IF(FLAG7.EQ.1)THEN
807 WRITE(*,*)'CHOOSE ONE OF THE FOLLOWING CONDITIONS'
WRITE(*,*)' EDGE IN THE VICINITY OF SECTION # 1 => 1'
NSEG = NELEM/NEPS
WRITE(*,801)NSEG
801 FORMAT(5x,'EDGE IN THE VICINITY OF SECTION # ',I4,' => 2')
WRITE(*,*)' BOTH THE EDGES => 3'
READ(*,*)FLAG8
IF(FLAG8.EQ.1)THEN
GOTO 806
260
ELSE IF(FLAG8.EQ.2)THEN
GOTO 806
ELSE IF(FLAG8.EQ.3)THEN
GOTO 806
ELSE
WRITE(*,*)'OPTION # ',FLAG8,' IS INVALID'
GOTO 807
END IF
ELSE
FLAG8=0
270
END IF

806 DO MM=1,30
WRITE(*,*)
END DO
WRITE(*,*)'Program running. . .'
```

```

CALL CHKINP(NELEM,NEPS,FLAG1)
  IF (FLAG1.EQ.1) THEN
    GO TO 20
  END IF
  NSEG = NELEM/NEPS
  CALL VINPUT(SIG1,SIG2,NELE,NELEM,VOL,SIGY,
1 PAPP,UNITS)
  CALL RNODE(SIG1,SIG2,NSEG,NELEM,NEPS,
1 RSEG,RSTR,RLOC,ELELOC,I)
  CALL RESULT(RSEG,RLOC,ELELOC,RSTR,NEPS,I)
  CALL CALCU(I,RSTR1,RSTR2,RSTR3,KJ,RSEG,RSTR,
1 ICOUNT,RSEGG)
  WRITE(19,*) 'Maximum R-Node Stress'
  WRITE(20,*) 'Average R-Node Stress'
  WRITE(21,*) 'Minimum R-Node Stress'
  BIG1=0.0
  KJ=KJ-1
  DO 155 IPP=1,KJ
    WRITE(19,*) RSEGG(IPP),RSTR1(IPP)
    IF(RSTR1(IPP).GT.BIG1)BIG1=RSTR1(IPP)
    WRITE(20,*) RSEGG(IPP),RSTR2(IPP)
    WRITE(21,*) RSEGG(IPP),RSTR3(IPP)
155 CONTINUE
  WRITE(24,*) 'The highest r-node stress value = ',big1,' ',units
  CALL INTERPOL(FLAG3,RSTR1,RSTR2,RSTR3,NSEG,
1 KJ,RSEGG,ORSTR,MEMO,FLAG8)
  CALL RDNODE(NNUM,XCORD,YCORD,NSEG,NTOT,MEMO)
  CALL MAXTHK(NNUM,XCORD,YCORD,THKMAX,NTOT,
1 THICK,ORSTR,SIGMA_N1,MEMO,BIGRST,REFTHK,STHK)
  CALL RTHICK(ORSTR,SIGMA_N1,THKMAX,TRSEG,NSEG,

```

```

1 MEMO,BIGRST,REFTHK,FLAG4,STHK,FLAG9)
  CALL NTHICK(TRSEG,TNSEC,NTOT,MEMO,ASPECT,THKMAX)
  CALL NLIST(TNSEC,NTOT,XCORD,YCORD,XCOORD,YCOORD, 310
1 THICK,FLAG2,MEMO,PERCENT,FLAG5,THKMAX)
  CALL NODES(XCOORD,YCOORD,NTOT,MEMO,NEPS,NNUM)
  CALL RDELEM(NELEM)

  CLOSE(28)
  CLOSE(27)
  CLOSE(26)
  CLOSE(25)
  CLOSE(24)
  CLOSE(23)
  CLOSE(22)
  CLOSE(21)
  CLOSE(20)
  CLOSE(19)
  CLOSE(18)
  CLOSE(17)
  CLOSE(16)
  CLOSE(15)
  GO TO 58
56 PRINT *,'The first input file ',fname1,' is not existing. 330
1 Re-enter another file name'
  GO TO 53
57 PRINT *,'The second input file ',fname2,' is not existing.
1 Re-enter another file name'
  GO TO 54
58 WRITE(*,*)'Program completed'
  STOP

```

END

340

* MESSAGE

SUBROUTINE MESSAGE

```
WRITE(*,*) 'THIS PROGRAM DETERMINES THE OPTIMUM SHAPE OF'  
WRITE(*,*) 'A GIVEN STRUCTURE USING THE R-NODE METHOD.'  
WRITE(*,*) 'THE OUTPUT FILES "nlist.new" and "elist.new" '  
WRITE(*,*) 'REPRESENTS THE NODAL COORDINATES AND THE ELEMENT'  
WRITE(*,*) 'CONNECTIVITY AND CAN BE DIRECTLY INPUT INTO ANSYS'  
WRITE(*,*)  
WRITE(*,*) 'THE NODAL COORDINATES AND ELEMENT CONNECTIVITY'  
WRITE(*,*) 'ARE SUITABLE ONLY FOR ANSYS STIF-42 ELEMENTS'  
WRITE(*,*)  
WRITE(*,*) '          . . . . .hit < r e t u r n > to continue'  
READ(*,*)  
DO MM=1,30  
WRITE(*,*)  
END DO  
RETURN  
END
```

350

360

* CHECK INPUT FOR CORRECTNESS

```
SUBROUTINE CHKINP(NELEM,NEPS,FLAG1)  
INTEGER FLAG1  
FLAG1=0  
R=FLOAT(NELEM)
```

```

R1=FLOAT(NEPS)
R2=R/R1
I=NELEM/NEPS
R3=FLOAT(I)
IF(R3.NE.R2)THEN
  FLAG1=1
  WRITE(*,21)
21  FORMAT(1X,'INPUT ERROR: Check and reinput total number of
1 elements',/,1X,'or No. of elements per segment. . . .')
  END IF
  RETURN
  END

```

370

* *READ INPUT FILE (strs1.out and strs2.out)*

```

SUBROUTINE VINPUT(SIG1,SIG2,NELE,NELEM,VOL,
1 SIGY,PAPP,UNITS)
  CHARACTER*(*) UNITS
  DIMENSION SIG1(NELEM),SIG2(NELEM),NELE(NELEM),
1 VOL(NELEM)

```

380

* *READ FIRST LINEAR ANALYSIS STRESS LISTING*

```

READ(15,25)
25  FORMAT(////////)
  K=NELEM/41
  J=NELEM-K*41
  I=1
  DO 30 K1=1,K
  DO 35 K2=1,41

```

390

```

      READ(15,*)NELE(I),SIG1(I)
35    I=I+1
      READ(15,40)
40    FORMAT(////)
30    CONTINUE
      DO 45 J1=1,J
      READ(15,*)NELE(I),SIG1(i)
45    I=I+1

*    READ SECOND LINEAR ANALYSIS STRESS LISTING

      READ(16,50)
50    FORMAT(/////))
      I=1
      DO 55 K1=1,K
      DO 60 K2=1,41
      READ(16,*)A,SIG2(I),VOL(I)
60    I=I+1
      READ(16,65)
65    FORMAT(////)
55    CONTINUE
      DO 70 J1=1,J
      READ(16,*)A,SIG2(I),VOL(I)
70    I=I+1

      SUMM=0.0
      SUMX=0.0
      VOLU=0.0

```

* *To find the biggest of the second linear stress value*

```

BIGG=0.0
BIGG1=0.0
DO K=1,NELEM
IF(SIG2(K).GT.BIGG)BIGG=SIG2(K)
END DO
DO K=1,NELEM
IF(SIG1(K).GT.BIGG1)BIGG1=SIG1(K)
END DO

DO K=1,NELEM
SUMN=(SIG2(K)**2)*VOL(K)
SUMY=(SIG1(K)**2)*VOL(K)
VOLU=VOLU+VOL(K)
SUMM=SUMM+SUMN
SUMX=SUMX+SUMY
WRITE(22,*)SUMX,VOLU
WRITE(23,*)SUMM,VOLU
END DO
RMO=SIGY*SQRT(VOLU)/SQRT(SUMM)
DENOM=(SIGY**2+(RMO*BIGG)**2)/(2.0*SIGY**2)
PLBOYL=SIGY/BIGG*PAPP
RMO1=SIGY*SQRT(VOLU)/SQRT(SUMX)
DENOM1=(SIGY**2+(RMO1*BIGG1)**2)/(2.0*SIGY**2)
PLBOYL1=SIGY/BIGG1*PAPP
WRITE(24,*)'Applied pressure      = ',PAPP,' ',UNITS
WRITE(24,*)'Yield stress = ',SIGY,' ',UNITS
WRITE(24,*)'Maximum stress:'
WRITE(24,*)'  I linear analysis = ',BIGG1,' ',UNITS
WRITE(24,*)'  II linear analysis = ',BIGG,' ',UNITS

```

```

WRITE(24,*)'Classical limit load:'
WRITE(24,*)'  I linear analysis = ',PLBOYL1,' ',UNITS
WRITE(24,*)'  II linear analysis = ',PLBOYL,' ',UNITS      460
WRITE(24,*)'Value of m0:'
WRITE(24,*)'  I linear analysis = ',RMO1
WRITE(24,*)'  II linear analysis = ',RMO
WRITE(24,*)'Value of the denominator:'
WRITE(24,*)'  I linear analysis = ',DENOM1
WRITE(24,*)'  II linear analysis = ',DENOM
WRITE(24,*)'m0 x P:'
WRITE(24,*)'  I linear analysis = ',RMO1*PAPP,' ',UNITS
WRITE(24,*)'  II linear analysis = ',RMO*PAPP,' ',UNITS
WRITE(24,*)'m0 x P/Denominator:'      470
WRITE(24,*)'  I linear analysis = ',RMO1*PAPP/DENOM1.
1 ' ',UNITS
WRITE(24,*)'  II linear analysis = ',RMO*PAPP/DENOM.
1 ' ',UNITS
WRITE(24,*)'Total volume           = ',VOLU
RETURN
END

```

• *CALCULATE R-NODE STRESSES AND LOCATIONS* 480

```

SUBROUTINE RNODE(SIG1,SIG2,NSEG,NELEM,NEPS,
1 RSEG,RSTR,RLOC,ELELOC,I)
  INTEGER RSEG,ELELOC
  REAL M1,M2
  DIMENSION SIG1(NELEM),SIG2(NELEM),RSEG(NELEM),
1 RSTR(NELEM),RLOC(NELEM),ELELOC(NELEM)

```

```

I=1
DO 85 J=1,NSEG                                490
DO 85 K=1,NEPS-1
IJK=(J-1)*NEPS+K
M1=SIG1(IJK+1)-SIG1(IJK)
M2=SIG2(IJK+1)-SIG2(IJK)
SLOPE=ABS(M1-M2)
IF (SLOPE.LE.0.00001) THEN
    GOTO 85
END IF
X=(SIG2(IJK)-SIG1(IJK))/(M1-M2)+FLOAT(K)-0.5
Y=M1*(SIG2(IJK)-SIG1(IJK))/(M1-M2)+SIG1(IJK)    500
RK=FLOAT(K)+0.5
RK1=FLOAT(K)-0.5
IF(X.LE.RK.AND.X.GE.RK1) THEN
    RSTR(I)=Y
    RLOC(I)=X
    RSEG(I)=J
    ELELOC(I)=IJK
    I=I+1
END IF
85 CONTINUE                                    510
RETURN
END

```

• *DISPLAY RESULTS*

```

SUBROUTINE RESULT(RSEG,RLOC,ELELOC,RSTR,NEPS,I)
INTEGER RSEG,ELELOC

```

```

DIMENSION RSEG(I),RLOC(I),ELELOC(I),RSTR(I)
WRITE(17,95)
95  FORMAT(1X,'SEGMENT NO      LOCATION          R-NODE STRESS')
WRITE(17,100)
100 FORMAT(1X,'          R-NODE      ELEMENTS          ')
DO 105 II=1,I-1
IE1=RSEG(II)
IE2=ELELOC(II)
IE3=ELELOC(II) + 1
WRITE(17,110)IE1,RLOC(II),IE2,IE3,RSTR(II)
110 FORMAT(1X,I4,2X,F9.5,2X,I5,2X,I5,2X,F13.5)
WRITE(18,111) IE1,RSTR(II)
111 FORMAT(1X,I10,2X,F13.5)
105 CONTINUE
RETURN
END

```

- DETERMINES THE HIGHEST, AVERAGE AND THE
- LOWEST R-NODE STRESSES

```

SUBROUTINE CALCU(I,RSTR1,RSTR2,RSTR3,KJ,
1 RSEG,RSTR,ICOUNT,RSEGG)
INTEGER RSEGG,RSEG,COUNT
DIMENSION RSTR1(I),RSTR2(I),RSTR3(I),RSEG(I),
1 RSTR(I),ICOUNT(I)
DIMENSION RSEGG(I)
COUNT=1
IJ=1
KJ=1
GOTO 125

```

```

130  IJ=IJ+1
125  INTA=RSEG(IJ)
      INTB=RSEG(IJ+1)
      IF(INTA.NE.INTB) GOTO 135
      COUNT=COUNT+1
      IF(IJ.EQ.I-1) GOTO 140
      GOTO 130
135  ICOUNT(KJ)=COUNT
      COUNT=1
      RSEGG(KJ)=RSEG(IJ)

      KJ=KJ+1
      IF(IJ.EQ.I-1) GOTO 140
      GOTO 130

140  ICOUNT(KJ)=1

      MM=1
      DO 145 IP=1,KJ
      BIG=-1E20
      AVG=0.0
      SMALL=1e20
      L=ICOUNT(IP)
      DO 150 IQ=1,L
      IF(RSTR(MM).GT.BIG) BIG=RSTR(MM)
      AVG=RSTR(MM)+AVG
      IF(RSTR(MM).LT.SMALL) SMALL=RSTR(MM)
150  MM=MM+1
      RSTR1(IP)=BIG
      RSTR2(IP)=AVG/L

```

```
RSTR3(IP)=SMALL
145 CONTINUE
RETURN
END
```

580

• *LINEAR INTERPOLATION OF THE R-NODE STRESSES*

```
SUBROUTINE INTERPOL(FLAG3,RSTR1,RSTR2,RSTR3,NSEG,
1 KJ,RSEGG,ORSTR,MEMO,FLAG8)
INTEGER FLAG3,RSEGG,FLAG8
DIMENSION RSTR1(MEMO),RSTR2(MEMO),RSTR3(MEMO),
1 RSEGG(MEMO),ORSTR(MEMO)
```

590

```
DO KO1=1,NSEG
ORSTR(KO1)=0.0
END DO
```

```
IF(FLAG3.EQ.1)THEN
DO KO2=1,KJ
KP1=RSEGG(KO2)
ORSTR(KP1)=RSTR1(KO2)
END DO
```

600

```
ELSE
IF(FLAG3.EQ.2)THEN
DO KO2=1,KJ
KP1=RSEGG(KO2)
ORSTR(KP1)=RSTR2(KO2)
END DO
ELSE
```

```

      IF(FLAG3.EQ.3)THEN
        DO KO2=1,KJ
          KP1=RSEGG(KO2)
          ORSTR(KP1)=RSTR3(KO2)
        END DO
      END IF
    END IF
  END IF

  IF(FLAG8.EQ.1)GOTO 802
  IF(FLAG8.EQ.3)GOTO 803
  KP2=RSEGG(1)
  DO KO3=1,KP2-1
    ORSTR(KO3)=ORSTR(KP2)
  END DO

  IF(FLAG8.EQ.2)GOTO 803
802  KP3=RSEGG(KJ)
    DO KO4=KP3+1,NSEG
      ORSTR(KO4)=ORSTR(KP3)
    END DO

803  IF(FLAG8.EQ.1.OR.FLAG8.EQ.3)THEN
      DO KSP=1,KJ
        RSEGG(KJ+2-KSP)=RSEGG(KJ+1-KSP)
      END DO
      KJ=KJ+1
      RSEGG(1)=1
      ORSTR(1)=0.0001
    END IF

```

IF(FLAG8.EQ.2.OR.FLAG8.EQ.3)THEN

KJ=KJ+1

640

RSEGG(KJ)=NSEG

ORSTR(NSEG)=0.0001

END IF

DO KO5=1,KJ-1

KP5=RSEGG(KO5)

KP6=RSEGG(KO5+1)

IDIFF=KP6-KP5

DO KO6=1,IDIFF-1

650

KP4=KP5+KO6

ORSTR(KP4)=ORSTR(KP5)+(FLOAT(KP4-KP5)*

1 (ORSTR(KP6)-ORSTR(KP5))/FLOAT(IDIFF))

END DO

END DO

=====

* *msp* *C H E C K P O I N T - I*

do icht1=1,nseg

write(80,*)'ORSTR(',icht1,') = ',orstr(icht1)

end do

660

=====

RETURN

END

* *READS NODE LISTING FOR THE SELECTED NODES*
SUBROUTINE RDNODE(NNUM,XCORD,YCORD,NSEG,
1 NTOT,MEMO)

```
DIMENSION NNUM(MEMO),XCORD(MEMO),YCORD(MEMO)
NTOT=(NSEG+1)*2
```

670

```
      READ(25,703)
703  FORMAT(//////////)
      GOTO 714
713  REWIND(25)
      READ(25,715)
715  FORMAT(///)
714  K=NTOT/20
      J=NTOT-K*20
      IO1=1
      DO K1=1,K
      DO K2=1,20
      READ(25,*,ERR=713)NNUM(IO1),XCORD(IO1),YCORD(IO1).a.b.c.d
      IO1=IO1+1
      END DO
      READ(25,704,ERR=713)
704  FORMAT(/)
      END DO
      DO J1=1,J
      READ(25,*,ERR=713)NNUM(IO1),XCORD(IO1),YCORD(IO1).a.b.c.d
      IO1=IO1+1
      END DO
```

680

690

```
=====
```

```
* msp          CHECK POINT - II
      do ichk1=1,ntot
      write(81,*)'NNUM(' ,ichk1,') = ',nnum(ichk1),'  XCORD(' ,
1 ichk1,') = ',xcord(ichk1),'  YCORD(' ,ichk1,') = ',
1 ycord(ichk1)
```

end do

=====

RETURN

700

END

* DETERMINES THE MAXIMUM SECTION THICKNESS
* AND THE CORRESPONDING R-NODE STRESS - SIGMA_N1
SUBROUTINE MAXTHK(NNUM,XCORD,YCORD,THKMAX,
1 NTOT,THICK,ORSTR,SIGMA_N1,MEMO,BIGRST,REFTHK,STHK)
DIMENSION NNUM(MEMO),XCORD(MEMO),YCORD(MEMO)
DIMENSION THICK(MEMO),ORSTR(MEMO),STHK(MEMO)
NTOTAL=NTOT/2
THKMAX=0.0
DO IO2=1,NTOTAL
THICK(IO2)=SQRT((YCORD(IO2+NTOTAL)-YCORD(IO2))**2
1 +(XCORD(IO2+NTOTAL)-XCORD(IO2))**2)
IF(THICK(IO2).GT.THKMAX) THEN
THKMAX=THICK(IO2)
MARK1=IO2
END IF
END DO
RMARK1=ORSTR(MARK1-1)
RMARK2=ORSTR(MARK1)
SIGMA_N1=MAX(RMARK1,RMARK2)
DO KO2A=1,NTOTAL-1
IF(THICK(KO2A).GE.THKMAX.AND.ORSTR(KO2A).
1 GT.SIGMA_N1) THEN
SIGMA_N1=ORSTR(KO2A)
THKMAX=THICK(KO2A)
END IF

710

720

```

END DO
BIGRST=0.0
DO KO2B=1,NTOTAL-1
  IF(ORSTR(KO2B).GT.BIGRST)THEN
    BIGRST=ORSTR(KO2B)
    REFTHK=MAX(THICK(KO2B),THICK(KO2B+1))
  END IF
END DO

```

730

```

DO KGOD=1,NTOTAL-1
  STHK(KGOD)=(THICK(KGOD)+THICK(KGOD+1))/2.0
END DO

```

740

```

=====
* msp          CHECK POINT - III
do ichk1=1,ntotal
write(82,*)'THICK(' ,ichk1,' ) = ',thick(ichk1)
end do
write(82,*)'THKMAX = ',thkmax
write(82,*)'SIGMA_N1 = ',sigma_n1
do ichk11=1,ntotal-1
write(83,*)'STHK(' ,ichk11,' ) = ',sthk(ichk11)
end do

```

750

```

=====
RETURN
END

```

- * DETERMINES THE THICKNESS OF THE R-NODE SECTIONS
SUBROUTINE RTHICK(ORSTR,SIGMA_N1,THKMAX,TRSEG,
1 NSEG,MEMO,BIGRST,REFTHK,FLAG4,STHK,FLAG9)
DIMENSION ORSTR(MEMO),TRSEG(MEMO),STHK(MEMO)

INTEGER FLAG4,FLAG9

IF(FLAG4.EQ.1)THEN

DO KO7A=1,NSEG

TRSEG(KO7A)=STHK(KO7A)*SQRT(ORSTR(KO7A)/BIGRST)

760

END DO

END IF

IF(FLAG4.EQ.2)THEN

DO KO7=1,NSEG

TRSEG(KO7)=STHK(KO7)*SQRT(ORSTR(KO7)/ORSTR(FLAG9))

END DO

END IF

=====

* *msp* CHECK POINT - IV

770

do ichk1=1,nseg

write(84,*)'TRSEG(' ,ichk1,') = ',trseg(ichk1)

end do

=====

RETURN

END

* DETERMINES THE NODE THICKNESS LIST

SUBROUTINE NTHICK(TRSEG,TNSEC,NTOT,MEMO.

1 ASPECT,THKMAX)

780

DIMENSION TRSEG(MEMO),TNSEC(MEMO)

NTOTAL=NTOT/2

THKMIN=ASPECT*THKMAX

TNSEC(1)=TRSEG(1)

TNSEC(NTOTAL)=TRSEG(NTOTAL-1)

DO KO8=2,NTOTAL-1

TNSEC(KO8)=MAX(TRSEG(KO8-1),TRSEG(KO8))

```

END DO
DO KO8A=1,NTOTAL
  IF(TNSEC(KO8A).LT.THKMIN)THEN
    WRITE(*,711)KO8A,TNSEC(KO8A),THKMIN
711  FORMAT(1X,'THICKNESS OF NODAL SEC. #',I3,'=',
1 F7.3,' LESS THAN PRESCRIBED MIN. OF',F7.3)
    WRITE(*,*)'THICKNESS CORRECTION PERFORMED'
    TNSEC(KO8A)=THKMIN
  END IF
END DO

=====
* msp          C H E C K   P O I N T   -   V
  do  ichk1=1,ntotal
  write(85,*)'TNSEC(',ichk1,') = ',tnsec(ichk1)
  end do
=====

RETURN
END

*  DETERMINES THE NEW NODE LIST
SUBROUTINE NLIST(TNSEC,NTOT,XCORD,YCORD,XCOORD,
1 YCOORD,THICK,FLAG2,MEMO,PERCENT,FLAG5,THKMAX)
  DIMENSION TNSEC(MEMO),XCORD(MEMO),YCORD(MEMO)
  DIMENSION XCOORD(MEMO),YCOORD(MEMO),
1 THICK(MEMO)
  INTEGER FLAG2,FLAG5
  NTOTAL=NTOT/2
  DO KO9=1,NTOTAL
    SP=(100.0-PERCENT)/100.0
    IF(FLAG5.EQ.2)THEN
810

```

```

      DELT=THICK(KO9)*SP-TNSEC(KO9)
    END IF
    IF(FLAG5.EQ.1)THEN
      DELT=THICK(KO9)*SP-TNSEC(KO9)
      IF(DELT.LT.0.0)THEN
        DELT=THICK(KO9)-TNSEC(KO9)
        IF(DELT.LT.0.0)THEN
          DELT=THKMAX-TNSEC(KO9)
          IF(DELT.LT.0.0)THEN
            DELT=0.0
          END IF
        END IF
      END IF
    END IF
    IF(FLAG5.EQ.3)THEN
      DELT=(1.0-PERCENT/100.0)*(THICK(KO9)-TNSEC(KO9))
    END IF

    DELX=DELT*ABS(XCORD(KO9)-XCORD(KO9+NTOTAL))
    1 /THICK(KO9)
    DELY=DELT*ABS(YCORD(KO9)-YCORD(KO9+NTOTAL))
    1 /THICK(KO9)

=====
* msp      C H E C K   P O I N T   -   V I
*      write(*,*)'DELT = ',delt
*      write(*,*)'DELX = ',delx
*      write(*,*)'DELY = ',dely
*      write(*,*)'FLAG2 = ',flag2
=====
      IF(FLAG2.EQ.1)THEN

```

820

830

840

```

      IF(YCORD(K09).GE.YCORD(K09+NTOTAL))THEN
        YCOORD(K09)=YCORD(K09)-DELY/2.0
        YCOORD(K09+NTOTAL)=YCORD(K09+NTOTAL)
1 +DELY/2.0
      ELSE
        YCOORD(K09)=YCORD(K09)+DELY/2.0
        YCOORD(K09+NTOTAL)=YCORD(K09+NTOTAL)
1 -DELY/2.0
      END IF
      IF(XCORD(K09).GE.XCORD(K09+NTOTAL))THEN
        XCOORD(K09)=XCORD(K09)-DELX/2.0
        XCOORD(K09+NTOTAL)=XCORD(K09+NTOTAL)
1 +DELX/2.0
      ELSE
        XCOORD(K09)=XCORD(K09)+DELX/2.0
        XCOORD(K09+NTOTAL)=XCORD(K09+NTOTAL)
1 -DELX/2.0
      END IF
    END IF
    IF(FLAG2.EQ.2)THEN
      IF(YCORD(K09).GE.YCORD(K09+NTOTAL))THEN
        YCOORD(K09)=YCORD(K09)
        YCOORD(K09+NTOTAL)=YCORD(K09+NTOTAL)
1 +DELY
      ELSE
        YCOORD(K09)=YCORD(K09)
        YCOORD(K09+NTOTAL)=YCORD(K09+NTOTAL)
1 -DELY
      END IF
      IF(XCORD(K09).GE.XCORD(K09+NTOTAL))THEN

```

850

860

870

```

        XCOORD(KO9)=XCORD(KO9)
        XCOORD(KO9+NTOTAL)=XCORD(KO9+NTOTAL)
1 +DELX
        ELSE
        XCOORD(KO9)=XCORD(KO9)
        XCOORD(KO9+NTOTAL)=XCORD(KO9+NTOTAL)
1 -DELX
        END IF
    END IF
    IF(FLAG2.EQ.3)THEN
        IF(YCORD(KO9).GE.YCORD(KO9+NTOTAL))THEN
            YCOORD(KO9)=YCORD(KO9)-DELY
            YCOORD(KO9+NTOTAL)=YCORD(KO9+NTOTAL)
        ELSE
            YCOORD(KO9)=YCORD(KO9)+DELY
            YCOORD(KO9+NTOTAL)=YCORD(KO9+NTOTAL)
        END IF
        IF(XCORD(KO9).GE.XCORD(KO9+NTOTAL))THEN
            XCOORD(KO9)=XCORD(KO9)-DELX
            XCOORD(KO9+NTOTAL)=XCORD(KO9+NTOTAL)
        ELSE
            XCOORD(KO9)=XCORD(KO9)+DELX
            XCOORD(KO9+NTOTAL)=XCORD(KO9+NTOTAL)
        END IF
    END IF
    IF(FLAG2.EQ.4)THEN
        DELX=DELX/2.0
        DELY=DELY/2.0
        IF(YCORD(KO9).GE.YCORD(KO9+NTOTAL))THEN
            YCOORD(KO9)=YCORD(KO9)

```

```

        YCOORD(KO9+NTOTAL)=YCORD(KO9+NTOTAL)
1 +DELY
        ELSE
        YCOORD(KO9)=YCORD(KO9)
        YCOORD(KO9+NTOTAL)=YCORD(KO9+NTOTAL)
1 -DELY
        END IF
        IF(XCORD(KO9).GE.XCORD(KO9+NTOTAL))THEN
        XCOORD(KO9)=XCORD(KO9)
        XCOORD(KO9+NTOTAL)=XCORD(KO9+NTOTAL)
1 +DELX
        ELSE
        XCOORD(KO9)=XCORD(KO9)
        XCOORD(KO9+NTOTAL)=XCORD(KO9+NTOTAL)
1 -DELX
        END IF
        END IF
        IF(FLAG2.EQ.5)THEN
        DELX=DELX/2.0
        DELY=DELY/2.0
        IF(YCORD(KO9).GE.YCORD(KO9+NTOTAL))THEN
        YCOORD(KO9)=YCORD(KO9)-DELY
        YCOORD(KO9+NTOTAL)=YCORD(KO9+NTOTAL)
        ELSE
        YCOORD(KO9)=YCORD(KO9)+DELY
        YCOORD(KO9+NTOTAL)=YCORD(KO9+NTOTAL)
        END IF
        IF(XCORD(KO9).GE.XCORD(KO9+NTOTAL))THEN
        XCOORD(KO9)=XCORD(KO9)-DELX
        XCOORD(KO9+NTOTAL)=XCORD(KO9+NTOTAL)

```

```

ELSE
  XCOORD(KO9)=XCORD(KO9)+DELX
  XCOORD(KO9+NTOTAL)=XCORD(KO9+NTOTAL)
END IF
END IF
END DO
=====
* msp          C H E C K   P O I N T   -   V I I
*   do  ichk1=1,ntotal
*   write(*,*)'XCOORD(',ichk1,') = ',zcoord(ichk1),
*   1 'YCOORD(',ichk1,') = ',ycoord(ichk1)
*   end do
=====
RETURN
END

*   OUTPUTS THE LIST OF NODES SUITABLE FOR ANSYS
SUBROUTINE NODES(XCOORD,YCOORD,NTOT,MEMO,
1 NEPS,NNUM)
  DIMENSION XCOORD(MEMO),YCOORD(MEMO),NNUM(MEMO)
  NTOTAL=NTOT/2
  DO KQ1=1,NTOT
    WRITE(26,707)NNUM(KQ1),XCOORD(KQ1),YCOORD(KQ1)
707  FORMAT(1X,'N',',I5,',',F11.7,',',F11.7)
    END DO
    DO KQ1A=1,NTOTAL
      WRITE(26,708)NNUM(KQ1A),NNUM(KQ1A+NTOTAL),NEPS-1
708  FORMAT(1X,'FILL',',I5,',',I5,',',I5)
    END DO
  RETURN

```

END

* *READS THE ELEMENT LIST OF ANSYS AND PRODUCES* 970
* *ANSYS READABLE ELEMENT LIST*

SUBROUTINE RDELEM(NELEM)

```
      READ(27,705)
705  FORMAT(////////////////)
      GOTO 722
720  REWIND(27)
      REWIND(28)
      READ(27,719)
890
719  FORMAT(///)
722  K=NELEM/20
      J=NELEM-K*20
      IO1=1
      DO K1=1,K
      DO K2=1,20
      READ(27,*,ERR=720)NENUM,IA,IB,IC,ID,NI,NJ,NK,NL
      WRITE(28,709)NI,NJ,NK,NL
709  FORMAT(1X,'E','I5','I5','I5','I5','I5')
      IO1=IO1+1
890
      END DO
      READ(27,706,ERR=721)
706  FORMAT(//)
      GOTO 728
721  IF(J.EQ.0) THEN
      GOTO 712
      ELSE
```

```
        GOTO 720
    END IF
728  END DO
                                           1000
    DO J1=1,J
    READ(27,*,ERR=720)NENUM,IA,IB,IC,ID,NI,NJ,NK,NL
    WRITE(28,710)NI,NJ,NK,NL
710  FORMAT(1X,'E','I5','I5','I5','I5')
    IO1=IO1+1
    END DO
712  RETURN
    END
```

Appendix C

ANSYS Commands Listing of Mechanical Components and Structures

All ANSYS commands listing for the problems given in Chapter 4 are provided in this section. Some typical inelastic analysis listings using ANSYS are also provided. Finally, listings for the layered beam problems are given.

C.1 Isotropic Components

C.1.1 Linear Elastic Analysis

C.1.1.1 Thick Cylinder Subjected to Internal Pressure

/BATCH

```
*SET,RI,3           ! INNER RADIUS (inch)
*SET,RO,9           ! OUTER RADIUS (inch)
*SET,NELEM,90       ! NO. OF ELEMENTS ACROSS THE CROSS-SECTION
```

```

*SET,THICK,(RO-RI)/NELEM ! THICKNESS (ENSURES SQUARE ELEMENTS)

*SET,YS,30E03           ! YIELD STRENGTH (psi)
*SET,YM,30E06           ! YOUNG'S MODULUS (psi)
*SET,POISSON,0.3        ! POISSON'S RATIO
*SET,PRSR,10E03         ! INTERNAL PRESSURE (psi)

/PREP7                   ! ENTER PREPROCESSOR
/TITLE,THICK CYLINDER UNDER INTERNAL PRESSURE
ANTYPE,0
ET,1,42,0,0,1,0,0       ! ELEMENT TYPE - PLANE42 (FOUR NODED ISOPARAMETRIC)
                          ! AXISYMMETRIC OPTION
MP,EX,1,YM               ! YOUNG'S MODULUS
MP,NUXY,,0.3            ! POISSON'S RATIO

N,1,RI                   ! DEFINE NODES
N,NELEM+1,RO
FILL,1,NELEM+1
N,NELEM+2,RI,THICK
N,2*(NELEM+1),RO,THICK
FILL,NELEM+2,2*(NELEM+1)

*DO,K,1,NELEM           ! DEFINE ELEMENTS
E,K,K+1,NELEM+K+2,NELEM+K+1
*ENDDO

FINISH                   ! EXIT PREPROCESSOR

/SOLUTION                ! ENTER SOLUTION ROUTINE

```

```

ANTYPE,0           ! STATIC ANALYSIS

D,ALL,UY,0        ! DISPLACEMENT BOUNDARY CONDITION

NSEL,S,LOC,X,RI   ! APPLY UNIFORM INTERNAL PRESSURE
SF,ALL,PRES,PRSR
NSEL,ALL

SAVE              ! SAVE DATA-BASE
SOLVE            ! SOLVE EQUATIONS

FINISH           ! EXIT SOLUTION ROUTINE

/INP,rnodemac     ! INPUT MACRO FOR R-NODE ANALYSIS...
C*** /INP,repeat  ! ...(OR) INPUT MACRO FOR REPEATED ELASTIC ANALYSIS

EXIT

```

C.1.1.2 Indeterminate Beam Subjected to Uniform Load

```
/BATCH
```

```

*SET,LENG,20      * LENGTH OF THE BEAM (inch)
*SET,THIK,1.00   * THICKNESS OF THE BEAM (inch)
*SET,NDIV1,100   * NUMBER OF DIVISIONS ALONG THE LENGTH OF THE BEAM
*SET,NDIV2,10    * NUMBER OF DIVISIONS ALONG THE WIDTH OF THE BEAM
*SET,PRSR,25     * ARBITRARY APPLIED PRESSURE (psi)
*SET,YM,30E06    * YOUNG'S MODULUS (psi)

```

```
*SET,YS,30E03          * YIELD STRESS (psi)

/PREP7
/TITLE,INDETERMINATE BEAM
ET,1,42                ! PLANE STRESS OPTION
MP,EX,1,YM
MP,NUXY,,0.3

K,1
K,2,LENG
K,3,LENG,THIK
K,4,0,THIK

L,1,2,NDIV1
L,2,3,NDIV2
L,3,4,NDIV1
L,4,1,NDIV2

A,4,1,2,3

TYPE,1
MAT,1
AMESH,ALL

FINI

/SOLU
ANTYPE,0

NSSEL,,LOC,X,0
```

D,ALL,ALL,0

NALL

NSEL,,LOC,X,LENG

NSEL,R,LOC,Y,0

D,ALL,UY,0

NALL

NSEL,,LOC,Y,THIK

SF,ALL,PRES,PRSR

NALL

SAVE

SOLVE

FINISH

/INP,rnodemac ! INPUT MACRO FOR R-NODE ANALYSIS...

C*** /INP,repeat ! ...(OR) INPUT MACRO FOR REPEATED ELASTIC ANALYSIS

EXIT

C.1.1.3 Torispherical Head Subjected to Uniform Pressure

/BATCH

! ALL DIMENSIONS IN METERS

! R/D = 0.12

! BASIC CONSTANTS

```

*SET,PI,3.1415926536
*SET,YM,206.85E06 ! YOUNG'S MODULUS (KPa)
*SET,YS,206.85E03 ! YIELD STRESS (KPa)
*SET,PRSR,200.0 ! INTERNAL PRESSURE (Kpa)

```

```

! BASIC INPUTS

```

```

! THE SYMBOLS USED ARE AS PER MASSONET AND SAVE

```

```

*SET,T,2.54E-02 ! WALL THICKNESS (m)
*SET,LSBYD,0.8 ! LS BY D (LS IS THE RADIUS OF THE HEAD)
*SET,RBYD,0.12 ! R BY D (R IS THE RADIUS OF THE TORUS)
*SET,TBYD,1/300 ! T BY D (T IS THE THICKNESS AND D IS THE
! DIAMETER OF THE CYLINDER)

```

```

! DERIVED DIMENSIONS

```

```

! THE SYMBOLS USED ARE MY OWN

```

```

*SET,PHITWO,ASIN((0.5-RBYD)/(LSBYD-RBYD))*180/PI
*SET,PHI1,90.0-PHITWO
*SET,D,T/TBYD ! INSIDE DIAMETER OF THE CYLINDER
*SET,RK,RBYD*D ! RADIUS OF THE KNUCKLE
*SET,RH,LSBYD*D ! RADIUS OF THE HEAD
*SET,HH,RH-(RH-RK)*COS(PHITWO*PI/180.0) ! HEIGHT OF THE TORISPHERICAL HEAD
*SET,A,D/2-RK ! DISTANCE FROM AXIS TO KNUCKLE CENTER
*SET,RI,D/2.0 ! INNER RADIUS OF THE CYLINDRICAL PORTION

```

```
*SET,RO,RI+T           ! OUTER RADIUS OF THE CYLINDRICAL PORTION
*SET,H,1.2*5.0*SQRT(RO*T) ! HEIGHT FROM BASE TO LOWER KNUCKLE
```

```
!           E L E M E N T   S I Z E   P A R A M E T E R S
```

```
*SET,NDIV1,6
*SET,NDIV2,70
*SET,NDIV3,30
*SET,NDIV4,120
```

```
/PREP7
ANTYPE,0
ET,1,42,0,0,1,0,0
MP,EX,1,YM
MP,NUXY,,0.3
```

```
K,1,RI
K,2,RO
K,3,RI,H
K,4,RO,H
```

```
! LOCAL CO-ORDINATE SYSTEM FOR THE KNUCKLE
LOCAL,11,1,A,H
```

```
CSYS,11
K,5,RK,PHI1
K,6,RK+T,PHI1
CSYS,0
```

! LOCAL CO-ORDINATE SYSTEM FOR THE HEAD
LOCAL,12,1,0,H+HH-RH

CSYS,12
K,7,RH,90
K,8,RH+T,90

CSYS,0

L,1,2,NDIV1
L,3,4,NDIV1
L,5,6,NDIV1
L,7,8,NDIV1

L,1,3,NDIV2
L,2,4,NDIV2

CSYS,11
L,3,5,NDIV3
L,4,6,NDIV3

CSYS,12
L,5,7,NDIV4
L,6,8,NDIV4

CSYS,0

A,1,2,4,3
AMESH,1

CSYS,11

A,3,4,6,5

AMESH,2

CSYS,12

A,5,6,8,7

AMESH,3

CSYS,0

SFL,5,PRES,PRSR

CSYS,11

SFL,7,PRES,PRSR

CSYS,0

CSYS,12

SFL,9,PRES,PRSR

CSYS,0

SFTRAN

NSEL,,LOC,X,0

D,ALL,UX,0

```

NSEL,ALL

NSEL,,LOC,Y,0
D,ALL,UY,0
NSEL,ALL

FINISH

/SOLUTION
SAVE
SOLVE

FINISH

/INP,rnodemac           ! INPUT MACRO FOR R-NODE ANALYSIS...
C*** /INP,repeat       ! ...(OR) INPUT MACRO FOR REPEATED ELASTIC ANALYSIS

EXIT

```

C.1.1.4 Spherical Pressure Vessel with a Cylindrical Nozzle Subjected to Uniform Internal Pressure

```

/BATCH

!           B A S I C   C O N S T A N T S

*SET,YM,200.00E06      ! YOUNG'S MODULUS (KPa)
*SET,YS,300.00E03     ! YIELD STRENGTH (KPa)
*SET,PRSR,200         ! INTERNAL PRESSURE (KPa)

```

```

!           B A S I C   I N P U T S

*SET,RS,1.0           ! MEAN RADIUS OF THE SPHERE (m)
*SET,TS,0.25         ! THICKNESS OF THE SPHERICAL SHELL (m)
*SET,RN,0.20         ! MEAN RADIUS OF THE NOZZLE (m)

!           D E R I V E D   I N P U T S

*SET,TN,2.0*TS*RN/RS      ! THICKNESS OF THE NOZZLE (m)
*SET,H,1.2*5.0*SQRT(RN*TN) ! HEIGHT OF THE NOZZLE (m)

!           E L E M E N T   S I Z E   P A R A M E T E R S

*SET,NDIV1,45
*SET,NDIV2,6
*SET,NDIV3,11
*SET,NDIV4,38
*SET,NDIV5,10

/TITLE,INTERSECTION OF A SPHERICAL PRESSURE VESSEL WITH A CYLINDRICAL NOZZLE

/PREP7
ANTYPE,0
ET,1,42,0,0,1,0,0
MP,EX,1,YM
MP,NUXY,,0.3

RSI=RS-TS/2.0
RSO=RS+TS/2.0

```

RNI=RN-TN/2.0

RNO=RN+TN/2.0

K,1,RSD

K,2,RNO,SQRT(RSO**2-RNO**2)

K,3,RNO,SQRT(RSO**2-RNO**2)+TN/2.0+H

K,4,RNI,SQRT(RSO**2-RNO**2)+TN/2.0+H

K,5,RNI,SQRT(RSO**2-RNO**2)+TN/2.0

K,6,RNI,SQRT(RSI**2-RNI**2)

K,7,RSI

K,12

K,15,,-RSI

K,16,,-RSD

CSYS,1

L,1,2

CSYS,0

L,2,3

L,3,4

L,4,5

L,5,6

CSYS,1

L,6,7

CSYS,0

L,7,1

LOCAL,11,1,RNO+TN/2.0,SQRT(RSO**2-RNO**2)+TN/2.0

CSYS,11

LFILLT,1,2,TN/2.0,10

LDIV,8,0.5,11

CSYS,0
L,8,12
LCSL,10,6
LDELE,14
L,11,6
L,9,5

L,15,16
CSYS,1
L,15,7
L,16,1
CSYS,0

KDELE,10
KDELE,2
KDELE,12

LESIZE,1,,,NDIV1,0.3333
LESIZE,2,,,NDIV4,3
LESIZE,3,,,NDIV5
LESIZE,4,,,NDIV4,0.3333
LESIZE,5,,,NDIV3
LESIZE,6,,,NDIV5
LESIZE,7,,,NDIV5
LESIZE,8,,,NDIV2
LESIZE,9,,,NDIV3
LESIZE,10,,,NDIV5
LESIZE,11,,,NDIV2
LESIZE,12,,,NDIV1,0.3333
LESIZE,13,,,NDIV5

```
LESIZE,14,, ,NDIV5  
LESIZE,15,, ,NDIV1  
LESIZE,16,, ,NDIV1
```

```
CSYS,1  
A,15,16,1,7  
A,7,1,8,13  
CSYS,0  
A,13,8,11,6  
A,6,11,9,5  
A,5,9,3,4
```

```
ESHAPE,2  
AMESH,ALL
```

```
FINI
```

```
/SOLU  
ANTYPE,STATIC
```

```
SFL,4,PRES,PRSR  
SFL,5,PRES,PRSR
```

```
CSYS,1  
SFL,11,PRES,PRSR  
SFL,12,PRES,PRSR  
SFL,15,PRES,PRSR
```

```
CSYS,0  
SFTRAN
```

```

NSEL,,LOC,Y,SQRT(RSO**2-RNO**2)+TN/2.0+H
D,ALL,UY,0
NSEL,ALL

NSEL,,LOC,X,0
D,ALL,UX,0
NSEL,ALL

SAVE
SOLVE
FINI

/INP,rnodemac           ! INPUT MACRO FOR R-NODE ANALYSIS...
C*** /INP,repeat       ! ...(OR) INPUT MACRO FOR REPEATED ELASTIC ANALYSIS

EXIT

```

C.1.1.5 Pressure Vessel Support Skirt

```

/BATCH

*SET,PI,3.1415926536
*SET,DI,97.28           ! INNER DIAMETER OF THE CYLINDER (inch)
*SET,DO,101.28         ! OUTER DIAMETER OF THE CYLINDER (inch)
*SET,LC,30.0           ! LENGTH OF THE CYLINDER (inch)
*SET,DSK,110.07        ! DIAMETER OF THE SKIRT (inch)
*SET,SKA,18.05         ! ANGLE MADE BY THE SKIRT WITH THE VERTICAL (deg.)

```

```

*SET, YM, 30E06      ! YOUNG'S MODULUS (psi)
*SET, ENLD, 1122    ! END LOAD (psi)

*SET, NDIV1, 12     ! NUMBER OF DIVISIONS ACROSS THE THICKNESS
*SET, NDIV2, 28     ! 0.5 * NUMBER OF DIVISIONS ALONG THE CYLINDER'S LENGTH
*SET, NDIV3, 23     ! 0.5 * NUMBER OF DIVISIONS ALONG THE SKIRT
*SET, NDIV4, 5      ! NUMBER OF DIVISIONS ALONG THE ARC OF THE BEND

```

```

RI=DI/2.0
RO=DO/2.0
RSK=DSK/2.0
T=RO-RI
THETA=PI/180.0*SKA
H1=(RSK-RO+T/COS(THETA))/TAN(THETA)

```

```

/TITLE,PRESSURE VESSEL SUPPORT SKIRT

```

```

/PREP7
ANTYPE,STATIC
ET,1,42,0,0,1,0,0
MP,EX,1,YM
MP,NUXY,,0.3

```

```

K,1,RI
K,2,RO
K,3,RO,LC
K,4,RI,H1+LC+TAN(PI/2.0-THETA)*(RI-RSK)
K,5,RSK+T/COS(THETA),LC+H1
K,6,RSK,LC+H1

```

L,1,2

L,6,5

L,2,3

L,1,4

L,3,5

L,4,6

LOCAL,11,1,RO+T,LC-T

CSYS,11

LFILLT,3,5,T/2.0

LFILLT,4,6,3.0*T/2.0

CSYS,0

L,7,9

L,8,10

KDELE,3

KDELE,4

LDIV,3

LDIV,4

LDIV,5

LDIV,6

LESIZE,1,,,NDIV1

LESIZE,9,,,NDIV1

LESIZE,10,,,NDIV1

LESIZE,2,,,NDIV1

LESIZE,3,,,NDIV2,2

```
LESIZE,4,,NDIV2,2
LESIZE,11,,NDIV2,0.5
LESIZE,12,,NDIV2,0.5
```

```
LESIZE,5,,NDIV3,2
LESIZE,6,,NDIV3,2
LESIZE,13,,NDIV3,0.5
LESIZE,14,,NDIV3,0.5
```

```
LESIZE,7,,NDIV4
LESIZE,8,,NDIV4
```

```
A,1,2,3,4
A,4,3,7,9
CSYS,11
A,9,7,8,10
CSYS,0
A,10,8,11,12
A,12,11,5,6
```

```
ESHAPE,2
AMESH,ALL
```

```
FINISH
```

```
/SOLUTION
```

```
NSEL,,LOC,Y,H1 + LC
D,ALL,ALL,0
NSEL,ALL
```

```
SFL,1,PRES,ENLD
SFTRAN
```

```
SAVE
SOLVE
FINISH
```

```
/INP,rnodemac          ! INPUT MACRO FOR R-NODE ANALYSIS...
C*** /INP,repeat       ! ...(OR) INPUT MACRO FOR REPEATED ELASTIC ANALYSIS
```

```
EXIT
```

C.1.1.6 Rectangular Plate Partially Fixed on Three Sides

```
C*** FULL THREE-DIMENSIONAL MODEL
```

```
*SET,THIK,0.5          ! THICKNESS OF THE PLATE (inch)
*SET,LENG,15           ! LENGTH OF THE PLATE (inch)
*SET,WDTH,10           ! WIDTH OF THE PLATE (inch)

*SET,PRSR,25           ! APPLIED PRESSURE (psi)
*SET,YM,30E06          ! YOUNG'S MODULUS (psi)
*SET,YS,30E03          ! YIELD STRENGTH (psi)
```

```
/PREP7
```

```
/TITLE,RECTANGULAR PLATE PARTIALLY FIXED
```

```
ANTYPE,0
```

```
ET,1,45                ! ELEMENT TYPE IS SOLID45 (EIGHT NODED ISOPARAMETRIC
```

! SOLID ELEMENT)

MP,EX,1,YM

MP,NUXY,,0.3

K,1,0,0,0

K,2,WDTH,0,0

K,3,WDTH,THIK,0

K,4,0,THIK,0

K,5,0,0,LENG

K,6,WDTH,0,LENG

K,7,WDTH,THIK,LENG

K,8,0,THIK,LENG

L,1,2,1.2*WDTH

L,1,4,5

L,2,3,5

L,4,3,1.2*WDTH

L,1,5,1.2*LENG

L,4,8,1.2*LENG

L,3,7,1.2*LENG

L,2,6,1.2*LENG

L,5,8,5

L,7,6,5

L,7,8,1.2*WDTH

L,5,6,1.2*WDTH

V,1,2,6,5,4,3,7,8

VMESH,ALL

FINISH

```

/SOLUTION

NSEL,R,LOC,Z,0
D,ALL,ALL,0
NSEL,ALL

NSEL,S,LOC,X,WIDTH
NSEL,R,LOC,Z,0,0.33333*LENG
D,ALL,ALL,0
NSEL,ALL

NSEL,S,LOC,X,0
NSEL,R,LOC,Z,0,0.666667*LENG
D,ALL,ALL,0
NSEL,ALL

NSEL,S,LOC,Y,THICK
SF,ALL,PRES,PRSR
NSEL,ALL

SAVE

SOLVE

FINISH

/INP,rnodemac           ! INPUT MACRO FOR R-NODE ANALYSIS...
C*** /INP,repeat       ! ...(OR) INPUT MACRO FOR REPEATED ELASTIC ANALYSIS

```

EXIT

C.1.1.7 Rectangular Plate Partially Fixed and Partially Simply Supported

C*** FULL THREE-DIMENSIONAL MODEL

```
*SET,THIK,0.5      ! THICKNESS OF THE PLATE (inch)
*SET,LENG,15       ! LENGTH OF THE PLATE (inch)
*SET,WDTH,10       ! WIDTH OF THE PLATE (inch)

*SET,PRSR,25       ! ARBITRARY APPLIED PRESSURE (psi)
*SET,YM,30E06      ! YOUNG'S MODULUS (psi)
```

/PREP7

/TITLE,RECTANGULAR PLATE PARTIALLY FIXED AND PARTIALLY SIMPLY SUPPORTED.

ET,1,45

MP,EX,1,30E6

MP,NUXY,,0.3

K,1,0,0,0

K,2,WDTH,0,0

K,3,WDTH,THIK,0

K,4,0,THIK,0

K,5,0,0,LENG

K,6,WDTH,0,LENG

K,7,WDTH,THIK,LENG

K,8,0,THIK,LENG

```
L,1,2,1.2*WIDTH
L,1,4,5
L,2,3,5
L,4,3,1.2*WIDTH
L,1,5,1.2*LENG
L,4,8,1.2*LENG
L,3,7,1.2*LENG
L,2,6,1.2*LENG
L,5,8,5
L,7,6,5
L,7,8,1.2*WIDTH
L,5,6,1.2*WIDTH

V,1,4,8,5,2,3,7,6
VMESH,ALL
```

```
FINISH
```

```
/SOLUTION
```

```
NSEL,S,LOC,X,0.3333*WIDTH,0.66667*WIDTH
NSEL,R,LOC,Y,0
NSEL,R,LOC,Z,0
D,ALL,UY,0
NSEL,ALL
```

```
NSEL,S,LOC,X,WIDTH
NSEL,R,LOC,Z,0,0.33333*LENG
D,ALL,ALL,0
NSEL,ALL
```

NSEL,S,LOC,X,WDTH
NSEL,R,LOC,Z,0.66667*LENG,LENG
D,ALL,ALL,0
NSEL,ALL

NSEL,S,LOC,X,0
NSEL,R,LOC,Z,0.3333*LENG,0.66667*LENG
D,ALL,ALL,0
NSEL,ALL

NSEL,S,LOC,X,0,0.3333*WDTH
NSEL,R,LOC,Y,0
NSEL,R,LOC,Z,LENG
D,ALL,UY,0
NSEL,ALL

NSEL,S,LOC,X,0.66667*WDTH,WDTH
NSEL,R,LOC,Y,0
NSEL,R,LOC,Z,LENG
D,ALL,UY,0
NSEL,ALL

NSEL,S,LOC,Y,THIK
SF,ALL,PRES,PRSR
NSEL,ALL

SAVE
SOLVE

FINISH

```
/INP,rnodemac      ! INPUT MACRO FOR R-NODE ANALYSIS...  
C*** /INP,repeat   ! ...(OR) INPUT MACRO FOR REPEATED ELASTIC ANALYSIS
```

EXIT

C.1.1.8 Compact Tension Specimen

/BATCH

C***

C*** ELASTIC ANALYSIS OF A COMPACT-TENSION SPECIMEN

C*** SINGULAR STIF 2 ELEMENTS USED AROUND CRACK TIP

C***

/PREP7

A=0.0466 ! DIMENSIONS OF THE SPECIMEN (m)

B=0.003

W=.100

W1=.125

H=.060

R=0.0125

E=0.0275

S=0.003

D1=0.080

D2=0.075

YM=211E09 ! YOUNG'S MODULUS (Pa)

YS=488.43E06 ! YIELD STRENGTH (Pa)

MP,EX,1,YM
MP,NUXY,1,.33

K,1,A ! DEFINE KEY POINTS
K,2,W
K,3,W,H
K,4,,H
K,5,(W-W1),H
K,6,(W-W1),S
K,7,,S
K,8,(W-D1),S
K,9,(W-D2)
K,10,,E
K,11,,E,E
CIRCLE,10,R,11,4,,8

L,1,2 ! DEFINE LINES
*REPEAT,8,1,1
L,9,1
L,4,12
L,16,7
KSEL,S,LOC,X,-1E-6,1
LSLK,S,1
AL,ALL
KSEL,S,LOC,X,-1,1E-6
LSLK,S,1
AL,ALL
KSEL,ALL
LSEL,ALL

ET,1,PLANE2,,,3 ! DEFINE ELEMENTS

R,1,B

ESIZE,A/4

KSCON,1,A/16,1,9

AMESH,ALL

WSORT,X

FINISH

/SOLUTION

ANTYPE,0

NSEL,S,LOC,Y

NSEL,R,LOC,X,A,W

D,ALL,UY,0

NSEL,R,LOC,X,A

D,ALL,UX,0

NSEL,ALL

F,515,FY,20

F,516,FY,20

F,8,FY,20

F,9,FY,20

F,6,FY,20

SAVE

SOLVE

FINISH

```
/INP,rnodemac          ! INPUT MACRO FOR R-NODE ANALYSIS...
C*** /INP,repeat       ! ...(OR) INPUT MACRO FOR REPEATED ELASTIC ANALYSIS
```

```
EXIT
```

C.1.2 Non-linear Analysis

C.1.2.1 Isotropic Thick Cylinder Subjected to Internal Pressure

```
/BATCH

*SET,RI,3              ! INNER RADIUS (inch)
*SET,RO,9              ! OUTER RADIUS (inch)
*SET,NELEM,90          ! NO. OF ELEMENTS ACROSS THE CROSS-SECTION

*SET,THICK,(RO-RI)/NELEM ! THICKNESS (ENSURES SQUARE ELEMENTS)

*SET,YS,30E03          ! YIELD STRENGTH (psi)
*SET,YM,30E06          ! YOUNG'S MODULUS (psi)
*SET,POISSON,0.3      ! POISSON'S RATIO

/PREP7
/TITLE,THICK CYLINDER UNDER INTERNAL PRESSURE
ANTYPE,0
ET,1,42,0,0,1,0,0
MP,EX,1,YM
MP,NUXY,,0.3
TB,BKIN,1,1
TBDATA,1,YS,0
```

```

N,1,RI
N,NELEM+1,RO
FILL,1,NELEM+1
N,NELEM+2,RI,THICK
N,2*(NELEM+1),RO,THICK
FILL,NELEM+2,2*(NELEM+1)

*DO,K,1,NELEM
E,K,K+1,NELEM+K+2,NELEM+K+1
*ENDDO

FINISH

/SOLUTION

ANTYPE,0
NROPT,1,,OFF
AUTOTS,ON
PRED,ON,,ON
NCNV,0
OUTRES,ALL,ALL

D,ALL,UY,0

PRSR=15000 ! INTERNAL PRESSURE (psi)

TIME,1E-12

NSEL,S,LOC,X,RI

```

SF,ALL,PRES,1E-12

NSEL,ALL

SAVE

SOLVE

TIME,3

NSUBST,150

NSEL,S,LOC,X,RI

SF,ALL,PRES,3*PRSR

NSEL,ALL

SAVE

SOLVE

FINISH

EXIT

C.2 Two-Layered Beams

C.2.1 Linear Elastic Analysis

C.2.1.1 Beam Subjected to Pure Bending

/BATCH

/TITLE,LAMINATED (TWO-LAYERED) BEAM UNDER PURE BENDING

! BEAM DIMENSIONS

*SET,THICK,1.0 ! TOTAL THICKNESS OF THE BEAM (inch)
*SET,SPAN,10.0 ! SEMI-LENGTH OF THE BEAM (inch)
*SET,THICK1,0.667 ! THICKNESS OF THE BOTTOM LAYER (inch)
*SET,DPRSR,SPAN/2 ! DISTANCE TO WHICH UNIFORM PRESSURE IS APPLIED (inch)

*SET,NSPAN,50 ! NUMBER OF ELEMENTS ACROSS THE SPAN
*SET,NTHICK,18 ! NUMBER OF ELEMENTS ACROSS THE THICKNESS

*SET,THICK2,(THICK-THICK1) ! THICKNESS OF THE TOP LAYER (INCH.)

! MATERIAL PROPERTIES

*SET,YM1,10E06 ! YOUNG'S MODULUS OF THE TOP LAYER (psi)
*SET,YM2,30E06 ! YOUNG'S MODULUS OF THE BOTTOM LAYER (psi)
*SET,POISSON,0.3 ! POISSON'S RATIO OF BOTH THE LAYERS
*SET,YIELD1,10E03 ! YIELD STRESS OF THE TOP LAYER (psi)
*SET,YIELD2,30E03 ! YIELD STRESS OF THE BOTTOM LAYER (psi)

*SET,PRSR,25 ! EXTERNAL LOAD (psi)

```
/PREP7
ET,1,42
ET,2,42
MP,EX,1,YM1
MP,EX,2,YM2
MP,NUXY,1,POISSON
MP,NUXY,2,POISSON

K,1,0,0
K,2,SPAN
K,3,0,THICK1
K,4,SPAN,THICK1
K,5,0,THICK
K,6,SPAN,THICK

DUM=(THICK1/THICK)*NTHICK
K,7,SPAN+5
K,8,SPAN+10
L,7,8,DUM
*GET,NTHICK1,LINE,1,ATTR,NDIV
NTHICK2=NTHICK-NTHICK1
LDELE,1
KDELE,7,8

L,1,2,NSPAN
L,3,4,NSPAN
L,5,6,NSPAN
L,1,3,NTHICK1
L,2,4,NTHICK1
L,3,5,NTHICK2
```

L,4,6,NTHICK2

A,5,3,4,6

A,3,1,2,4

TYPE,1

MAT,1

AMESH,1

TYPE,2

MAT,2

AMESH,2

*GET,II,ELEM,0,COUNT

KK=1

JJ=NTHICK2*NSPAN+1

*DO,K1,1,NSPAN

*DO,K2,1,NTHICK2

*GET,P1,ELEM,KK,NODE,1

*GET,P2,ELEM,KK,NODE,2

*GET,P3,ELEM,KK,NODE,3

*GET,P4,ELEM,KK,NODE,4

TYPE,1

MAT,1

E,P1,P2,P3,P4

KK=KK+1

*ENDDO

*DO,K2,1,NTHICK1

*GET,P5,ELEM,JJ,NODE,1

```
*GET,P6,ELEM,JJ,NODE,2
*GET,P7,ELEM,JJ,NODE,3
*GET,P8,ELEM,JJ,NODE,4
TYPE,2
MAT,2
E,P5,P6,P7,P8
JJ=JJ+1
*ENDDO
*ENDDO
```

```
MODMSH,DETACH
```

```
EDELE,1,II
```

```
NUMCMP,ELEM
```

```
FINISH
```

```
/SOLUTION
```

```
NSEL,S,LOC,X,0
D,ALL,UX,0
NSEL,ALL
```

```
NSEL,S,LOC,X,SPAN/2
NSEL,R,LOC,Y,0
D,ALL,UY,0
NSEL,ALL
```

```
NSEL,S,LOC,Y,THICK
```

```
NSEL,R,LOC,X,1.1*SPAN/2,SPAN
SF,ALL,PRES,PRSR
NSEL,ALL
```

```
SAVE
SOLVE
```

```
FINISH
```

```
/INP,rnodemac          ! INPUT MACRO FOR R-NODE ANALYSIS...
```

```
EXIT
```

C.2.1.2 Simply-Supported Beam

```
/BATCH
```

```
/TITLE,LAMINATED (TWO-LAYERED) SIMPLY-SUPPORTED BEAM
```

```
! BEAM DIMENSIONS
```

```
*SET,THICK,1.0          ! TOTAL THICKNESS OF THE BEAM (inch)
*SET,SPAN,10.0         ! SEMI-LENGTH OF THE BEAM (inch)
*SET,THICK1,0.5        ! THICKNESS OF THE BOTTOM LAYER (inch)

*SET,NSPAN,50          ! NUMBER OF ELEMENTS ACROSS THE SPAN
*SET,NTHICK,18         ! NUMBER OF ELEMENTS ACROSS THE THICKNESS

*SET,THICK2,(THICK-THICK1) ! THICKNESS OF THE TOP LAYER (inch)
```

```

! MATERIAL PROPERTIES
*SET,YM1,10E06      ! YOUNG'S MODULUS OF THE TOP LAYER (psi)
*SET,YM2,10E06      ! YOUNG'S MODULUS OF THE BOTTOM LAYER (psi)
*SET,POISSON,0.3     ! POISSON'S RATIO OF BOTH THE LAYERS
*SET,YIELD1,10E03    ! YIELD STRESS OF THE TOP LAYER (psi)
*SET,YIELD2,30E03    ! YIELD STRESS OF THE BOTTOM LAYER (psi)

*SET,PRSR,25         ! EXTERNAL LOAD (psi)

/PREP7
ET,1,42
ET,2,42
MP,EX,1,YM1
MP,EX,2,YM2
MP,NUXY,1,POISSON
MP,NUXY,2,POISSON

K,1,0,0
K,2,SPAN
K,3,0,THICK1
K,4,SPAN,THICK1
K,5,0,THICK
K,6,SPAN,THICK

DUM=(THICK1/THICK)*NTHICK
K,7,SPAN+5
K,8,SPAN+10
L,7,8,DUM
*GET,NTHICK1,LINE,1,ATTR,NDIV

```

NTHICK2=NTHICK-NTHICK1

LDELE,1

KDELE,7,8

L,1,2,NSPAN

L,3,4,NSPAN

L,5,6,NSPAN

L,1,3,NTHICK1

L,2,4,NTHICK1

L,3,5,NTHICK2

L,4,6,NTHICK2

A,5,3,4,6

A,3,1,2,4

TYPE,1

MAT,1

AMESH,1

TYPE,2

MAT,2

AMESH,2

*GET,II,ELEM,0,COUNT

KK=1

JJ=NTHICK2*NSPAN+1

*DO,K1,1,NSPAN

*DO,K2,1,NTHICK2

*GET,P1,ELEM,KK,NODE,1

```
*GET,P2,ELEM,KK,NODE,2
*GET,P3,ELEM,KK,NODE,3
*GET,P4,ELEM,KK,NODE,4
TYPE,1
MAT,1
E,P1,P2,P3,P4
KK=KK+1
*ENDDO
*DO,K2,1,NTHICK1
*GET,P5,ELEM,JJ,NODE,1
*GET,P6,ELEM,JJ,NODE,2
*GET,P7,ELEM,JJ,NODE,3
*GET,P8,ELEM,JJ,NODE,4
TYPE,2
MAT,2
E,P5,P6,P7,P8
JJ=JJ+1
*ENDDO
*ENDDO

MODMSH,DETACH

EDELE,1,II

NUMCMP,ELEM

FINISH

/SOLUTION
```

```
NSEL,S,LOC,X,0
D,ALL,UX,0
NSEL,ALL
```

```
NSEL,S,LOC,X,SPAN
NSEL,R,LOC,Y,0
D,ALL,UY,0
NSEL,ALL
```

```
NSEL,S,LOC,Y,THICK
SF,ALL,PRES,PRSR
NSEL,ALL
```

```
SAVE
SOLVE
```

```
FINISH
```

```
/INP,rnodemac          ! INPUT MACRO FOR R-NODE ANALYSIS...
```

```
EXIT
```

C.2.1.3 Indeterminate Beam

```
/BATCH
```

```
/TITLE,LAMINATED (TWO-LAYERED) INDETERMINATE BEAM
```

```
! BEAM DIMENSIONS
```

```

*SET,THICK,1.0      ! TOTAL THICKNESS OF THE BEAM (inch)
*SET,SPAN,20.0     ! LENGTH OF THE BEAM (inch)
*SET,THICK1,0.5    ! THICKNESS OF THE BOTTOM LAYER (inch)

*SET,NSPAN,100     ! NUMBER OF ELEMENTS ACROSS THE SPAN
*SET,NTHICK,10     ! NUMBER OF ELEMENTS ACROSS THE THICKNESS

*SET,THICK2,(THICK-THICK1) ! THICKNESS OF THE TOP LAYER (inch)

! MATERIAL PROPERTIES
*SET,YM1,10E06     ! YOUNG'S MODULUS OF THE TOP LAYER (psi)
*SET,YM2,30E06     ! YOUNG'S MODULUS OF THE BOTTOM LAYER (psi)
*SET,POISSON,0.3   ! POISSON'S RATIO OF BOTH THE LAYERS
*SET,YIELD1,10E03  ! YIELD STRESS OF THE TOP LAYER (psi)
*SET,YIELD2,30E03  ! YIELD STRESS OF THE BOTTOM LAYER (psi)

*SET,PRSR,25      ! EXTERNAL LOAD (psi)

/PREP7
ET,1,42
ET,2,42
MP,EX,1,YM1
MP,EX,2,YM2
MP,NUXY,1,POISSON
MP,NUXY,2,POISSON

K,1,0,0
K,2,SPAN
K,3,0,THICK1

```

```
K,4,SPAN,THICK1
K,5,0,THICK
K,6,SPAN,THICK

DUM=(THICK1/THICK)*NTHICK
K,7,SPAN+5
K,8,SPAN+10
L,7,8,DUM
*GET,NTHICK1,LINE,1,ATTR,NDIV
NTHICK2=NTHICK-NTHICK1
LDELE,1
KDELE,7,8

L,1,2,NSPAN
L,3,4,NSPAN
L,5,6,NSPAN
L,1,3,NTHICK1
L,2,4,NTHICK1
L,3,5,NTHICK2
L,4,6,NTHICK2

A,5,3,4,6
A,3,1,2,4

TYPE,1
MAT,1
AMESH,1

TYPE,2
MAT,2
```

AMESH,2

*GET,II,ELEM,0,COUNT

KK=1

JJ=NTHICK2*NSPAN+1

*DO,K1,1,NSPAN

*DO,K2,1,NTHICK2

*GET,P1,ELEM,KK,NODE,1

*GET,P2,ELEM,KK,NODE,2

*GET,P3,ELEM,KK,NODE,3

*GET,P4,ELEM,KK,NODE,4

TYPE,1

MAT,1

E,P1,P2,P3,P4

KK=KK+1

*ENDDO

*DO,K2,1,NTHICK1

*GET,P5,ELEM,JJ,NODE,1

*GET,P6,ELEM,JJ,NODE,2

*GET,P7,ELEM,JJ,NODE,3

*GET,P8,ELEM,JJ,NODE,4

TYPE,2

MAT,2

E,P5,P6,P7,P8

JJ=JJ+1

*ENDDO

*ENDDO

MODMSH,DETACH

```
EDELE,1,II

NUMCMP,ELEM

FINISH

/SOLUTION

NSEL,S,LOC,X,0
D,ALL,ALL,0
NSEL,ALL

NSEL,S,LOC,X,SPAN
NSEL,R,LOC,Y,0
D,ALL,UY,0
NSEL,ALL

NSEL,S,LOC,Y,THICK
SF,ALL,PRES,PRSR
NSEL,ALL

SAVE
SOLVE

FINISH

/INP,rnodemac          ! INPUT MACRO FOR R-NODE ANALYSIS...

EXIT
```

C.2.2 Non-linear Analysis

C.2.2.1 Indeterminate Beam

```
/BATCH

/TITLE,LAMINATED (TWO-LAYERED) INDETERMINATE BEAM

! BEAM DIMENSIONS

*SET,THICK,1.0      ! TOTAL THICKNESS OF THE BEAM (inch.)
*SET,SPAN,20.0     ! LENGTH OF THE BEAM (inch.)
*SET,THICK1,0.8    ! THICKNESS OF THE BOTTOM LAYER (inch.)

*SET,NSPAN,100     ! NUMBER OF ELEMENTS ACROSS THE SPAN
*SET,NTHICK,10     ! NUMBER OF ELEMENTS ACROSS THE THICKNESS

*SET,THICK2,(THICK-THICK1) ! THICKNESS OF THE TOP LAYER (inch.)

! MATERIAL PROPERTIES

*SET,YM1,10E06     ! YOUNG'S MODULUS OF THE TOP LAYER (psi.)
*SET,YM2,30E06     ! YOUNG'S MODULUS OF THE BOTTOM LAYER (psi.)
*SET,POISSON,0.3   ! POISSON'S RATIO OF BOTH THE LAYERS
*SET,YIELD1,10E03  ! YIELD STRESS OF THE TOP LAYER (psi.)
*SET,YIELD2,30E03  ! YIELD STRESS OF THE BOTTOM LAYER (psi.)

/PREP7
```

ET,1,42
ET,2,42
MP,EX,1,YM1
MP,EX,2,YM2
MP,NUXY,1,POISSON
MP,NUXY,2,POISSON

K,1,0,0
K,2,SPAN
K,3,0,THICK1
K,4,SPAN,THICK1
K,5,0,THICK
K,6,SPAN,THICK

DUM=(THICK1/THICK)*NTHICK
K,7,SPAN+5
K,8,SPAN+10
L,7,8,DUM
=GET,NTHICK1,LINE,1,ATTR,NDIV
NTHICK2=NTHICK-NTHICK1
LDELE,1
KDELE,7,8

L,1,2,NSPAN
L,3,4,NSPAN
L,5,6,NSPAN
L,1,3,NTHICK1
L,2,4,NTHICK1
L,3,5,NTHICK2
L,4,6,NTHICK2

A,5,3,4,6

A,3,1,2,4

TB,BKIN,1,1

TBDATA,1,YIELD1,0

TYPE,1

MAT,1

AMESH,1

TB,BKIN,2,1

TBDATA,1,YIELD2,0

TYPE,2

MAT,2

AMESH,2

*GET,II,ELEM,0,COUNT

KK=1

JJ=NTHICK2*NSPAN+1

*DO,K1,1,NSPAN

*DO,K2,1,NTHICK2

*GET,P1,ELEM,KK,NODE,1

*GET,P2,ELEM,KK,NODE,2

*GET,P3,ELEM,KK,NODE,3

*GET,P4,ELEM,KK,NODE,4

TB,BKIN,1,1

TBDATA,1,YIELD1,0

TYPE,1

MAT,1

```
E,P1,P2,P3,P4
KK=KK+1
*ENDDO
*DO,K2,1,NTHICK1
*GET,P5,ELEM,JJ,NODE,1
*GET,P6,ELEM,JJ,NODE,2
*GET,P7,ELEM,JJ,NODE,3
*GET,P8,ELEM,JJ,NODE,4
TB,BKIN,2,1
TBDATA,1,YIELD2,0
TYPE,2
MAT,2
E,P5,P6,P7,P8
JJ=JJ+1
*ENDDO
*ENDDO

MODMSH,DETACH

EDELE,1,II

NUMCMP,ELEM

FINISH

/SOLUTION

ANTYPE,0
NROPT,1,,OFF
AUTOTS,ON
```

```
PRED,ON, ,ON  
NCNV,0  
OUTRES,ALL,ALL
```

```
NSEL,S,LOC,X,0  
D,ALL,ALL,0  
NSEL,ALL
```

```
NSEL,S,LOC,X,SPAN  
NSEL,R,LOC,Y,0  
D,ALL,UY,0  
NSEL,ALL
```

```
PRSR=100
```

```
! NULL SOLUTION FOR LOAD-DEFLECTION DISPLAY
```

```
TIME,1E-10  
NSEL,S,LOC,Y,THICK  
SF,ALL,PRES,1E-10  
NSEL,ALL  
SAVE  
SOLVE
```

```
TIME,3  
NSUBST,300  
NSEL,S,LOC,Y,THICK  
SF,ALL,PRES,3.0*PRSR  
NSEL,ALL  
SAVE
```

SOLVE

FINISH

EXIT

C.3 Two-Layered Cylinder under Uniform Internal Pressure

C.3.1 Linear Elastic Analysis

/BATCH

! A THICK CYLINDER PROBLEM - COMPOSITE CYLINDER

```
*SET,RI,10E-02           ! Inner radius (m)
*SET,RINT,20E-02        ! Interface radius (m)
*SET,RO,30E-02         ! Outer radius (m)
*SET,NELEM,50           ! No. of elements across the cross-section
*SET,NELEM1,(RINT-RI)*NELEM/(RO-RI) ! No. of elements in material 1

*SET,THICK,(RO-RI)/NELEM ! Thickness (Ensures Square Elements)

*SET,E1BYE2,3.1368
*SET,YIELD1,68.95E03    ! Yield Strength of Material 1 (kPa)
*SET,YIELD2,68.95E03    ! Yield Strength of Material 2 (kPa)
*SET,YM1,10E06         ! Young's Modulus
*SET,YM2,YM1*E1BYE2    ! Young's Modulus
*SET,POISSON,0.48      ! Poisson's Ratio
*SET,PRSR,50E03        ! Internal Pressure
```

```

/PREP7
/TITLE,Thick Cylinder Under Internal Pressure
ANTYPE,0
ET,1,42,0,0,1,0,0
MP,EX,1,YM1
MP,NUXY,1,POISSON

ET,2,42,0,0,1,0,0
MP,EX,2,YM2
MP,NUXY,2,POISSON

K,1
K,2,3
L,1,2,NELEM1
*GET,DUM,LINE,1,ATTR,NDIV
NELEM2=NELEM-DUM
NELEM1=NELEM-NELEM2
LDELE,1
KDELE,1,2

N,1,RI
N,NELEM1+1,RINT
FILL,1,NELEM1+1
N,NELEM+2,RI,THICK
N,NELEM+2+NELEM1,RINT,THICK
FILL,NELEM+2,NELEM+2+NELEM1

TYPE,1

```

```

MAT,1

*DO,K,1,NELEM1
E,K,K+1,NELEM+K+2,NELEM+K+1
*ENDDO

N,NELEM+1,RO
FILL,NELEM1+1,NELEM+1
N,2*(NELEM+1),RO,THICK
FILL,NELEM+NELEM1+2,2*(NELEM+1)

TYPE,2
MAT,2

*DO,K,1,NELEM2
E,NELEM1+K,NELEM1+K+1,NELEM+NELEM1+2+K,NELEM+NELEM1+1+K
*ENDDO

FINISH

/SOLUTION

ANTYPE,0

D,ALL,UY,0

NSEL,S,LOC,X,RI
SF,ALL,PRES,PRSR
NSEL,ALL

```

```
SAVE
SOLVE

FINISH

/inp,CYLMAC
```

C.3.2 Non-linear Analysis

```
/BATCH

! NON - LINEAR ANALYSIS
! A THICK CYLINDER PROBLEM - TWO-LAYERED CYLINDER

*SET,RI,8E-02 ! Inner radius = 3 in.
*SET,RINT,13E-02 ! Interface radius = 5 in.
*SET,RO,23E-02 ! Outer radius = 9 in.
*SET,NELEM,50 ! No. of elements across the cross-section
*SET,NELEM1,(RINT-RI)*NELEM/(RO-RI) ! No. of elements in material 1

*SET,THICK,(RO-RI)/NELEM ! Thickness (Ensures Square Elements)

*SET,YIELD1,68.95E03 ! Yield Strength of Material 1
*SET,YIELD2,206.85E03 ! Yield Strength of Material 2
*SET,YM1,10E06 ! Young's Modulus
*SET,YM2,30E06 ! Young's Modulus
*SET,POISSON,0.3 ! Poisson's Ratio
```

```

/PREP7
/TITLE,Thick Cylinder Under Internal Pressure
ANTYPE,0
ET,1,42,0,0,1,0,0
MP,EX,1,YM1
MP,NUXY,1,POISSON

ET,2,42,0,0,1,0,0
MP,EX,2,YM2
MP,NUXY,2,POISSON

K,1
K,2,3
L,1,2,NELEM1
*GET,DUM,LINE,1,ATTR,NDIV
NELEM2=NELEM-DUM
NELEM1=NELEM-NELEM2
LDELE,1
KDELE,1,2

N,1,RI
N,NELEM1+1,RINT
FILL,1,NELEM1+1
N,NELEM+2,RI,THICK
N,NELEM+2+NELEM1,RINT,THICK
FILL,NELEM+2,NELEM+2+NELEM1

```

```
TB,BKIN,1,1
TBDATA,1,YIELD1,0
TYPE,1
MAT,1

*DO,K,1,NELEM1
E,K,K+1,NELEM+K+2,NELEM+K+1
*ENDDO

N,NELEM+1,RO
FILL,NELEM+1,NELEM+1
N,2*(NELEM+1),RO,THICK
FILL,NELEM+NELEM+2,2*(NELEM+1)

TB,BKIN,2,1
TBDATA,1,YIELD2,0
TYPE,2
MAT,2

*DO,K,1,NELEM2
E,NELEM+K,NELEM+K+1,NELEM+NELEM+2+K,NELEM+NELEM+1+K
*ENDDO

FINISH

/SOLUTION

ANTYPE,0
NROPT,1,,OFF
AUTOTS,ON
```

```
PRED,ON,,ON  
NCNV,0  
OUTRES,ALL,ALL
```

```
D,ALL,UY,0
```

```
! NULL SOLUTION FOR THE LOAD-DEFLECTION DISPLAY
```

```
TIME,1E-10  
NSEL,S,LOC,X,RI  
SF,ALL,PRES,1E-10  
NSEL,ALL  
SAVE  
SOLVE
```

```
PRSR=100000.0
```

```
TIME,5.0  
NSUBST,600  
NSEL,S,LOC,X,RI  
SF,ALL,PRES,5.0*PRSR  
NSEL,ALL  
SAVE  
SOLVE
```

```
FINISH  
EXIT
```



```

! * NOTE: *
! * The parameters to be defined in the main program *
! * POISSON - Poisson's ratio *
! * YIELD1 - Yield Strength of I layer *
! * YIELD2 - Yield Strength of II layer *
! * YM1 - Young's Modulus of I layer *
! * YM2 - Young's Modulus of II layer *
! * Values to be given in this macro *
! * ARB1 - Arbitrary Number *
! * ALFA - Value of index (alpha) *
! *****

```

```

! -----
! I - L I N E A R   A N A L Y S I S
! -----

```

```

/POST1

```

```

*DIM,DUM1,ARRAY,1
*DIM,DUM2,ARRAY,1
*DIM,DUM3,ARRAY,1

```

```

SET,1
ETABLE,SIGC,S,EQV
ETABLE,VOL,VOLU
ETABLE,STRN,EPEL,X

```

```

! =====
! UNSORTED ELEMENT STRESSES AND VOLUMES ARE STORED IN THE FILE "estrsl"
! =====

```

```

*GET,MAX1,ELEM,0,COUNT

```

```

*CFOPEN,estrsl
*DO,KK,1,MAX1
*GET,SIGC1,ELEM,KK,ETAB,SIGC
*GET,VOL1,ELEM,KK,VOLU
DUM1(1)=KK
DUM2(1)=SIGC1
DUM3(1)=VOL1

```

```
*VWRITE,DUM1(1),DUM2(1),DUM3(1)
(x,f6.1,3x,e21.10,3x,e21.10)
*ENDDO
*CFCLOS
```

```
=====|
! UNSORTED ELEMENT X-STRAINS ARE STORED IN THE FILE "strain1" |
=====|
```

```
*CFOPEN, strain1
*DO, KK, 1, MAX1
*GET, STRN1, ELEM, KK, ETAB, STRN
DUM1(1)=KK
DUM2(1)=STRN1
*VWRITE,DUM1(1),DUM2(1)
(x,f6.1,3x,e21.10)
*ENDDO
*CFCLOS
```

```
!-----|

ARB1=100E03
ALFA=1
ZETA=YIELD1/YIELD2
PSI=YM1/YM2
ARB2=ARB1/((PSI**ALFA)*((ZETA-PSI)*ALFA+PSI))
```

```
*SET, MN, 3

*CFOPEN, EXVAL
*DO, J, 1, MAX1
*GET, STEQ, ELEM, J, ETAB, SIG
*GET, JJ, ELEM, J, ATTR, MAT
*IF, JJ, EQ, 1, THEN
*SET, ESEC, ARB1/(STEQ**ALFA)
*ELSE
*SET, ESEC, ARB2/(STEQ**ALFA)
*ENDIF
*CFWRITE, MP, EX, MN, ESEC
*CFWRITE, MP, NUXY, MN, POISSON
```

```
*SET, MN, MN+1
*ENDDO
*CFCLOS
```

```
!-----
!=====
ESEL, ALL
!=====
```

```
*SET, MN, 3

*CFOPEN, EXMOD
*DO, M, 1, MAX1
*CFWRITE, MAT, MN
*CFWRITE, EMODIF, M
*SET, MN, MN+1
*ENDDO
*CFCLOS
FINISH
```

```
!
! -----
! II - L I N E A R   A N A L Y S I S
! -----
```

```
/PREP7
RESUME
```

```
*USE, EXVAL
*USE, EXMOD
FINISH
```

```
/SOLU
SAVE
SOLVE
FINISH
```

```
/POST1
```

```
*DIM,DUM1,ARRAY,1
*DIM,DUM2,ARRAY,1
*DIM,DUM3,ARRAY,1

SET,1
ETABLE,SIGC,S,EQV
ETABLE,VOL,VOLU
ETABLE,STRN,EPEL,X
```

```
! =====|
! UNSORTED ELEMENT STRESSES AND VOLUMES ARE STORED IN THE FILE "estrs2"|
! =====|
```

```
*GET,MAX1,ELEM,0,NUM,MAX

*CFOPEN,estrs2
*DO,KK,1,MAX1
*GET,SIGC3,ELEM,KK,ETAB,SIGC
*GET,VOL2,ELEM,KK,VOLU
DUM1(1)=KK
DUM2(1)=SIGC3
DUM3(1)=VOL2
*VWRITE,KK,SIGC3,VOL2
(x,f6.1,3x,e21.10,3x,e21.10)
*ENDDO
*CFCLOSE
```

```
! =====|
! UNSORTED ELEMENT X-STRAINS ARE STORED IN THE FILE "strain2" |
! =====|
```

```
*CFOPEN,strain2
*DO,KK,1,MAX1
*GET,STRN1,ELEM,KK,ETAB,STRN
DUM1(1)=KK
DUM2(1)=STRN1
*VWRITE,DUM1(1),DUM2(1)
(x,f6.1,3x,e21.10)
*ENDDO
*CFCLOSE
```

FINISH

D.2 Two-Layered Cylindrical Shells

```
!           FILE - 'CYLMAC'
!  
!           #####
!           # ELASTIC MODULUS SOFTENING MACRO FOR R-NODE ANALYSIS #
!           # OF TWO LAYERED CYLINDRICAL SHELLS #
!           #####
!  
!           *****
!           * VALUES TO BE SUPPLIED: *
!           * MAIN PROGRAM : *
!           *           (1) YM1 *
!           *           (2) YM2 *
!           * IN THIS MACRO *
!           *           (1) ALFA *
!           *****
!  
! PROCEDURE:
! -----
! This macro uses Sigma_arb1 = Sigma_ref1
! Sigma_arb2 = Sigma_ref2
! Es1 = E1 * ((Sigma_ref1/Sigma_eqv1)**ALPHA) => Layer 1
! Es2 = E2 * ((Sigma_ref2/Sigma_eqv2)**ALPHA) => Layer 2
! "Sigma_ref1" and "Sigma_ref2" are determined from the theorem of
! nesting surfaces.
!  
!  
!           -----
!           I - L I N E A R   A N A L Y S I S
!           -----
```

/POST1

*DIM,DUM1,ARRAY,1
*DIM,DUM2,ARRAY,1
*DIM,DUM3,ARRAY,1

SET,1
ETABLE,SIGC,S,EQV
ETABLE,VOL,VOLU

!-----!
! SORTED ELEMENT STRESSES AND VOLUMES ARE STORED IN THE FILE "esort1"!
! UNSORTED ELEMENT STRESSES AND VOLUMES ARE STORED IN THE FILE "estrs1"!
!-----!

*GET,MAX1,ELEM,0,NUM,MAX

ESORT,ETAB,SIGC,0
/out,esort1
PRETAB,SIGC,VOL
/out
EUSORT

*CFOPEN,estrs1
*DO, KK, 1, MAX1
*GET, SIGC1, ELEM, KK, ETAB, SIGC
*GET, VOL1, ELEM, KK, VOLU
DUM1(1)=KK
DUM2(1)=SIGC1
DUM3(1)=VOL1
*VWRITE, DUM1(1), DUM2(1), DUM3(1)
(x, f6.1, 3x, e21.10, 3x, e21.10)
*ENDDO
*CFCLOSE

!-----!
SUM1=0.0
SUM2=0.0
SUM3=0.0
SUM4=0.0

```

*DO, KP, 1, MAX1
*GET, SIGC1, ELEM, KP, ETAB, SIGC
*GET, VOL1, ELEM, KP, VOLU
*GET, JJ, ELEM, KP, ATTR, MAT
*IF, JJ, EQ, 1, THEN
SUM1=SUM1+(SIGC1**2)*(VOL1)
SUM2=SUM2+VOL1
*ELSE
SUM3=SUM3+(SIGC1**2)*(VOL1)
SUM4=SUM4+VOL1
*ENDIF
*ENDDO
SREF1=SQRT(SUM1/SUM2)
SREF2=SQRT(SUM3/SUM4)

```

```

*CFOPEN, EXVAL

```

```

ALFA=1

```

```

*DO, MM, 1, MAX1
*GET, STEQ, ELEM, MM, ETAB, SIGC
*GET, JJ, ELEM, MM, ATTR, MAT
*IF, JJ, EQ, 1, THEN
*SET, ESEC, ((SREF1/STEQ)**ALFA)*YM1
*ELSE
*SET, ESEC, ((SREF2/STEQ)**ALFA)*YM2
*ENDIF
*CFWRITE, MP, EX, MM+2, ESEC
*CFWRITE, MP, NUXY, MM+2, POISSON
*ENDDO
*CFCLOS
ESEL, ALL

```

```

!-----

```

```

*SET, MN, 3

```

```

*CFOPEN, EXMOD
*DO, L, 1, MAX1
*CFWRITE, MAT, MN

```

```
•CFWRITE,EMODIF,L
•SET,MN,MN+1
•ENDDO
•CFCLOS
ESEL,ALL
FINISH
```

```
!
!  
!
```

```
-----  
I I - L I N E A R   A N A L Y S I S  
-----
```

```
/PREP7  
RESUME
```

```
EX,1,YM  
•USE,EXVAL  
•USE,EXMOD  
FINISH
```

```
/SOLU  
SAVE  
SOLVE  
FINISH
```

```
/POST1
```

```
•DIM,DUM1,ARRAY,1  
•DIM,DUM2,ARRAY,1  
•DIM,DUM3,ARRAY,1
```

```
SET,1  
ETABLE,SIGC,S,EQV  
ETABLE,VOL,VOLU
```

```
!=====  
! SORTED ELEMENT STRESSES AND VOLUMES ARE STORED IN THE FILE "esort2"  
! UNSORTED ELEMENT STRESSES AND VOLUMES ARE STORED IN THE FILE "estrs2"  
!=====
```

```
•GET,MAX1,ELEM,0,COUNT
```

```
ESORT,ETAB,SIGC,0
/out,esort2
PRETAB,SIGC,VOL
/out
EUSORT

*CFOPEN,estrs2
*DO, KK, 1, MAX1
*GET, SIGC3, ELEM, KK, ETAB, SIGC
*GET, VOL2, ELEM, KK, VOLU
DUM1(1)=KK
DUM2(1)=SIGC3
DUM3(1)=VOL2
*VWRITE, KK, SIGC3, VOL2
(x, f6.1, 3x, e21.10, 3x, e21.10)
*ENDDO
*CFCLOS

FINISH
```

Appendix E

Essential Macros for performing a Number of Elastic Iterations

The macros that are necessary for performing repeated elastic analyses are provided in the following sections. The file 'iter1' performs the initial elastic analysis and the subsequent analysis. The file 'iter2', which is input subsequently, performs the third elastic iteration. The file 'iter2' can be copied subsequently as 'iter3', 'iter4' etc. and after some minor changes (in places indicated by %%%%%%%%%%) they can be used for subsequent iterations. The file 'repeat' integrates all the 'iter' files so that the required number of elastic iterations can be carried out.

E.1 First Elastic Iteration - 'iter1'

```
! #####
! #           I T E R A T I O N   -   I           #
! #   ELASTIC MODULUS SOFTENING MACRO FOR R-NODE ANALYSIS   #
! #####
!
! .....
! * NOTE:
! * The parameter "YM" should be defined in the main program *
! .....
```

```
!-----  
!           I - L I N E A R   A N A L Y S I S  
!-----
```

```
/POST1
```

```
/nopr
```

```
*DIM,DUM1,ARRAY,1  
*DIM,DUM2,ARRAY,1  
*DIM,DUM3,ARRAY,1  
*DIM,DUM4,ARRAY,1  
*DIM,DUM5,ARRAY,1
```

```
SET,1  
ETABLE,SIGC,S,EQV  
ETABLE,VOL,VOLU
```

```
/out,esort1,../iterres/  
ESORT,ETAB,SIGC,0  
PRETAB,SIGC,VOL  
/out  
EUSORT
```

```
!=====  
! ELEMENT STRESSES AND VOLUMES ARE STORED IN THE FILE "estrs1"  
!=====
```

```
*GET,MAX1,ELEM,0,NUM,MAX
```

```
DUM4(1)=MAX1  
*CFOPEN,MAX1  
*VWRITE,DUM4(1)  
(1x,F15.2)  
*CFCLOSE
```

```
/sys,cp MAX1 RUN1
```

```

*DIM,ESEC1,ARRAY,MAX1      ! *****
*CFOPEN,estrsl,../iterres/ ! *****

*DO,K,1,MAX1
*GET,SIGC1,ELEM,K,ETAB,SIG
*GET,VOL1,ELEM,K,VOLU
DUM1(1)=K
DUM2(1)=SIGC1
DUM3(1)=VOL1
*VWRITE,DUM1(1),DUM2(1),DUM3(1)
(1x,f6.1,3x,e21.10,3x,e21.10)
*ENDDO
*CFCLOS
!-----
/nopr

c*** !-----
c*** ! NODAL STRESSES ARE STORED IN THE FILE "nstrs1"
c*** !-----

c*** *CFOPEN,nstrs1,../iterres/ ! *****
c*** *GET,MAX2,NODE,0,NUM,MAX

c*** *DO,K,1,MAX2
c*** *GET,SIGC2,NODE,K,S,EQV
c*** DUM1(1)=K
c*** DUM2(1)=SIGC2
c*** *VWRITE,DUM1(1),DUM2(1)
c*** (1x,f6.1,3x,e21.10)
c*** *ENDDO
c*** *CFCLOS
c*** !-----

!-----
! FOR SELECTIVE SOFTENING REMOVE THE COMMENT BELOW
c*** ESEL,S,ETAB,SIGC,YS,(YS*10E10)
!-----

```

```

*SET,MN,2
*SET,YS,100 ! Arbitrary Stress Value

*CFOPEN,EXVAL2,.../iterres/ ! ****

*GET,K,ELEM,O,COUNT

*DO,L,1,K
*GET,MIN1,ELEM,O,NUM,MIN
*GET,STEQ,ELEM,MIN1,ETAB,SIGC
*SET,ESEC1(L),(YS/STEQ)*YM ! ****
*CFWRITE,MP,EX,MN,ESEC1(L) ! ****
*SET,MN,MN+1
*SET,MIN1,MIN1+1
*IF,MIN1,LE,MAX1,THEN
ESEL,R,ELEM,,MIN1,MAX1
*ENDIF
*ENDDO
*CFCLOS
!-----
/nopr

!=====
ESEL,ALL
c*** ESEL,S,ETAB,SIGC,YS,(YS*10E10)
!=====

*CFOPEN,EXVAL,AUX ! ****
*DO,KK,1,MAX1,1
DUM5(1)=ESEC1(KK)
*VWRITE,DUM5(1) ! ****
(1x,E36.19)
*ENDDO
*CFCLOS

/nopr

*SET,MN,2

```

```

*CFOPEN,EXMOD,.../iterres/
*DO,LL,1,K
*GET,MIN1,ELEM,O,NUM,MIN
*CFWRITE,MAT,MN
*CFWRITE,EMODIF,MIN1
*SET,MN,MN+1
*SET,MIN1,MIN1+1
*IF,MIN1,LE,MAX1,THEN
ESEL,R,ELEM,,MIN1,MAX1
*ENDIF
*ENDDO
*CFCLOS
ESEL,ALL
FINISH

```

```
/nopr
```

```

!-----
!           I I   -   L I N E A R   A N A L Y S I S
!-----

```

```
/PREP7
RESUME
```

```

MP,EX,1,YM
/INP,EXVAL2,.../iterres/ ! ****
/INP,EXMOD,.../iterres/
FINISH

```

```
/SOLU
SAVE
SOLVE
FINISH
```

```
/POST1
RESUME
```

```

*DIM,DUM1,ARRAY,1
*DIM,DUM2,ARRAY,1
*DIM,DUM3,ARRAY,1

```

```

SET,1
ETABLE,SIGC,S,EQV
ETABLE,VOL,VOLU

/out,esort2,../iterres/
ESORT,ETAB,SIGC,0
PRETAB,SIGC,VOL
/out
EUSORT

*GET,MAX1,ELEM,0,NUM,MAX
*CFOPEN,estrs2,../iterres/ ! *****

*DO,K,1,MAX1
*GET,SIGC3,ELEM,K,ETAB,SIGC
*GET,VOL2,ELEM,K,VOLU
DUM1(1)=K
DUM2(1)=SIGC3
DUM3(1)=VOL2
*VWRITE,K,SIGC3,VOL2
(1x,f6.1,3x,e21.10,3x,e21.10)
*ENDDO
*CFCLOS
!-----

/nopr

c*** !=====
c*** ! NODAL STRESSES ARE STORED IN THE FILE "nstrs2"
c*** !=====

c*** *CFOPEN,nstrs2,../iterres/ ! *****
c*** *GET,MAX2,NODE,0,NUM,MAX

c*** *DO,K,1,MAX2
c*** *GET,SIGC4,NODE,K,S,EQV
c*** *VWRITE,K,SIGC4
c*** (x,f6.1,3x,e21.10)

```

```
c*** *ENDDDO
c*** *CFCLDS
c*** !-----
```

FINISH

```
/sys,cp ../itermac/iter1 iter1.aux
/sys,tail -20 iter1.aux > iter1a.aux
/sys,rm iter1.aux
/sys,cut -c2-72 iter1a.aux > vread.for
/sys,rm iter1a.aux
/sys,f77 -o vread vread.for
/sys,rm vread.for
/sys,vread
```

```
! program vread1
! open(unit=10,file='EXVAL.AUX',status='old')
! open(unit=11,file='MAX1',status='old')
! open(unit=12,file='EXVAL',status='unknown')
!
! read(11,*)max1
! do j=1,max1
! read(10,*)val
! write(12,15)j,val
!15 format(1x,'YMODU(',I4,')=',E32.19)
! end do
!
!
! close(12)
! close(11)
! close(10)
!
```

```
! stop
! end
```

E.2 Second Elastic Iteration - 'iter2'

```
! *****
! #           I T E R A T I O N   -   I I           #
! # ELASTIC MODULUS SOFTENING MACRO FOR R-NODE ANALYSIS #
! *****

/POST1

/nopr

RESUME

SET,1
ETABLE,SIGC,S,EQV

*GET,MAX1,ELEM,0,NUM,MAX

*DIM,YMODU,ARRAY,MAX1
*DIM,ESEC2,ARRAY,MAX1
*DIM,DUM1,ARRAY,1

/INP,EXVAL

/sys,rm EXVAL

! =====
! FOR SELECTIVE SOFTENING REMOVE THE COMMENT BELOW
c*** ESEL,S,ETAB,SIGC,YS,(YS*10E10)
! =====

*SET,MN,2
*SET,YST,100E12 ! Arbitrary Stress Value
```

```
*CFOPEN,EXVAL3,../iterres/ ! %%%%%%%%%%%%%%%%%%%%%%%%%%%%%%%%%%%%%%%%%%%%%%%%%%%%%%%%%%%%%%%%%%%%%%%%%%
```

```
*GET,KK,ELEM,0,COUNT
```

```
*DO,LL,1,KK  
*GET,MIN1,ELEM,0,NUM,MIN  
*GET,STEQ,ELEM,MIN1,ETAB,SIGC  
*SET,ESEC2(LL),(YST/STEQ)*YMODU(LL)  
*CFWRITE,MP,EX,MN,ESEC2(LL)  
*SET,MN,MN+1  
*SET,MIN1,MIN1+1  
*IF,MIN1,LE,MAX1,THEN  
ESEL,R,ELEM,,MIN1,MAX1  
*ENDIF  
*ENDDO  
*CFCLOS
```

```
!-----
```

```
/nopr
```

```
!-----
```

```
ESEL,ALL  
c*** ESEL,S,ETAB,SIGC,YS,(YS*10E10)
```

```
!-----
```

```
*CFOPEN,EXVAL,AUX  
*DO,KJ,1,MAX1  
DUM1(1)=ESEC2(KJ)  
*VWRITE,DUM1(1)  
(1x,E39.12)  
*ENDDO  
*CFCLOS
```

```
/nopr
```

```
!-----  
!           I I - L I N E A R   A N A L Y S I S  
!-----
```

```
/PREP7  
RESUME
```

```
EX,1,YM  
/INP,EXVAL3,../iterres/ ! XXXXXXXXXXXXXXXXXXXXXXXXXXXXXXXX  
/INP,EXMOD,../iterres/  
FINISH
```

```
/SOLU  
SAVE  
SOLVE  
FINISH
```

```
/POST1  
RESUME
```

```
SET,1  
ETABLE,SIGC,S,EQV  
ETABLE,VOL,VOLU
```

```
/out,esort3,../iterres/  
ESORT,ETAB,SIGC,0  
PRETAB,SIGC,VOL  
/out  
EUSORT
```

```
*GET,MAX1,ELEM,0,NUM,MAX  
*CFOPEN,estrs3,../iterres/ ! XXXXXXXXXXXXXXXXXXXXXXXXXXXXXXXX
```

```
*DO,KL,1,MAX1  
*GET,SIGC3,ELEM,KL,ETAB,SIGC  
*GET,VOL3,ELEM,KL,VOLU  
*VWRITE,KL,SIGC3,VOL3  
(1x,f6.1,3x,e21.10,3x,e21.10)  
*ENDDO
```

```

•CFCLOS
!-----

/nopr

c*** !=====
c*** ! NODAL STRESSES ARE STORED IN THE FILE "nstrs2"
c*** !=====

c*** •CFOPEN,nstrs3 ! *****
c*** •GET,MAX2,NODE,0,NUM,MAX

c*** •DO,K,1,MAX2
c*** •GET,SIGC4,NODE,K,S,EQV
c*** •WRITE,K,SIGC4
c*** (1x,f6.1,3x,e21.10)
c*** •ENDDO
c*** •CFCLOS
c*** !-----

FINISH

/sys,vread

```

E.3 Macro that Links all the Individual Elastic Iteration Macros - 'repeat'

```

/inp,iter1,..../itermac/
/sys,mv RUN1 RUN2      ! Indicator in the problem directory to see
                       ! how many iterations have been completed
/inp,iter2,..../itermac/
/sys,mv RUN2 RUN3
/inp,iter3,..../itermac/

```

```
/sys,mv RUN3 RUN4
/inp,iter4,../itermac/
/sys,mv RUN4 RUN5
/inp,iter5,../itermac/
/sys,mv RUN5 RUN6
/inp,iter6,../itermac/
/sys,mv RUN6 RUN7
/inp,iter7,../itermac/
/sys,mv RUN7 RUN8
/inp,iter8,../itermac/
/sys,mv RUN8 RUN9
/inp,iter9,../itermac/
/sys,mv RUN9 RUN10
/inp,iter10,../itermac/
/sys,mv RUN10 RUN11
/inp,iter11,../itermac/
/sys,mv RUN11 RUN12
/inp,iter12,../itermac/
/sys,mv RUN12 RUN13
/inp,iter13,../itermac/
/sys,mv RUN13 RUN14
/inp,iter14,../itermac/
/sys,mv RUN14 RUN15

/sys,rm vread
/sys,rm MAX1
/sys,rm EXVAL
/sys,rm EXVAL.AUX
```

Appendix F

Input File for determining the Elastic Moduli Ratio for a Two-Layered Cylinder

This following file is to be input into the Maple¹⁹ software for determining the elastic moduli values for a two-layered thick cylinder subjected to internal pressure.

F.1 Axisymmetric Two-Layered Cylinder under Plane-Strain Conditions

```
Digits:=15;
```

```
nu:=0.3;
```

```
ex1:=1;
```

```
sigy1:=1;
```

```
sigy2:=1;
```

```
cr1:=3;
```

```
cr2:=5;
```

```
cr3:=9;
```

```

cp1:=1;
pii:=evalf(Pi);

szz:=nu*(stt+srr);
e1:=(srr-nu*(stt+szz))/e-er;
e2:=(stt-nu*(srr+szz))/e-et;
ans:=solve({e1,e2},{srr,stt});

```

10

```

# Radial stress
subs(er=c1-c2/r^2,rhs(ans[1]));
sr:=subs(et=c1+c2/r^2,");

```

20

```

# Hoop stress
subs(er=c1-c2/r^2,rhs(ans[2]));
st:=subs(et=c1+c2/r^2,");

```

```

subs(r=r1,sr);
e3:="+p1=0;

```

```

subs(r=r2,sr);
e4:="+p2=0;

```

30

```

ans1:=solve({e3,e4},{c1,c2});

```

```

con1:=rhs(ans1[1]);
con2:=rhs(ans1[2]);

```

```

e5:=con1*cr2+con2/cr2;

```

```

subs(p1=cp1,");

```

```
subs(r1=cr1,");
subs(r2=cr2,");
disp1:=subs(e=ex1,");
```

40

```
subs(p2=0,e5);
subs(p1=p2,");
subs(r1=cr2,");
subs(r2=cr3,");
disp2:=subs(e=ex2,");
```

```
e8:=disp1-disp2;
```

50

```
pint:=solve("=0,p2);
```

```
subs(ans1[1],sr);
subs(ans1[2],");
subs(p1=cp1,");
subs(p2=pint,");
subs(r1=cr1,");
subs(r2=cr2,");
sr1:=subs(e=ex1,");
```

60

```
subs(ans1[1],st);
subs(ans1[2],");
subs(p1=cp1,");
subs(p2=pint,");
subs(r1=cr1,");
subs(r2=cr2,");
st1:=subs(e=ex1,");
```

```
sz1:=nu*(sr1+st1);
```

70

```
subs(ans1[1],sr);  
subs(ans1[2],");  
subs(r1=cr2,");  
subs(r2=cr3,");  
subs(p1=pint,");  
subs(p2=0,");  
sr2:=subs(e=ex2,");
```

```
subs(ans1[1],st);  
subs(ans1[2],");  
subs(r1=cr2,");  
subs(r2=cr3,");  
subs(p1=pint,");  
subs(p2=0,");  
st2:=subs(e=ex2,");
```

80

```
sz2:=nu*(sr2+st2);
```

```
seqv1:=(1/2)*((sr1-st1)^2+(st1-sz1)^2+(sz1-sr1)^2)*2*pii*r;  
seqv2:=(1/2)*((sr2-st2)^2+(st2-sz2)^2+(sz2-sr2)^2)*2*pii*r;
```

90

```
v1:=pii*(cr2^2-cr1^2);  
v2:=pii*(cr3^2-cr2^2);
```

```
e9:=int(seqv1,r=cr1..cr2);  
e10:=int(seqv2,r=cr2..cr3);
```

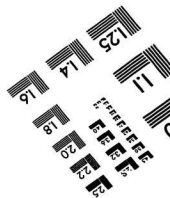
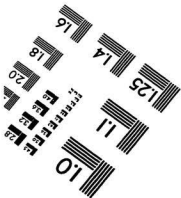
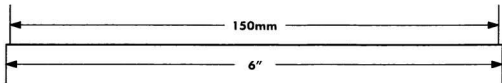
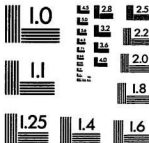
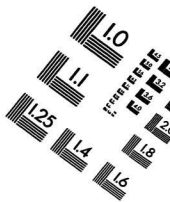
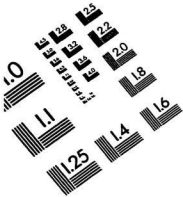
```
m01:=simplify(sigy1*sqrt(v1)/sqrt(e9));
```

```
m02:=simplify(sigy2*sqrt(v2)/sqrt(e10));
```

100

```
e11:=simplify(m01/m02);
```

TEST TARGET (QA-3)



APPLIED IMAGE, Inc
1653 East Main Street
Rochester, NY 14609 USA
Phone: 716/482-0300
Fax: 716/288-5989

© 1993, Applied Image, Inc., All Rights Reserved



